

The Texas Medical Center Library

DigitalCommons@TMC

---

The University of Texas MD Anderson Cancer  
Center UTHealth Graduate School of  
Biomedical Sciences Dissertations and Theses  
(Open Access)

The University of Texas MD Anderson Cancer  
Center UTHealth Graduate School of  
Biomedical Sciences

---

8-2017

# IDENTIFYING THE IMMUNE RELATED METABOLIC PROPERTIES OF PANCREATIC CANCER USING NUCLEAR MAGNETIC RESONANCE SPECTROSCOPY AND DYNAMIC MAGNETIC RESONANCE SPECTROSCOPIC IMAGING WITH HYPERPOLARIZED PYRUVATE

Joseph Weygand

Follow this and additional works at: [https://digitalcommons.library.tmc.edu/utgsbs\\_dissertations](https://digitalcommons.library.tmc.edu/utgsbs_dissertations)



Part of the [Medical Biophysics Commons](#)

---

## Recommended Citation

Weygand, Joseph, "IDENTIFYING THE IMMUNE RELATED METABOLIC PROPERTIES OF PANCREATIC CANCER USING NUCLEAR MAGNETIC RESONANCE SPECTROSCOPY AND DYNAMIC MAGNETIC RESONANCE SPECTROSCOPIC IMAGING WITH HYPERPOLARIZED PYRUVATE" (2017). *The University of Texas MD Anderson Cancer Center UTHealth Graduate School of Biomedical Sciences Dissertations and Theses (Open Access)*. 783.

[https://digitalcommons.library.tmc.edu/utgsbs\\_dissertations/783](https://digitalcommons.library.tmc.edu/utgsbs_dissertations/783)

This Thesis (MS) is brought to you for free and open access by the The University of Texas MD Anderson Cancer Center UTHealth Graduate School of Biomedical Sciences at DigitalCommons@TMC. It has been accepted for inclusion in The University of Texas MD Anderson Cancer Center UTHealth Graduate School of Biomedical Sciences Dissertations and Theses (Open Access) by an authorized administrator of DigitalCommons@TMC. For more information, please contact [digitalcommons@library.tmc.edu](mailto:digitalcommons@library.tmc.edu).

The  
**TMC** LIBRARY  
Health Sciences Resource Center

**IDENTIFYING THE IMMUNE RELATED METABOLIC  
PROPERTIES OF PANCREATIC CANCER USING NUCLEAR  
MAGNETIC RESONANCE SPECTROSCOPY AND DYNAMIC  
MAGNETIC RESONANCE SPECTROSCOPIC IMAGING WITH  
HYPERPOLARIZED PYRUVATE**

by

Joseph Weygand, B.A.

APPROVED:

---

Advisory Professor – Pratip Bhattacharya, Ph.D.

---

Florencia McAllister, M.D.

---

Richard Wendt III, Ph.D.

---

Victor Krasnykh, Ph.D.

---

Jason Fleming, M.D.

---

Niki Millward, Ph.D.

APPROVED:

---

**Dean**, The University of Texas MD Anderson Cancer Center UTHealth Graduate  
School of Biomedical Sciences.

**IDENTIFYING THE IMMUNE RELATED METABOLIC  
PROPERTIES OF PANCREATIC CANCER USING NUCLEAR  
MAGNETIC RESONANCE SPECTROSCOPY AND DYNAMIC  
MAGNETIC RESONANCE SPECTROSCOPIC IMAGING WITH  
HYPERPOLARIZED PYRUVATE**

A

THESIS

Presented to the Faculty of

The University of Texas

MD Anderson Cancer Center UTHealth

Graduate School of Biomedical Sciences

in Partial Fulfillment

of the Requirements

for the Degree of

MASTER OF SCIENCE

by

Joseph Weygand, B.A.

Houston, Texas

August 2017

## Acknowledgements

*I would like to thank my thesis advisor: Dr. Pratip Bhattacharya. It has been a pleasure working in your laboratory for the past eighteen months.*

*I would also like to thank my SMS thesis committee members for their guidance through this project: Dr. Jason Fleming, Dr. Florencia McAllister, Dr. Richard Wendt, Dr. Viktor Krasnykh, and Dr. Niki Zacharias-Millward. A special thank you goes to Dr. Wendt for coordinating the medical physics program and always being available for students.*

*I would also like to thank our research collaborators: Dr. Cullen Taniguchi, Dr. Florencia McAllister, Dr. Jason Fleming, and Dr. Imad Shureiqi, and the various members of their laboratories. I must also acknowledge Kumar Kaluarachchi for his work in maintaining the NMR core facility and all the people that keep the small animal imaging facility afloat, namely Jorge de la Cerda, Charles Kingsley, Dr. James Bankson, and Dr. John Hazle.*

*I would like to thank every member of Dr. Bhattacharya's laboratory, especially Dr. Prasanta Dutta for all his help during the various hyperpolarization experiments.*

*Lastly, I would like to thank my parents, Donna M. Weygand and Joseph L. Weygand, for all their support over the years.*

# **IDENTIFYING THE IMMUNE RELATED METABOLIC PROPERTIES OF PANCREATIC CANCER USING NUCLEAR MAGNETIC RESONANCE SPECTROSCOPY AND DYNAMIC MAGNETIC RESONANCE SPECTROSCOPIC IMAGING WITH HYPERPOLARIZED PYRUVATE**

By: Joseph Weygand, B.A.

Chair of Advisory Committee: Pratip Bhattacharya, Ph.D.

Despite its relatively low incidence, pancreatic cancer was the fourth leading cause of cancer-related death in the US in 2015. This is due in part to pancreatic cancer's natural resistance to both chemotherapy and radiotherapy. Immunotherapy presents an attractive potential treatment approach, but initial trials in mice have proved ineffective. Because cancer cells exhibit a significant increase in metabolic activity relative to normal tissue, an understanding of the metabolic function of tumors in systems with different levels of immunocompetence is a critical first step to develop an understanding of the immune-related metabolic properties of the tumor, which have potential application in assessing a tumor's response to immunotherapy.

Magnetic resonance (MR) is an intrinsically low sensitivity technique, but dynamic nuclear polarization allows one to increase the MR signal by five orders of magnitude. As described by the Warburg effect, even in the presence of an ample amount of oxygen, tumors preferentially metabolize their energy via the inefficient process of glycolysis in which pyruvate is ultimately converted into lactate. Thus, by hyperpolarizing  $^{13}\text{C}$ -labelled pyruvate, one can spectroscopically observe the conversion of pyruvate to lactate in real time and quantify a tumor's glycolytic conversion flux *in vivo*. In addition, the application of high-resolution  $^1\text{H}$  nuclear magnetic resonance metabolomics allows one globally analyze the entire water-soluble

metabolome and quantify the relative concentrations of each metabolite in an extracted tumor tissue sample. By applying MR spectroscopic imaging with hyperpolarized pyruvate and NMR metabolomics, this study identifies clear metabolic biomarkers that can facilitate the assessment of metabolic changes between pancreatic tumors in mice cultivated in both immunocompromised and immunocompetent environments.

# Table of Contents

Approval Page .....	i
Title Page .....	ii
Acknowledgements .....	iii
Abstract .....	iv
Table of Contents .....	vi
List of Illustrations .....	viii
1. Introduction and Background .....	1
1.1 Pancreatic Cancer .....	1
1.2 The Immune System .....	3
1.3 Immunotherapy .....	5
1.4 Cancer Metabolism .....	7
1.5 NMR Spectroscopy .....	8
1.6 Hyperpolarization .....	10
1.7 Hypothesis and Aims .....	16
1.8 Research Approach .....	17
2. Materials and Methods .....	18
2.1 Mouse Model .....	18
2.2 NMR Metabolomics Experimental Methods .....	20
2.3 Hyperpolarization Experimental Methods .....	23
2.4 Statistical Methods .....	25
3. Results .....	26
3.1 NMR Spectroscopic Data .....	26

3.2	Hyperpolarization Data .....	32
4.	Discussion .....	36
4.1	Histological Staining .....	36
4.2	The Effects of Immune Infiltration .....	41
4.3	Lactate Metabolism .....	42
4.4	Problems and Pitfalls .....	46
4.5	Future Direction .....	48
5.	Conclusion .....	51
6.	Supplementary Section.....	53
7.	Citations .....	57
8.	Vita .....	100



# List of Illustrations

Figure 1-1: A Representative NMR Spectrum .....	8
Figure 1-2: The HyperSense DNP Polarizer used at MD Anderson .....	11
Figure 1-3: A T <sub>2</sub> -weighted Coronal Image that Illustrates Two Dimensions of the Voxel in which Spectroscopic Data are Acquired .....	12
Figure 1-4: A Representative Time-integrated Spectrum .....	14
Figure 1-5: A Dynamic Spectrum Depicting the Conversion of Pyruvate into Lactate ..	14
Figure 2-1: A Cohort of Immunocompetent C57BL/6 Mice .....	18
Figure 2-2: A Cohort of Immunocompromised Nude Mice .....	19
Figure 2-3: A Nude Mouse with a Subcutaneously-injected Pancreatic Tumor Growing in its Flank .....	19
Figure 2-4: A 500 MHz Bruker NMR Spectrometer .....	22
Figure 2-5: Representative NMR Spectra of Tumor Samples Taken from the Immunocompetent and Immunocompromised mice .....	23
Figure 2-6: A 7 T Bruker Small Animal MRI Scanner .....	25
Figure 3-1: Relative Concentrations of Various Metabolites Found in Larger Tumor Samples .....	27
Figure 3-2: Ratio of the Relative Concentrations of Various Metabolites Found in the	

C57BL/6 Mice to the Relative Concentration of Various Metabolites Found in the Nude	
Mice for the Larger Tumor Samples .....	28
Figure 3-3: Negative Control Experimental Data that Show the Relative Concentrations	
of Various Metabolites Found in Healthy Pancreatic Tissue .....	29
Figure 3-4: Relative Concentrations of Various Metabolites Found in Smaller Tumor	
Samples .....	30
Figure 3-5: Ratio of the Relative Concentrations of Various Metabolites Found in the	
C57BL/6 Mice to the Relative Concentration of Various Metabolites Found in the Nude	
Mice for the Smaller Tumor Samples .....	31
Figure 3-6: Glycolytic Dependence, Smaller Tumors .....	33
Figure 3-7: Glycolytic Dependence, Larger Tumors .....	34
Figure 3-8: Dynamic Spectroscopy, Smaller Tumors, Cohort 1 .....	34
Figure 3-9: Dynamic Spectroscopy, Smaller Tumors, Cohort 2 .....	35
Figure 3-10: Dynamic Spectroscopy, Larger Tumors .....	36
Figure 4-1: H&E Staining of Tumors at the Earlier Time Point in Tumor Progression .	37
Figure 4-2: H&E Staining of Tumors at the Later Time Point in Tumor Progression ...	38
Figure 4-3: Color Coded H&E Stain of a Tumor Taken from the Immunocompetent	
Mice .....	39

Figure 4-4: Color Coded H&E Stain of a Tumor Taken from the Immunocompromised Mice .....	40
Figure 4-5: Dynamic Spectroscopy, Failed Experiment Due to Low SNR .....	46
Figure 4-6: Glycolytic Dependence, Failed Experiment Due to Low SNR .....	47
Supplementary Figure 1: Glycolytic dependence, small tumors, cohort 1 .....	53
Supplementary Figure 2: Glycolytic dependence, small tumors, cohort 2 .....	53
Supplementary Figure 3: Time-integrated spectra, small tumors, cohort 1 .....	54
Supplementary Figure 4: Time-integrated spectra, small tumors, cohort 2 .....	55
Supplementary Figure 5: Time-integrated spectra, large tumors .....	56

# 1. Introduction and Background

## 1.1 Pancreatic Cancer

In 2015, nearly 49,000 new cases of pancreatic cancer were diagnosed in the United States [1]. Despite this low incidence relative to other malignancies, pancreatic cancer was the fourth leading cause of cancer-related death in both men and women, as it was responsible for over 40,000 mortalities [1] in the United States in 2015 alone. Pancreatic cancer has an abysmal five-year survival rate of 7 % [1], and the median survival of patients diagnosed with a pancreatic malignancy is typically measured in months [2]. One of the main factors leading to pancreatic cancer's exorbitantly high rate of morbidity is its natural resistance to both chemotherapy and radiotherapy [3]. Thus, it is pertinent to explore new treatment modalities that can potentially extend the lives of these patients without compromising their quality of life.

The pancreas is a small, pear-shaped organ found in the upper left quadrant of the abdominal cavity [4]. It is located behind the stomach, sits on top of the curve of the duodenum [5], and rests below the liver. The pancreas has functional roles in both the endocrine and digestive systems [6]. The main endocrine function of the pancreas, spearheaded by the islets of Langerhans [7], is to produce insulin and glucagon, hormones that regulate the body's blood glucose level [8-11]. The main digestive function of the pancreas is the production of the enzymes amylase, lipase, and trypsin which are involved in the catabolism of starch, fat, and polypeptides, respectively [12]. Numerous epidemiological studies [13-15] have identified age [16] and cigarette smoking [17,18] to be the two most commonly reported risk factors for pancreatic cancer. Other potential risk factors include alcohol consumption [19,20], family history [21,22], and occupational exposure to carcinogens [23,24].

Pancreatic ductal adenocarcinoma is far and away the most common form of pancreatic cancer [25]. Like many other malignancies, pancreatic ductal adenocarcinoma is known to be caused by the accumulation of acquired genetic mutations [26]. Greater than 85% of pancreatic carcinomas exhibit *K-ras* mutations [27-29], which are strongly correlated with both alcohol and cigarette consumption [30-32]. In addition, the tumor-suppressor genes TP53 [33], SMAD4 [34], CDKN2A [35], p16 [36-38], and MADH4 [39] are often inactivated in pancreatic tumors. As in other types of cancer, many growth factors and their receptors are overexpressed in pancreatic malignancies. Vascular endothelial growth factor [40,41] and interleukin 8 [42] are both overexpressed in pancreatic cancer and are critical in initiating angiogenesis which is necessary to satisfy the tumor's increased demand for nutrients and oxygen [43]. Other studies have shown that fibroblast growth factor [44], epidermal growth factor [45], tumor necrosis factor  $\alpha$  [46], transforming growth factor  $\beta$  [47], interleukin 1 [48], and interleukin 6 [49] are also upregulated in pancreatic tumors.

When determining treatment approaches it is often helpful to classify pancreatic tumors into three categories: localized and resectable, locally advanced and unresectable, or metastatic [50]. A pancreatic tumor is deemed localized and potentially resectable if it does not encroach on the superior mesenteric artery or the coeliac axis and there is no evidence of distant metastatic disease [26]. Pancreatic tumors are classified as resectable in approximately 15-20% of patients and are often treated with a pancreaticoduodenectomy and adjuvant fluorouracil-based chemoradiation [51]. The five-year survival of these patients improves to 20% [52]. A locally advanced and unresectable tumor is defined as such when the disease encases a vascular structure but there is still no evidence of distant metastatic disease [26]. The standard of care for these patients is fluorouracil-based chemoradiation [53]. Treatment approaches for metastatic

pancreatic cancer are only palliative [54] in nature. The chemotherapeutic agent gemcitabine serves as the standard of care when there is evidence of distant metastatic disease [55].

## **1.2 The Immune System**

The immune system is a functional biological system consisting of cells, tissues, and organs that protect a host from foreign invaders [56]. It is conventionally dichotomized into two intrinsic defense systems [57] that act independently of each other: the innate defense system and the adaptive defense system. The innate immune system is nonspecific [58] and contains two lines of defense. The first line of defense includes external body membranes, namely the skin and mucous membranes [59] that act as a physical barrier against pathogens and other foreign invaders.

The second line of defense utilizes phagocytes [60], natural killer cells [61], and antimicrobial proteins [62] to fight off pathogens when the first line of defense has been compromised. Phagocytes, such as macrophages [63] and neutrophils [64], ingest foreign bacteria in a process known as phagocytosis [65,66]. Natural killer cells, a group of defensive cells found mainly in lymph [67], kill target invaders by inducing them to undergo apoptosis [68]. Antimicrobial proteins, such as interferons [69] and complement proteins [70], contribute to the innate defense system by either attacking microorganisms directly or by obstructing their propensity to reproduce. Inflammation, a response intended to prevent the spread of harmful agents to neighboring tissue, to remove cellular debris and other pathogens, and to set the stage for the repair process to begin, is a hallmark of the second line of defense [71].

The adaptive immune system is characterized by three notable properties. Firstly, it is specific, as the adaptive immune response is initiated by specific pathogens and foreign substances. It is systemic, as the adaptive immune response is not limited to the site of the initial infection. Lastly, it has the ability to remember pathogens after an initial exposure and will subsequently mount an even stronger attack against these previously encountered foreign substances [71]. The adaptive immune system can be further subclassified into humoral immunity [72] and cell-mediated immunity [73].

Humoral immunity is mediated by antibodies [74] located in the fluids of the body, namely blood and lymph [75]. These antibodies, also called immunoglobulins [76], are secreted by B lymphocytes [77] in response to a particular invading antigen [78]. The antibody then binds with the antigen at a specific binding site [79,80] to form an antibody-antigen complex [81,82], which causes the antigen to be rendered inactive via neutralization [83] and tagged for destruction via agglutination [84], precipitation [85], or complement fixation [86].

Cell-mediated immunity is controlled directly by T lymphocytes [87]. These T lymphocytes are activated in a two-step process [88] both involving interactions with antigen presenting cells. First T cell antigen receptors bind to an antigen-major histocompatibility complex at the surface of an antigen presenting cell [89]. Then the T cell receptors induce a costimulatory signal when they bind with molecules on antigen presenting cells [90]. Signaling in cell-mediated immunity is controlled by a class of proteins known as cytokines [91], which include both interferons [92] and interleukins [93]. There are many types of T lymphocytes that contribute to cell-mediated immunity; important examples include helper T cells [94], cytotoxic T cells [95], and regulatory T cells [96]. Helper T cells aid in the activation of B and T lymphocytes and induce B and T cell proliferation [97]. Cytotoxic T cells, as the name implies,

can directly attack and kill antigens [98]. Regulatory T cells lessen the immune response [99] by releasing inhibitory cytokines [100].

### **1.3 Immunotherapy**

As mentioned previously, one of the causes leading to the exorbitantly high morbidity of pancreatic cancer is its intrinsic resistance to both chemotherapy [101,102] and radiotherapy [103]. Immunotherapy has exhibited substantial success in treating other forms of cancer such as melanoma [104], so there was much hope [105] that it would be implemented into pancreatic cancer with equal success and provide an attractive new treatment options to numerous pancreatic cancer patients.

The aim of immunotherapy in cancer is to stimulate an effective immune response in the patient against his or her tumor [106]. This can be accomplished by stimulating the recruitment and activation [107,108] of T cells that can recognize tumor-specific antigens. In addition, monoclonal antibodies can also activate and inhibit molecules of the immune system and, as a result, induce an antitumor immune response [109]. Moreover, monoclonal antibodies can be conjugated to either chemotherapeutic [110] or radiotherapeutic [111] agents and have been implemented in treating lymphoma [112-118], leukemia [119,120], and other hematologic malignancies [121]. Both approaches, the recruitment and activation of T cells and monoclonal antibodies, present attractive options towards the treatment of pancreatic cancer [122].

Although not originally recognized as such [123], immune evasion is now considered one of the hallmarks of cancer [124]. Tumor cells learn to survive in a chronically inflamed microenvironment, evade immune recognition, and suppress immune responses [125,126]. In particular, the inhibition of T cell recognition of pancreatic tumors and the subsequent



suppression of the immune response may be due to many factors [122] such as the upregulation of molecules involved in immune inhibition [127-134], deficiencies in immune-cell localization [135-148], the loss of immune-regulation signals [149-151], and the loss of co-stimulatory factors [152-154]. The progression of a successful immune response mandates that many immunological checkpoints be passed [155]. Thus, any clinically successful immunotherapy must be able to overcome these inhibitory checkpoints [156].

One key type of the immunotherapeutic approach takes advantage of the receptor [157-159] program death 1 (PD-1) and its ligands PD-L1 and PD-L2 [160]. PD-1 is a receptor of the immunoglobulin superfamily that downregulates T cell antigen receptor signaling [161]. In particular, when PD-L1 or PD-L2 bind to PD-1, an inhibitory signal [162-164] is transmitted to the T cell, which reduces cytokine production and suppresses T cell proliferation [165]. PD-L1 is commonly overexpressed in tumors [166-169], and the expression of PD-L1 is negatively correlated with survival in pancreatic cancer [170]. Thus, treatment with PD-L1 neutralizing antibodies will downregulate PD-L1 expression and, as a result, inhibit the suppression of T cell proliferation [171,172]. Other treatment approaches that block the inhibitory effects of the receptor Cytotoxic T lymphocyte- associated antigen 4 (CTLA-4) are currently being explored by MD Anderson immunologist James P. Allison and others [173-188].

Despite the incredible potential, initial trials implementing immunotherapy into pancreatic cancer treatment regimens have been disappointing [189-192], and the reasons as to why are not well understood. An overarching goal in the community is to obtain a more mechanistic understanding of immunotherapy's failure in pancreatic cancer, but this is a very complex problem that must be approached from numerous angles. Because metabolic function is severely dysregulated in cancer [193], one avenue of approaching this problem is through

studying the immune-related metabolic properties of pancreatic cancer. More specifically, observing the metabolome of pancreatic tumors cultivated in different immune environments could serve as a critical first step in understanding the failure of immunotherapy in pancreatic cancer.

#### **1. 4 Cancer Metabolism**

Metabolism is the net sum of all the physical and chemical processes taking place within an organism that result in the biological processing of energy and materials [194]. Metabolism is typically subdivided into two categories [195]: catabolism and anabolism. Catabolism is the breakdown of complex molecules into simpler end products and results in the release of chemical energy [196]. Anabolism, on the other hand, is the buildup of simple molecules into larger, more complex units and necessarily requires the input of energy [197]. Most metabolic reactions are catalyzed by enzymes, so the vital regulation of metabolic function is accomplished via the modulation of the activities of these enzymes [198].

Metabolic function is severely dysregulated in cancer [199], and this dysregulation of metabolism is considered one of the hallmarks of cancer [200,201]. Normal differentiated cells typically metabolize energy via oxidative phosphorylation under standard oxygen conditions but switch to anaerobic glycolysis under hypoxic conditions [202]. In contrast, even in the presence of an ample supply of oxygen, tumor cells tend to metabolize energy via the inefficient [203] process of glycolysis rather than the more energy-efficient process of oxidative phosphorylation [204-209]. This upregulation of aerobic glycolysis [210,211] in cancerous cells ultimately leads to an increased production of lactic acid [212] relative to healthy cells. This phenomenon was

first described [213] by Otto Warburg [214-216] in 1924 and has since been coined the Warburg effect [217-220]. Because metabolomics is downstream from gene expression and protein synthesis [221,222], studying the metabolism of pancreatic tumors cultivated in different immune environments may provide crucial insight into how the immune environment alters the function of pancreatic tumor cells.

## 1.5 NMR Spectroscopy

The first magnetic resonance-based technique used in this project to interrogate tumor metabolism was nuclear magnetic resonance (NMR) metabolomics. NMR metabolomics is a spectroscopic technique that allows one to quantitatively interrogate the water-soluble metabolome. It relies upon the same guiding principles as magnetic resonance imaging (MRI) except for the fact that the gradient coils responsible for spatial encoding in MRI are not present in NMR.

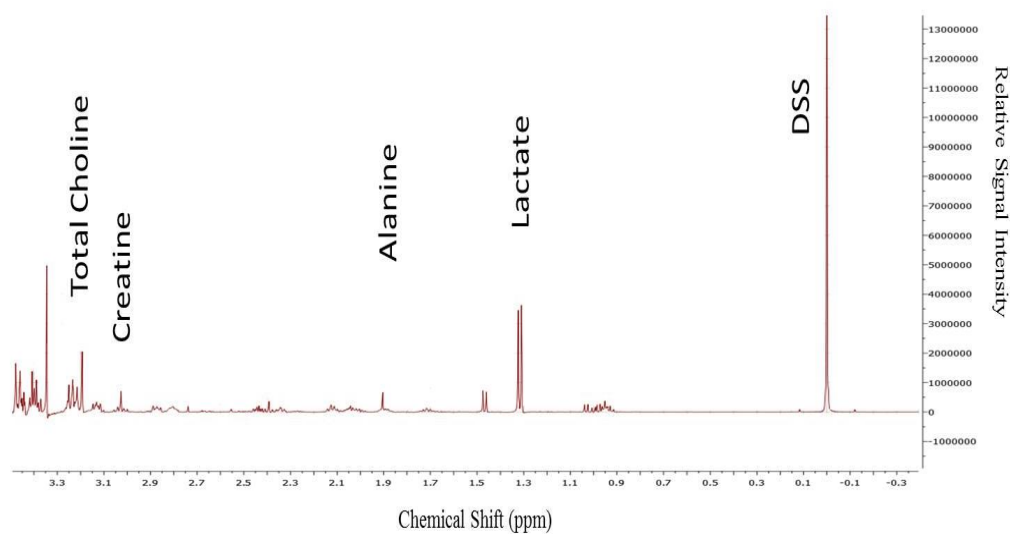


**Figure 1-1: A representative NMR spectrum**

As in MRI, a strong, static magnetic field is established to polarize the spins, resulting in a net magnetization in the direction of the field. This magnetization is then transferred into a plane orthogonal to the direction of the field via a pulse of electromagnetic radiation in the radiofrequency regime. These spins will precess about the magnetic field, and, by Faraday's law of induction [223-225], this changing magnetic field will induce an electromotive force, which can be detected and measured as a current through a coil. The chemical environment in which a proton is located will perturb the magnitude of the net magnetic field experienced by that proton [226]. Thus, a proton in a given molecule will experience a slightly different magnetic field than a proton in a different molecule or even a nonequivalent proton in that same molecule. Since the precessional frequency of a spin, known as the Larmor frequency [227], is proportional to the magnetic field experienced by that spin, protons in different chemical environments will precess at slightly different frequencies. Therefore, the signal detected in the coil will be a superposition of numerous, individual frequency components. By taking the Fourier transformation of this signal, one can transform the signal into the temporal frequency domain to obtain an NMR spectrum, as shown in Figure 1-1. Here, the vertical axis represents relative signal intensity, while the horizontal axis represents chemical shift which is a relative measure of deviation from a standard resonance frequency. Chemical shift is measured in parts per million (ppm) relative to the Larmor frequency of a spin subject to the static magnetic field. A group of equivalent protons in a given molecule will resonate at a specific chemical shift, so it is possible to identify the presence of certain metabolites by observing the location of the peaks in the NMR spectrum. The relative concentration of these metabolites can then be determined by integrating under a given peak in the frequency domain [228-232].

It is important to note that NMR metabolomics provides a static snapshot of pancreatic tumor metabolism literally frozen in time. The samples that we subject to NMR spectroscopy have been resected from mice following euthanasia and flash frozen. Thus, we are observing the static metabolic properties of that tumor at the time of euthanasia. In addition, NMR metabolomics, in theory, allows us to globally analyze the entire water-soluble metabolome. Because there can be multiple unrelated molecules that resonate at the same chemical shift, it is not always possible to identify every molecule with 100% certainty. However, many of the common metabolites and metabolic pathways are easily identifiable, so a large amount of metabolic information can be ascertained in an NMR spectroscopic experiment.

## 1.6 Hyperpolarization

Although the static, *ex vivo* data obtained in NMR metabolomics are very illuminating, it is also advantageous to interrogate real-time tumor metabolism in a living system. Unfortunately, however, MRI is a relatively low sensitivity technique [233]. This is due to the fact that when a sample is placed in a magnetic field, the spins in the sample will either align or anti-align with the field [234,235]. Aligning with the field is a lower energy state than anti-aligning, so the number of spins that will align with the field,  $N_-$ , will be greater than the number of spins that anti-align,  $N_+$ . In particular, the net NMR signal is proportional to the polarization,  $P$ , which is given by the following relation [236]:

$$P = \frac{N_- - N_+}{N_- + N_+} = \tanh\left(\frac{\gamma \hbar B_0}{2k_B T}\right) \quad \text{Equation (1)}$$

Here,  $\gamma$  is the gyromagnetic ratio of the nucleus,  $\hbar$  is the reduced Planck's constant,  $B_0$  is the strength of the static magnet field,  $k_B$  is the Boltzmann constant, and  $T$  is the temperature. At

typical clinical field strengths, for every million spins, only a few more spins populate the lower energy state. Since the net magnetization is the vector sum of the individual dipole moments, it is proportional to the difference of the number of spins that align with the field and the number of spins that anti-align with the field [237]. This sensitivity problem is typically avoided since most clinical imaging techniques focus on hydrogen atoms [238]. Sensitivity issues are not as dire in hydrogen-based MRI due to the high natural abundance of hydrogen in the body [239-240] and its comparably large gyromagnetic ratio of 42.58 MHz/T [241]. If one wishes to image MR-visible nuclei other than hydrogen, however, one needs a technique that increases sensitivity.



**Figure 1-2: The HyperSense DNP Polarizer used at MD Anderson**

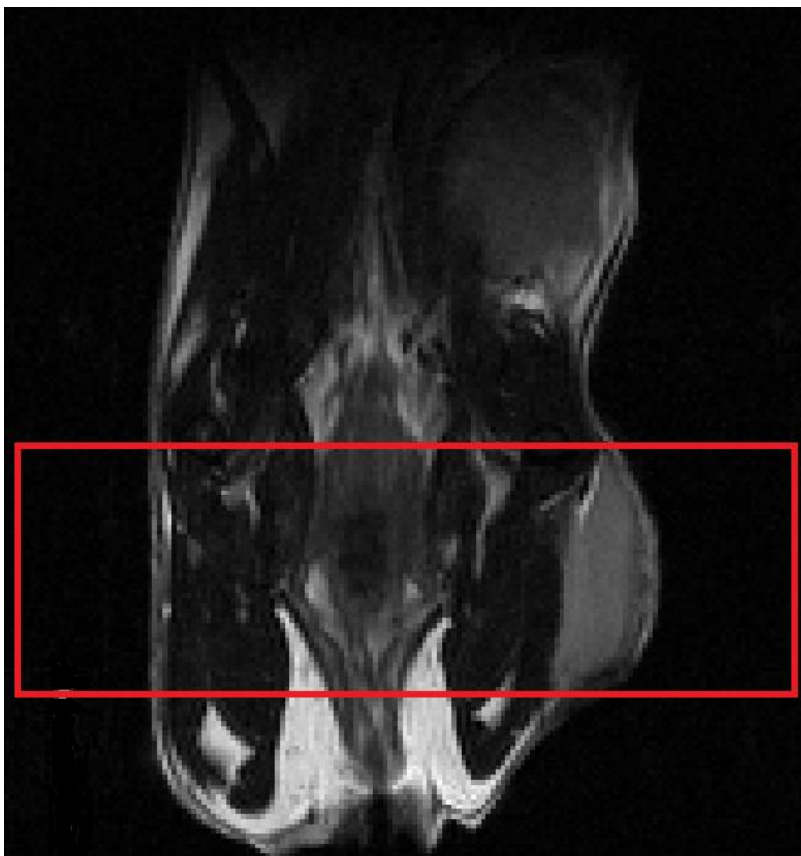


**Figure 1-3: A  $T_2$ -weighted coronal image that illustrates two dimensions of the voxel in which spectroscopic data are acquired**

Hyperpolarization refers to the driving of the nuclear spin polarization far from its thermal equilibrium distribution [242]. In particular, spins are preferentially driven to a given energy state so that the signal is enhanced considerably [243]. Hyperpolarization can be achieved through a variety of methods: optical pumping [244], parahydrogen-induced polarization [245-247], brute force polarization [248-249], and dynamic nuclear polarization (DNP). The preferred hyperpolarization technique of focus in this treatise was DNP. Polarization of nuclear spins in DNP is accomplished in an amorphous solid state [250] at very low temperatures, on the order of 1 K. Unpaired free electrons, in the form of an organic free radical, are added to the sample, and the high electron spin polarization is transferred to the nuclear spins via microwave irradiation

[251]. At MD Anderson, this is accomplished using a HyperSense DNP Polarizer, shown in Figure 1-2, that is produced by Oxford Instruments. This mechanism of polarization transfer was originally proposed by the physicist Albert Overhauser [252] in 1953. Previous studies have demonstrated that polarizations of nearly 100% and 50% can be achieved for  $^1\text{H}$  and  $^{13}\text{C}$ , respectively [253,254], which constitutes a greater than 10,000-fold increase in sensitivity [255].

Because glycolysis, in which pyruvate is converted into lactate, is upregulated in cancer, pyruvate is the substrate that we choose to hyperpolarize to probe pancreatic tumor metabolism [256]. By observing the flux of pyruvate to lactate, one can obtain a measure of how glycolytic a tumor is [257]. This is accomplished by labelling pyruvate with  $^{13}\text{C}$ , hyperpolarizing the  $^{13}\text{C}$ , and injecting the labelled pyruvate into the subject. The pyruvate will perfuse into the tumor and be converted into lactate. This real-time pyruvate-to-lactate conversion is captured using dynamic magnetic resonance spectroscopic imaging (MRSI). Similarly to conventional magnetic resonance spectroscopic imaging, a voxel is placed over a region of interest in which spectroscopy is to be performed. Figure 1-3 illustrates the placement of this voxel on a coronal view of a  $T_2$ -weighted anatomical scan of a mouse with a pancreatic tumor implanted in its flank. The voxel position is chosen as to contain as much of the tumor volume as possible. Spectroscopic data are acquired every two seconds, and these  $^{13}\text{C}$  spectra are integrated over time to produce a time-integrated  $^{13}\text{C}$  spectrum. Figure 1-4 depicts a representative time-integrated spectrum acquired in one of our imaging experiments. Here, the vertical axis represents the relative signal intensity in arbitrary units, which is essentially the time integrated sum of all spectra acquired. The horizontal axis represents  $^{13}\text{C}$  chemical shift. Pyruvate and lactate are labelled in the figure for convenience.



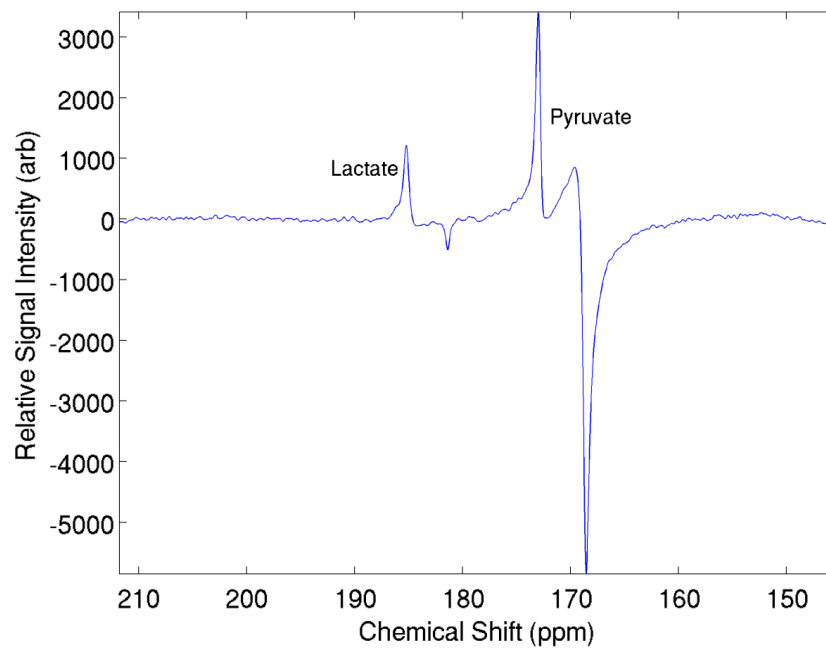


**Figure 1-4: A representative time-integrated spectrum**

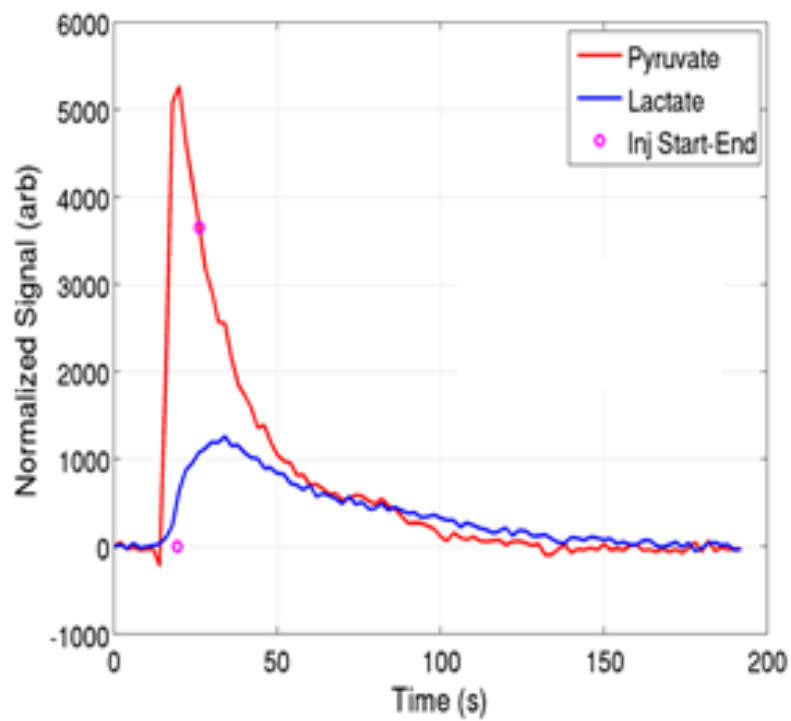


**Figure 1-5: A dynamic spectrum depicting the conversion of pyruvate into lactate**

The individual peak intensities of pyruvate and lactate can be plotted as a function of time, as is shown in Figure 1-5. Here, pyruvate is shown in red, lactate is shown in blue, and the dots indicating the start time and end time of the pyruvate injection are shown in pink.

Immediately following injection, the pyruvate concentration rises rapidly and then decays via  $T_1$  relaxation [258]. Shortly after the injection, one can see the lactate concentration rising, indicating its conversion from pyruvate. Ultimately, that signal also decays due to  $T_1$  relaxation.

The glycolytic flux can be quantified using the metric  $nLac$  given the time-dependent concentrations of pyruvate [Pyruvate] and lactate [Lactate]:

$$nLac = \frac{\int ([Lactate]) dt}{\int ([Lactate] + [Pyruvate]) dt} \quad \text{Equation (2)}$$

Essentially,  $nLac$  is the time-integrated hyperpolarized lactate concentration normalized by the total time-integrated hyperpolarized signal, pyruvate plus lactate. Here, the integrals run from  $t = 0$  to  $t = \infty$ .

Magnetic resonance spectroscopic imaging of hyperpolarized pyruvate has its challenges. The biggest challenge faced is the spin-lattice relaxation of the hyperpolarized pyruvate [259], which depends on numerous factors but typically has a time constant on the order of tens of seconds to minutes [260]. Thus, the success of this technique inherently depends on the ability of the pyruvate to perfuse to the tumors rapidly relative to the  $T_1$  decay of the signal. This shall be discussed further in later sections.

## 1.7 Hypothesis and Aims

The ultimate aim of this project was to interrogate the immune environment's effect on the metabolism of pancreatic tumors. Pancreatic tumor metabolism has been probed using two different magnetic resonance-based techniques: nuclear magnetic resonance spectroscopy and magnetic resonance spectroscopic imaging of hyperpolarized pyruvate. These two techniques provide distinctly different yet complimentary information. NMR spectroscopy provides a static snapshot of tumor metabolism and allows one to interrogate the entire water-soluble metabolome. Most key metabolites can be identified, and their concentrations can be quantified. In addition, the metabolic pathways that are important in pancreatic tumor metabolism can be determined. MRSI using hyperpolarized pyruvate, on the other hand, focuses on a single metabolic pathway, aerobic glycolysis, by quantifying the glycolytic conversion flux from pyruvate to lactate. This technique provides a dynamic picture of pancreatic tumor metabolism and allows us to understand how pyruvate is metabolized *in vivo*. The specific aims of this project can be articulated as follows:

Specific Aim 1: *Perform NMR metabolomics to identify clear metabolic biomarkers characteristic of pancreatic tumors resected from mice with different levels of immune system functionality.* Studying the global metabolic profile of *ex vivo* tumors in systems with different levels of immunocompetence is a critical first step toward developing an understanding of the immune-related metabolic properties of the tumor, which have potential application in assessing a tumor's response to immunotherapy. **We hypothesize that it is possible to identify clear metabolic biomarkers that can predict the immune environment in which a pancreatic tumor was harvested.**

Specific Aim 2: *Quantify the pyruvate-to-lactate conversion flux of pancreatic tumors in living mice with different levels of immune system functionality via real-time hyperpolarized  $^{13}\text{C}$  pyruvate MRSI.* Pyruvate-to-lactate flux is a well-established biomarker that can quantitatively assess how glycolytic a tumor is, which tends to correlate with tumor growth and aggressiveness. Normally, MR imaging is not sufficiently sensitive to image nuclei other than hydrogen. However, dynamic nuclear polarization (DNP) is a technique that allows us to preferentially drive nuclear spins to a given energy state and, as a result, increase the sensitivity of MR imaging by roughly five orders of magnitude. This will allow us to image  $^{13}\text{C}$ -labeled pyruvate and capture its conversion to lactate in real-time. **We hypothesize that pancreatic tumors harvested in different immune environments will exhibit different levels of dependence on aerobic glycolysis.**

## 1.8 Research Approach

Mice can be bred to possess varying levels of immunocompetence, which is an organism's ability to produce a normal immune response after being exposed to an antigen [261]. In particular, the hairless mouse mutant breed typically referred to as “nude” mice is immunocompromised, as these athymic mice are born without the ability to produce viable T cells [262]. C57BL/6 mice, on the other hand, have a properly functioning immune system [263]. Pancreatic tumors were cultivated in both sets of mice, and the metabolism of both were observed in order to study the immune environment's influence on pancreatic tumor metabolism. Both NMR spectroscopy and MRSI with hyperpolarized pyruvate were employed to study metabolism. In addition, these experiments were performed at two separate time points in tumor

development: one at an earlier stage when the tumors were small, ~1 cm in diameter, and one at a later time point when the tumors were larger, ~1.5 cm in diameter.

## **2. Materials and Methods**

### **2.1 Mouse Model**

The animal model was developed in a collaborating laboratory and utilized both the immunocompetent C57BL/6 mice and the immunocompromised nude mice. All procedures were performed in accordance with regulations of the Animal Care and Use Committee of the University of Texas MD Anderson Cancer Center.



**Figure 2-1: A cohort of immunocompetent C57BL/6 mice**



**Figure 2-2: A cohort of immunocompromised nude mice**



**Figure 2-3: A nude mouse with a subcutaneously-injected pancreatic tumor growing in its flank**

A cohort of five C57BL/6 mice is shown in Figure 2-1, and a cohort of five athymic nude mice is shown in Figure 2-2. When the mice reached approximately nine weeks of age, our collaborators injected approximately one million K8484 pancreatic tumor cells into the flanks of the mice. This cell line was syngeneic to C57BL/6 background and derived from mouse tumors with an oncogenic KRAS mutation (G12D) and a homozygous null mutation in p53. A nude mouse with a subcutaneously injected tumor growing in its flank is shown in Figure 2-3.

## **2.2 NMR Metabolomics Experimental Methods**

When the tumors reached their appropriate size, either approximately 1 cm or 2 cm in diameter, the mice were euthanized. The tumors were resected from the flank and immediately frozen in liquid nitrogen. The samples were then stored at -80°C until further analysis was performed.

Each sample was weighed, crushed, and immersed in 3 mL of methanol-to-water mixture (2:1) with 0.5 mL of polymer vortex beads inside a 15 mL test tube. Mechanical homogenization was performed by vortexing the tubes for 15 seconds, soaking the samples in liquid nitrogen for one minute, allowing the mixture to thaw, and repeating this process three times.. The samples were then subjected to centrifugation for ten minutes to physically separate the water-soluble metabolites from the proteins and other cellular constituents. The supernatant was extracted and subjected to rotary evaporation in order to remove the methanol. The samples were further dehydrated by placing them on a lyophilizer overnight, leaving just a collection of metabolites in powder form remaining. These metabolites were then immersed in a solution of 600  $\mu$ L of  $^2\text{H}_2\text{O}$ , 36  $\mu$ L of  $\text{PO}_4$  buffer, and 4  $\mu$ L of 80 mM DSS (4,4-dimethyl-4-silapentane-1-sulfonic acid). The

PO<sup>4</sup> buffer was added in order to stabilize any potential pH variations, and the DSS served as the reference standard to which we normalized the spectral signal from each metabolite.

NMR spectroscopy was performed on a Bruker AVANCE III HD<sup>®</sup> NMR scanner (Bruker Bio Spin Corporation, The Woodlands, TX) at a temperature of 298 K. The <sup>1</sup>H resonant frequency was 500 MHz, which corresponds to a static field strength of 11.7 T. The scanner possesses a triple resonance (<sup>1</sup>H, <sup>13</sup>C, <sup>15</sup>N) cryogenic temperature probe with a Z-axis shielded gradient. Water suppression was performed using a pre-saturation technique. The spectra were collected with a 10240 Hz spectral width, a 90° pulse width, a scan delay of 6.0 s, and an acquisition time of 1.09 s (16,000 complex points). Two hundred and fifty-six scans were acquired and averaged, so that the total scan time was 32 minutes and 49 seconds. Here,  $t_{\text{rel}} + t_{\text{max}}$  was nearly 8 s so that it was greater than  $3 \cdot T_1$  of the metabolites observed [264]. Apodization of the time domain signal was performed using an exponential function. The 500 MHz Bruker scanner used in all NMR metabolomics experiments is shown in Figure 2-4. Figure 2-5 depicts representative NMR spectra of tumor samples taken from the immunocompetent and immunocompromised mice.

After the spectra were acquired, metabolic profiling was performed in the Chenomx NMR Suite 8.1 software (Chenomx Inc., Edmonton, Canada). Quantification of the metabolites was then performed using the MestReNova software (Mestrelab Research, A Coruña, Spain) by integrating a nonzero region centered about the chemical shift at which the metabolite is known to resonate. This integral value is then normalized by the value of the integral of the DSS reference peak. Since the NMR signal is directly proportional to the amount of material in the test tube, this value is further normalized by the mass obtained prior to immersion in the



methanol-to-water mixture. Prior to integration, phase and baseline corrections were performed manually in MestReNova.



**Figure 2-4: A 500 MHz Bruker NMR spectrometer**

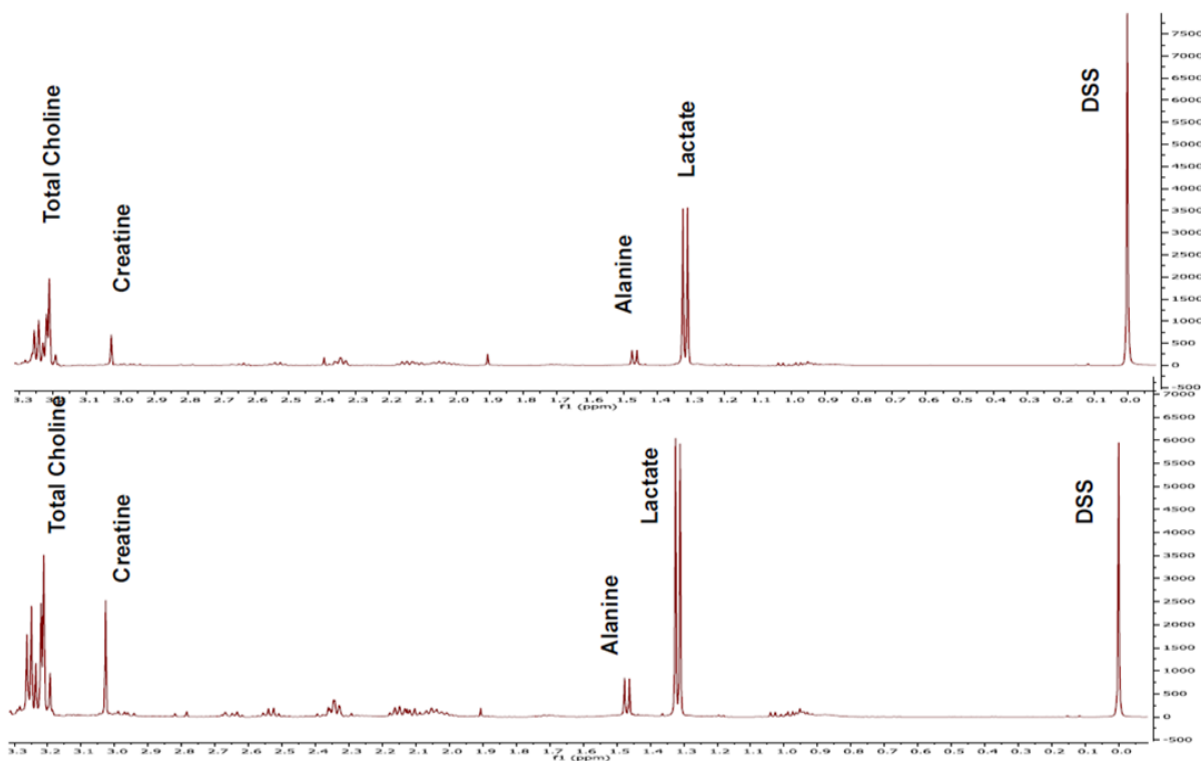


**Figure 2-5: Representative NMR spectra of tumor samples taken from the immunocompetent and immunocompromised mice**

### 2.3 Hyperpolarization Experimental Methods

20  $\mu$ L of [1- $^{13}\text{C}$ ]-enriched pyruvic acid ( Isotec, Sigma-Aldrich) samples containing 15 mM OX63 trityl radical (Oxford Instruments Molecular Biotools, Abingdon, UK) were doped with 1.0 mM concentrations of ProHance containing  $\text{Gd}^{3+}$  ions. Hyperpolarization was accomplished at 3.35 T and at the extremely low temperature of 1.4 K using a HyperSense DNP Polarizer (Oxford Instruments, Abingdon, United Kingdom). The pyruvic acid was bombarded with 94.082 GHz microwaves for approximately one hour so that the high electron spin polarization of the trityl radicals could be transferred to the nuclear spins at the  $^{13}\text{C}$  atoms in the

pyruvic acid. Since DNP must be performed in the solid state, the pyruvic acid was rapidly dissolved in Tris/EDTA and NaOH at 310.15 K, which yielded 80 mmol/L of pyruvate at a physiological pH. 200  $\mu$ L of this hyperpolarized substrate was then injected into the mouse via a catheter inserted into the tail vein. The injection typically lasted from 10 to 12 seconds and was performed with the mouse placed in the lateral decubitus position. The mouse was anesthetized with isoflurane throughout the entirety of the procedure [265].

Each  $^{13}\text{C}$  spectrum was acquired using a 7 T Bruker scanner with a 30 cm bore BioSpec magnet. This small animal scanner is shown in Figure 2-6. The scanner was equipped with a Bruker gradient and shim system BGA-12 that has maximum gradient amplitude of 200 mT/m and a rise time of 80  $\mu$ s. The linear radiofrequency coil was dual-tuned for both  $^1\text{H}$  and  $^{13}\text{C}$  and had a 36 mm inner radius.  $T_1$ -weighted proton images were taken for positioning, which were immediately followed by rapid gradient echo multiplane scout scans for localization.  $T_2$ -weighted scans were acquired in axial, coronal, and sagittal planes and subsequently used for positioning the voxel in which  $^{13}\text{C}$  spectroscopy is performed. The imaging parameters of the  $T_2$ -weighted scans were: echo time TE = 17 ms, repetition time TR = 2.5 s, 4 cm field of view, 156  $\mu$ m x 156  $\mu$ m in-plane resolution, 20° flip angle, ten 2-mm slices, and 4 averages [266].

A series of slice-selective  $^{13}\text{C}$  spectra (field-of-view 40 x 40 mm, slice thickness 8 mm on the tumor) were collected right after injection of hyperpolarized pyruvate using the spFLASH sequence. A total of 90 transients were acquired with the time delay between each transient being 2 s (total time 3 minutes). Each transient utilized a 20° flip angle of excitation pulse (Gauss pulse) and 2048 data points. Acquired data was processed both in MATLAB (MathWorks Inc., Natick, MA) and TopSpin (Bruker BioSpin GmbH, Ettingen, Germany). The dynamic spectra were manually phased and line-broadening was applied (10 Hz). The area under the spectral

peaks for pyruvate and lactate were integrated over the entire array. The normalized lactate (nLac) ratio was calculated as lactate over the sum of pyruvate and lactate signals.



**Figure 2-6: A 7 T Bruker small animal MRI scanner**

## **2.4 Statistical Methods**

To determine if statistical significance was achieved in both NMR spectroscopy and hyperpolarization experiments, we performed an unpaired, two-sample, two-tailed t-test with equal variance [267]. Significance was achieved if the p-value  $\alpha < 0.05$ . All statistical analyses were performed in Microsoft Excel (Microsoft Corporation, Redmond, WA).

## 3. Results

### 3.1 NMR Spectroscopic Data

NMR spectroscopy was performed for tumors at a later time point in tumor progression, approximately three weeks after the tumor cells had been injected into the flank of the mice. The tumors at the time of euthanasia were approximately 2 cm in diameter. Spectroscopic data were collected for ten mice in total, five of which were nude mice and five of which were C57BL/6 mice. Here, the immunocompetent C57BL/6 mice exhibited significantly higher baseline metabolic activity than the immunocompromised nude mice. This is illustrated in Figure 3-1 where the relative concentration levels of various metabolites are shown for both cohorts of mice. The vertical axis depicts relative concentration, which is a unitless quantity that characterizes the concentration of the given metabolite per unit mg of sample relative to the concentration of the added reference standard. The horizontal axis depicts some of the common metabolites that were present in the spectra. The error bars shown in this figure are the calculated standard errors for a given metabolite found in a given group of mice. In particular, we observed significantly higher relative concentrations of the following metabolites: lactate ( $p = 0.020$ ), alanine ( $p = 0.014$ ), creatine ( $p = 0.00013$ ), total choline ( $p = 0.046$ ), methionine ( $p = 0.0015$ ), glutamate ( $p = 0.018$ ), glutathione ( $p = 0.012$ ), oxaloacetate ( $p = 0.029$ ), glycine ( $p = 0.015$ ), aspartate ( $p = 0.0033$ ), and taurine ( $p = 0.012$ ).

This metabolic difference between the immunocompetent mice and the immunocompromised mice was quite drastic, as it was observed that the immunocompetent mice are more metabolically active than the immunocompromised mice by an average of 93%. In Figure 3-2, a bar graph is presented that shows the ratio of metabolic concentration for a given

metabolite between the two cohorts of mice. In this figure, each metabolite that was properly identified is shown, and one can see that the immunocompetent mice demonstrate higher baseline metabolic activity than the immunocompromised mice by a factor slightly less than two. Here, GPC is an abbreviation for sn-Glycero-3-phosphocholine, which along with phosphocholine is an important choline derivative [268].

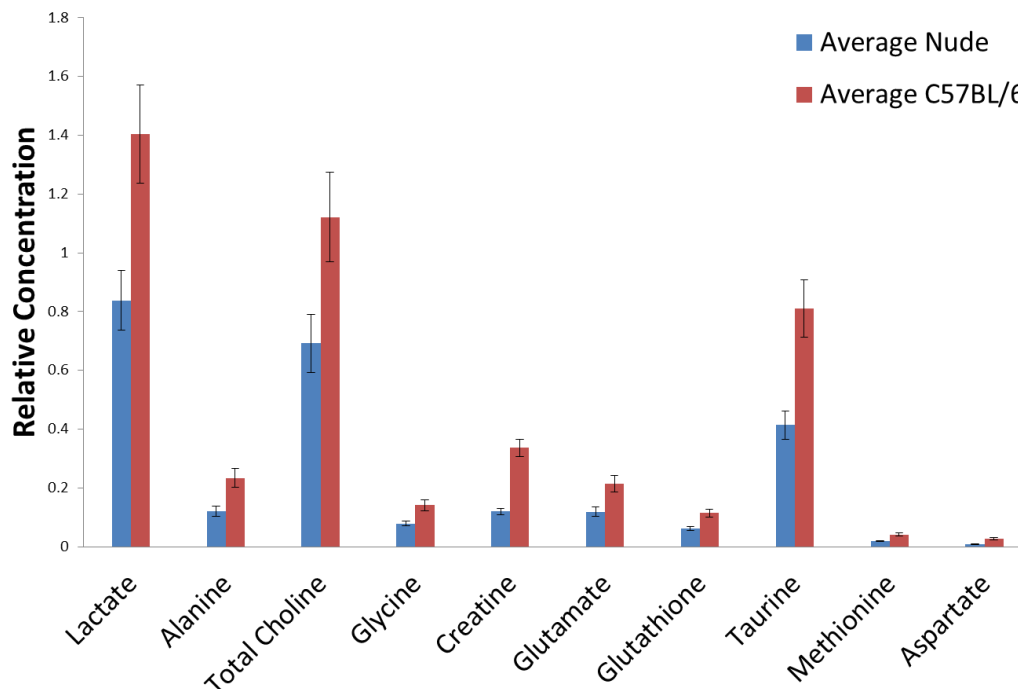


**Figure 3-1: Relative concentrations of various metabolites found in larger tumor samples**

Since there exist genomic differences between the two cohorts of mice, it was entirely possible that these metabolic differences are simply the product of these genomic differences and are not the metabolic properties of pancreatic tumors cultivated in different immune environments. Thus, a negative control experiment was performed in which the same two groups of mice, C57BL/6 and nude, were not injected with pancreatic tumors. The mice were euthanized, and healthy pancreatic tissue was resected. NMR metabolomics was then performed, and the metabolic differences seen in the pancreatic tumor tissue samples were not observed. In

fact, many metabolites were found in slightly higher concentrations in the immunocompromised mice. The only exception to this was creatine in which the immunocompetent mice exhibited significantly higher concentrations ( $p = 0.036$ ). Note, however, that this difference in creatine concentration in this negative control experiment is much less than that found in the pancreatic tumor tissue samples in which a p-value of 0.00013 was achieved. This is illustrated in Figure 3-3 where the relative concentration levels of various metabolites are shown for both cohorts of mice in this negative control experiment.

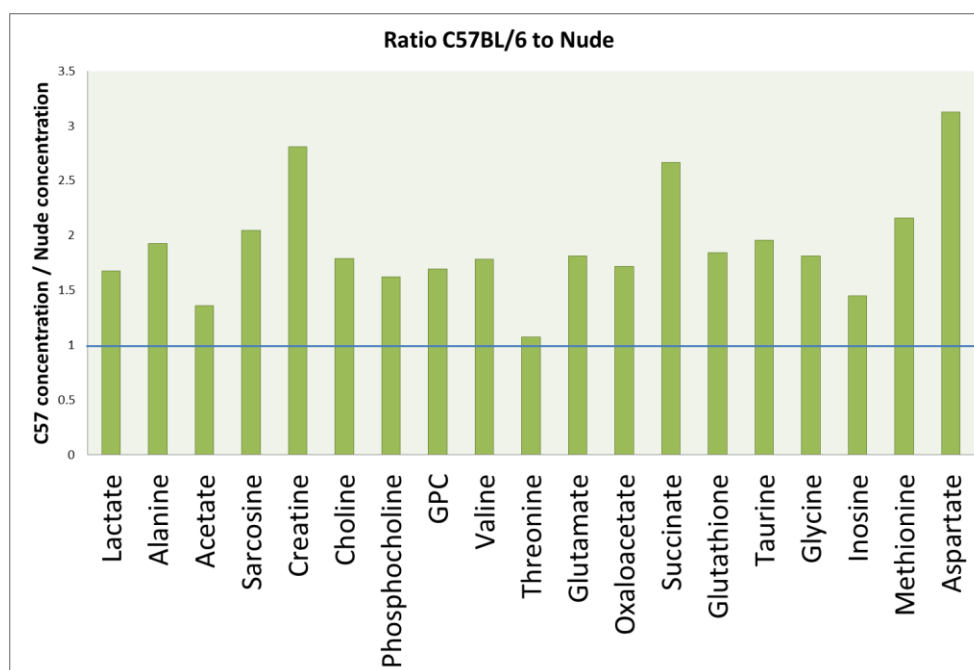


**Figure 3-2: Ratio of the relative concentrations of various metabolites found in the C57BL/6 mice to the relative concentration of various metabolites found in the nude mice to for the larger tumor samples**

These control data suggest that the metabolic differences observed are, in fact, immune-related metabolic properties of pancreatic tumors and not simply genetic differences between the breeds of mice. It should also be mentioned that the tumors from both cohorts of mice were more metabolically active than the healthy pancreatic tissue, which was to be expected.

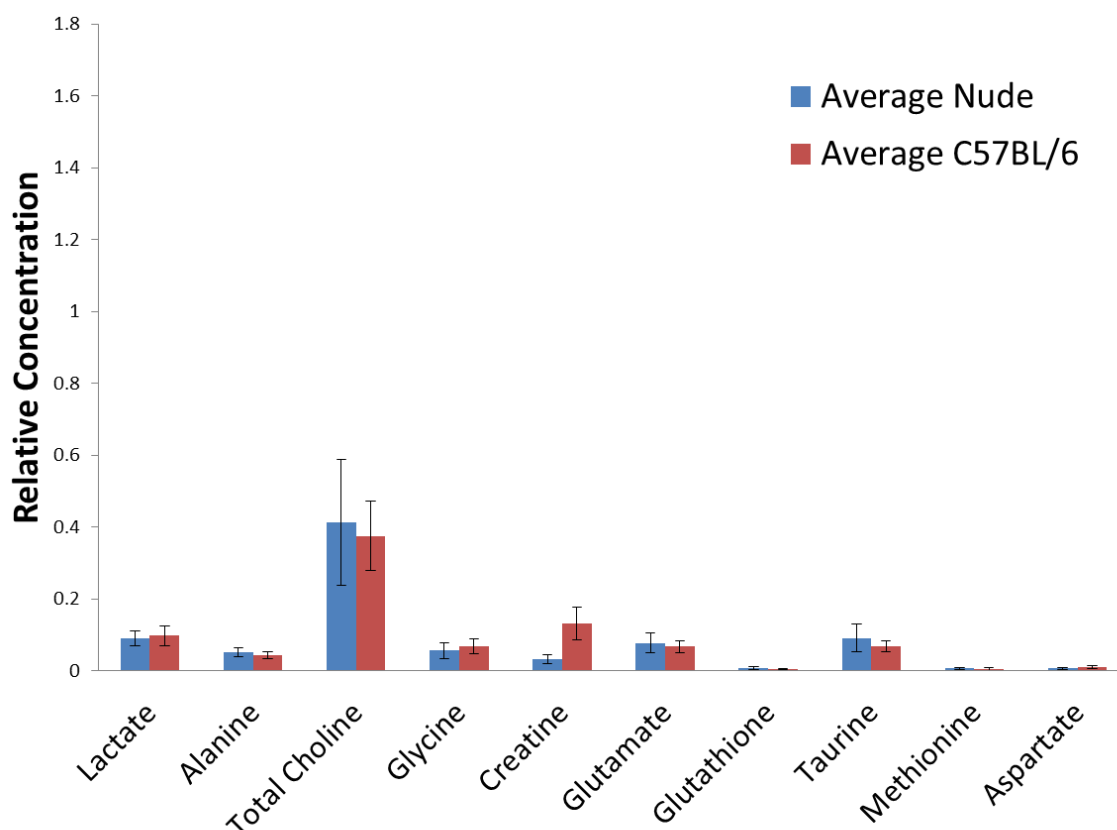


**Figure 3-3: Negative control experimental data that show the relative concentrations of various metabolites found in healthy pancreatic tissue**

These data were further validated by performing NMR metabolomics at an earlier stage in tumor progression, approximately two weeks after the tumor cells were injected into the flank of the mice. The tumors at the time of euthanasia were approximately 1 cm in diameter. Spectroscopy was performed for ten mice in total as well, five of which were nude mice and five of which were C57BL/6 mice. As in the earlier experiment, the immunocompetent C57BL/6 mice exhibited significantly higher baseline metabolic activity than the immunocompromised nude mice. Specifically, statistically significantly higher relative concentrations were observed in the C57BL/6 mice for the following metabolites: lactate ( $p = 0.0034$ ), alanine ( $p = 0.00066$ ),



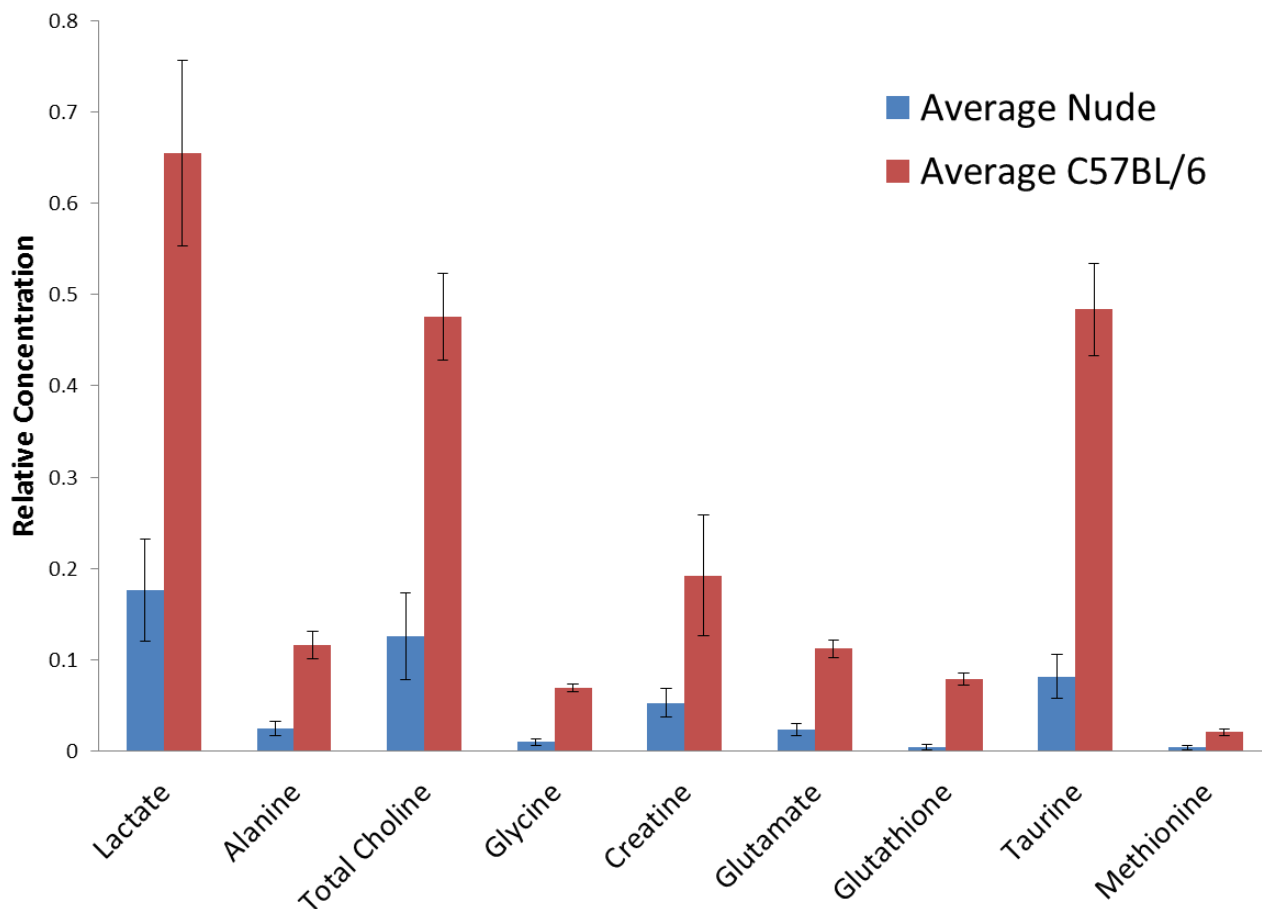


**Figure 3-4: Relative concentrations of various metabolites found in smaller tumor samples**

total choline ( $p = 0.00080$ ), valine ( $p = 0.0035$ ), succinate ( $p = 0.000024$ ), methionine ( $p = 0.0032$ ), glutamate ( $p = 0.000063$ ), glutathione ( $p = 0.0000070$ ), oxaloacetate ( $p = 0.000027$ ), glycine ( $p = 0.0000050$ ), and taurine ( $p = 0.000095$ ). The relative concentration levels of various metabolites are illustrated in Figure 3-4 for both cohorts of mice. Again, the vertical axis depicts relative concentration, while the horizontal axis lists some of the common metabolites that were found in the spectra.

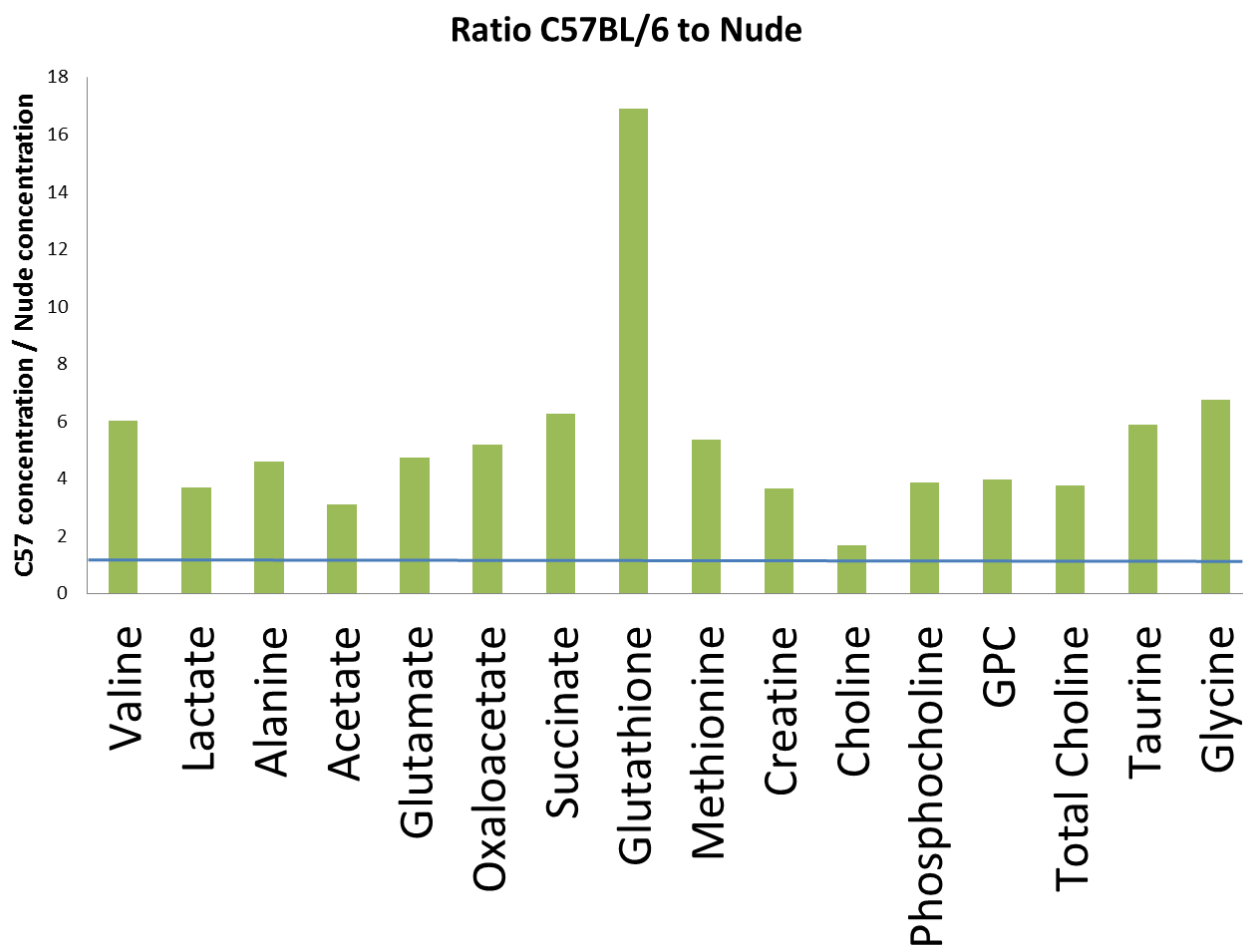


**Figure 3-5: Ratio of the relative concentrations of various metabolites found in the C57BL/6 mice to the relative concentration of various metabolites found in the nude mice for the smaller tumor samples**

The metabolic difference between the immunocompetent mice and the immunocompromised mice was even more pronounced at this earlier time point in tumor progression, as it was observed that the immunocompetent mice are more metabolically active than the immunocompromised mice by an average of 435%. In Figure 3-5, a bar graph is depicted that presents the ratio of metabolic concentration for a given metabolite between the two cohorts of mice, as in Figure 3-2. One can see that the immunocompetent mice demonstrate

higher baseline metabolic activity than the immunocompromised mice by a factor slightly greater than five.

Because lactate is so important in cancer metabolism, it should be noted that lactate concentration is higher by factors of 3.71 and 1.68 in the immunocompetent mice relative to the immunocompromised mice at the earlier and later timepoint in tumor progression, respectively.

### **3.2 Hyperpolarization Data**

In total, successful hyperpolarization data was acquired for 25 mice, 16 at the earlier time point in tumor progression, and 9 at the later time point in tumor progression. The mice imaged at the earlier time point came from two separate cohorts, 2 immunocompromised mice and 4 immunocompetent mice in the first cohort and 5 immunocompromised mice and 5 immunocompetent mice in the second cohort. Of the mice imaged at the later time point 5 were immunocompromised, and 4 were immunocompetent. In addition, an unsuccessful attempt at imaging another cohort of mice at the later time point, 3 immunocompromised mice and 3 immunocompetent mice, was made. The data from this unsuccessful experiment will not be presented in this section. However, this experiment will be mentioned further in the discussion section. In addition, the reasons why this experiment was a failure and how this failed experiment affected the progression of this project will be explored further in that section.

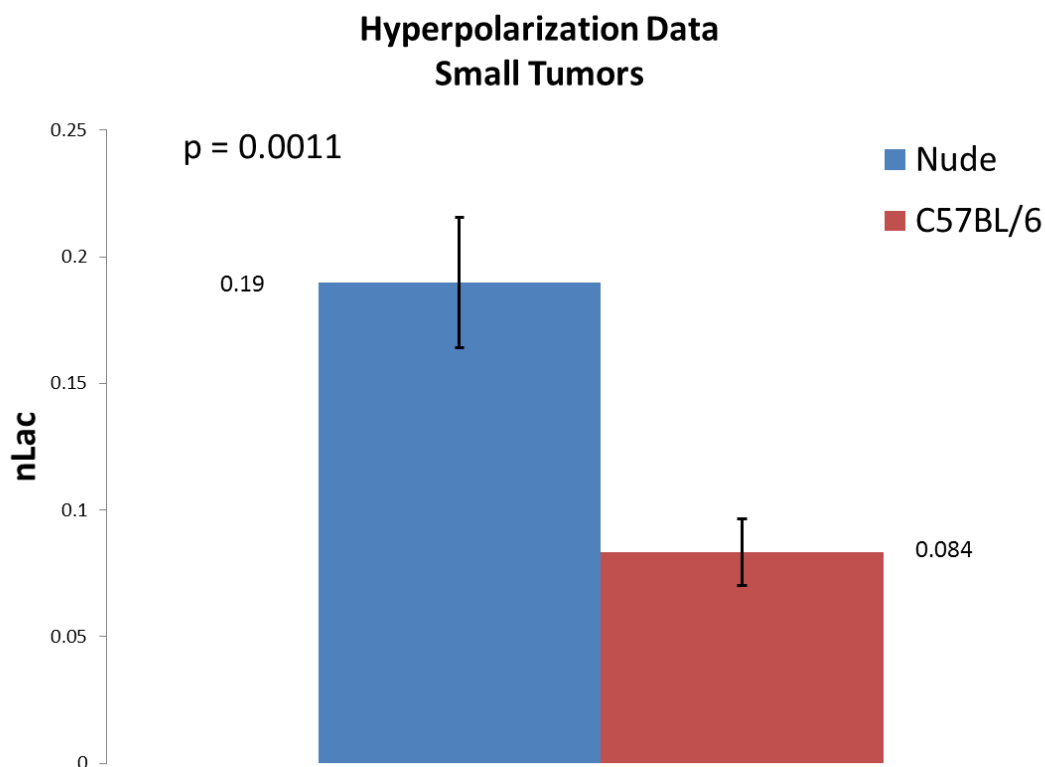


**Figure 3-6: Glycolytic dependence, smaller tumors**

For both the smaller and larger tumors it was found that the immunocompromised nude mice exhibited statistically significantly higher glycolytic dependence than the immunocompetent C57BL/6 mice. In particular, p-values of 0.0011 and 0.016 were achieved for the earlier and later time points, respectively. Here, glycolytic dependence is quantified via the metric nLac, which is defined in Equation 2 found in the introductory hyperpolarization section. Figure 3-4 and Figure 3-5 illustrate the nLac differential for the smaller and larger tumors, respectively. One should also note that glycolytic dependence increased as tumor size increased for both breeds of mice. For the smaller tumors, the hyperpolarization data were acquired using two different cohorts, so the result of each is included in the Supplementary Section at the end

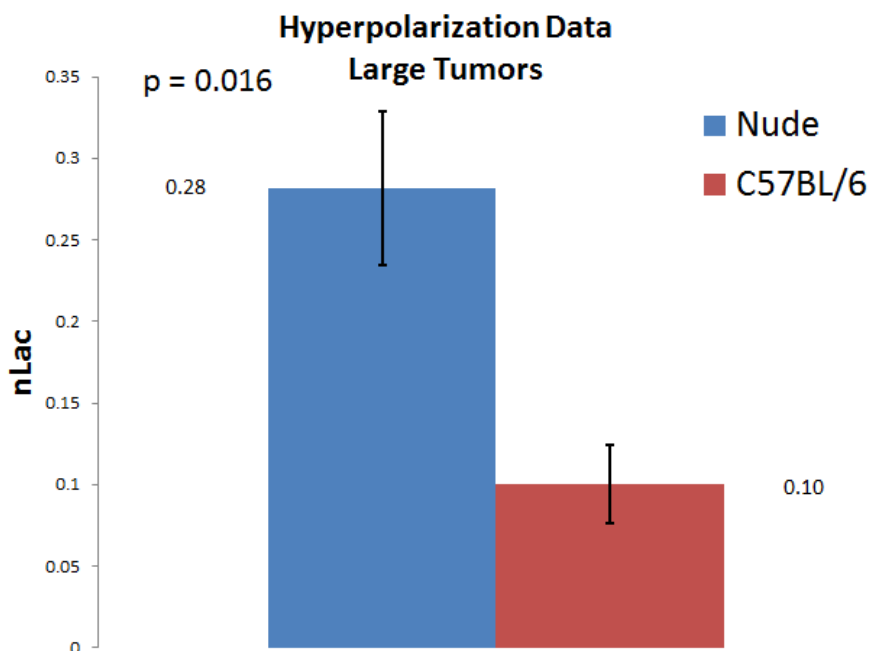
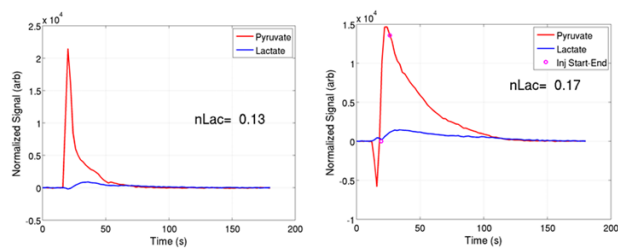


**Figure 3-7: Glycolytic dependence, larger tumors**

Nude



C57BL/6

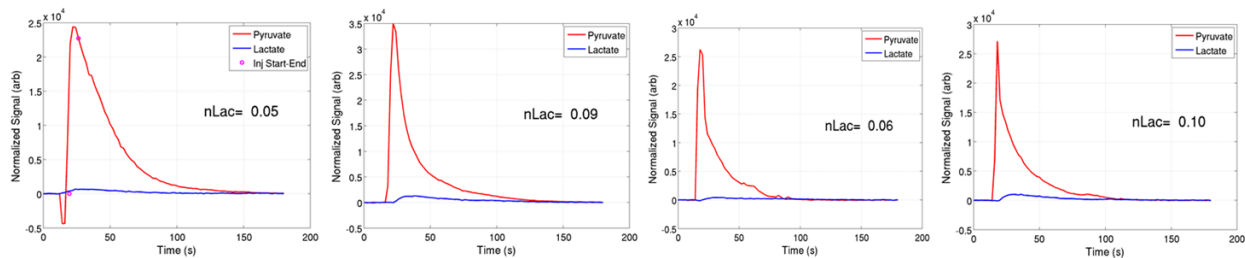


**Figure 3-8: Dynamic spectroscopy, smaller tumors, cohort 1**

## Nude

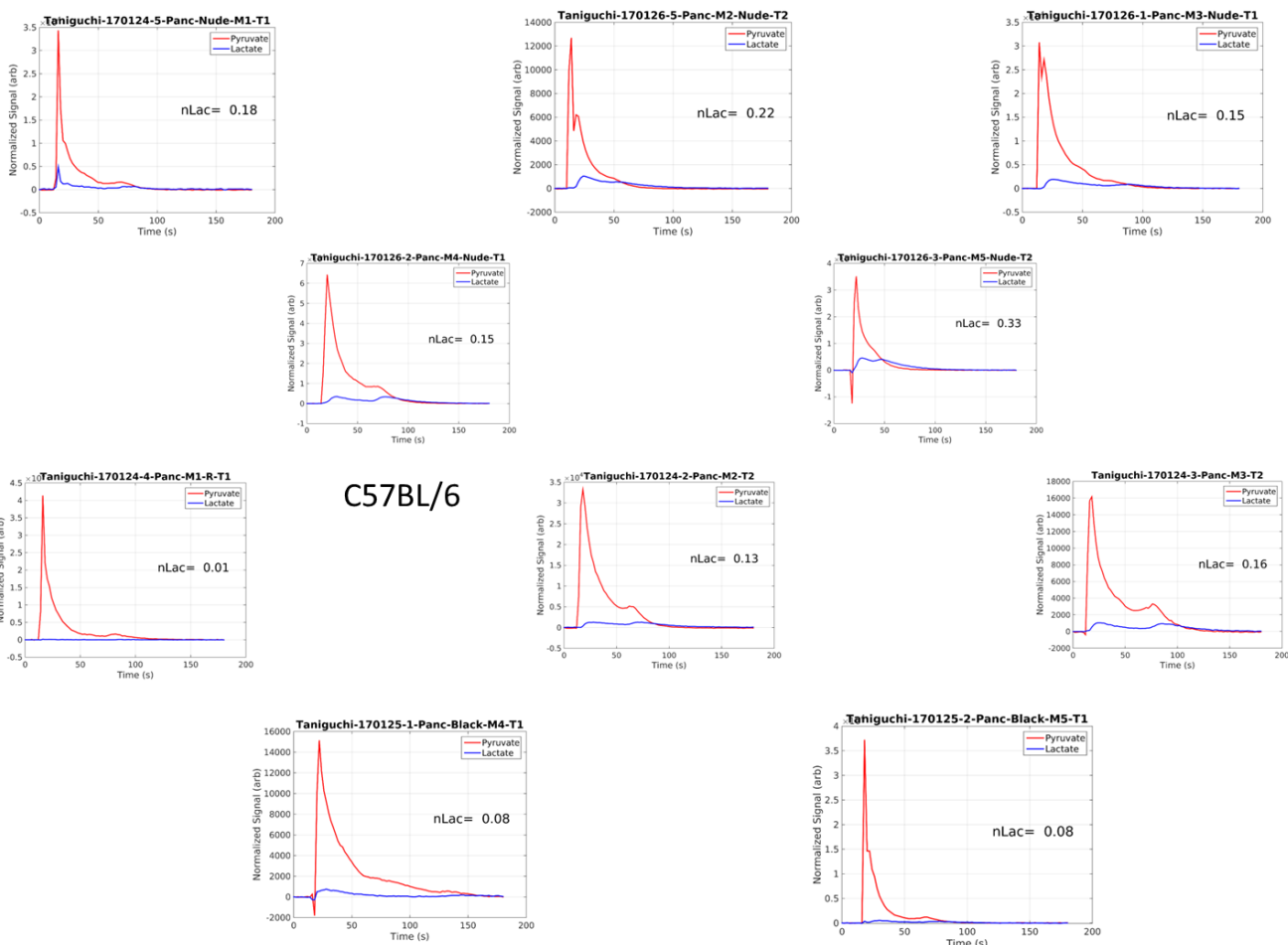
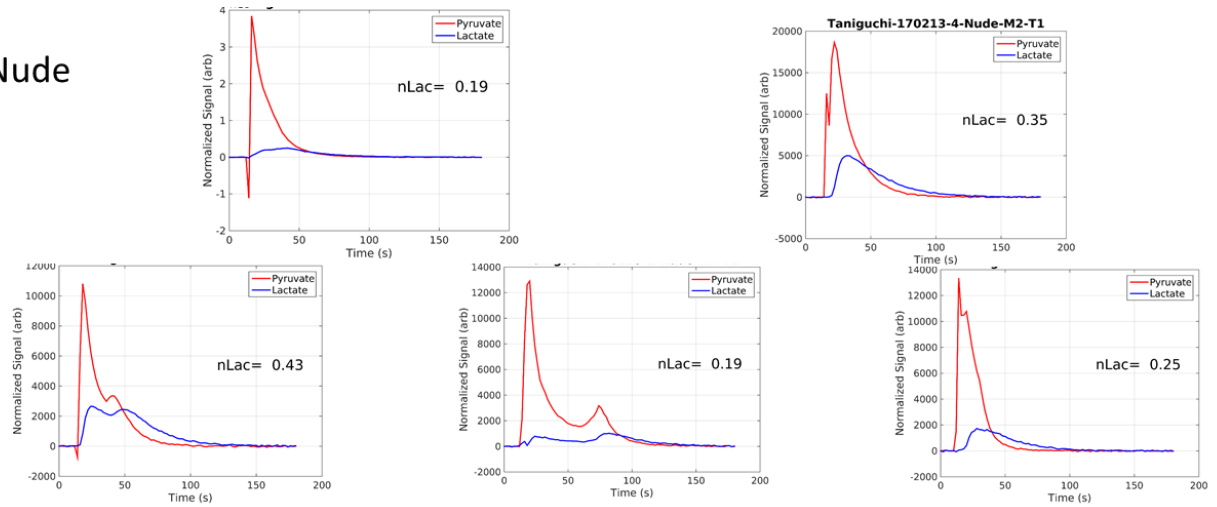


**Figure 3-9: Dynamic spectroscopy, smaller tumors, cohort 2**

of this thesis as Supplementary Figure 1 and Supplementary Figure 2. The dynamic spectra for the 25 mice successfully imaged are shown in Figure 3-8, Figure 3-9, and Figure 3-10. In these spectra, normalized signal intensity is shown on the vertical axis, and time is shown on the horizontal axis. Pyruvate is shown in red, and lactate is shown in blue. The 25 time-integrated spectra are shown in Supplementary Figure 3, Supplementary Figure 4, and Supplementary Figure 5.

Nude



C57BL/6

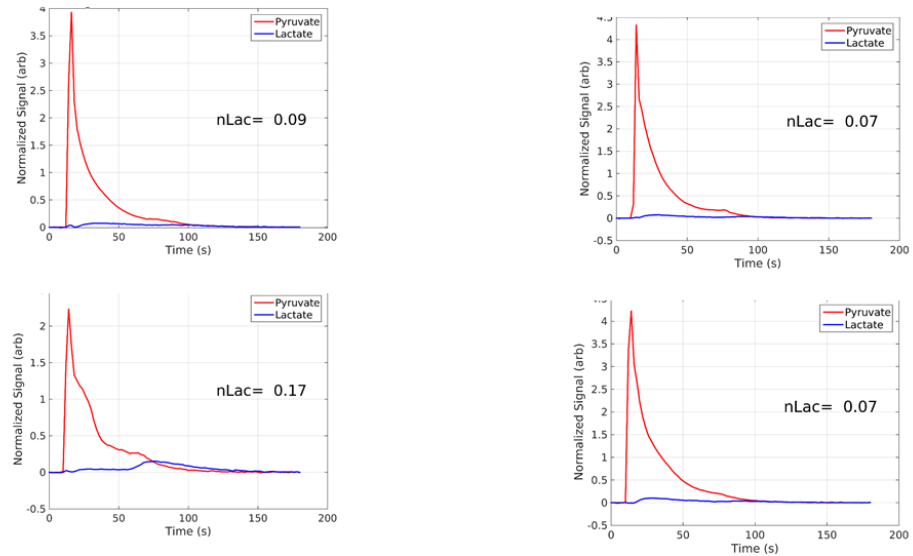


**Figure 3-10: Dynamic spectroscopy, larger tumors**

## 4. Discussion

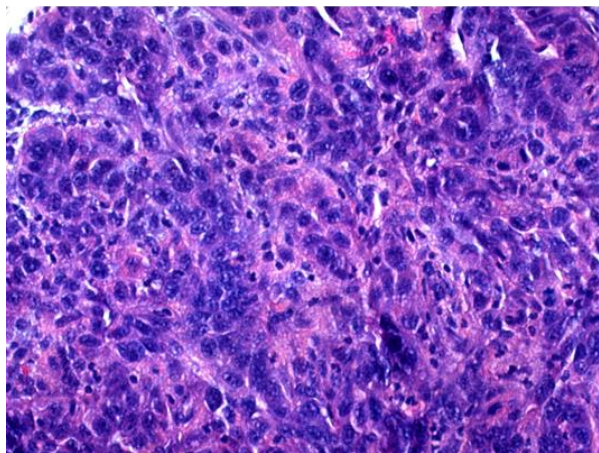
### 4.1 Histological Staining

Following the imaging experiments, the mice were euthanized, and the tumors were resected. Some of this tissue was used for NMR spectroscopy, but the rest of it was given to a

colleague who subjected it to histological staining. Histology is the study of microscopic structures such as cells and tissues [269]. The most widely employed type of histological staining experiment is the hematoxylin and eosin (H&E) stain [270]. Hematoxylin is a basic dye that stains basophilic structures purplish blue. The cellular nucleus is basophilic and is, thus, stained with hematoxylin. Eosin is an acidic dye that stains acidophilic structures red or pink. The cytoplasm and most connective tissue fibers are acidophilic and are stained with eosin.

## Smaller tumors

Immunocompetent



Immunocompromised

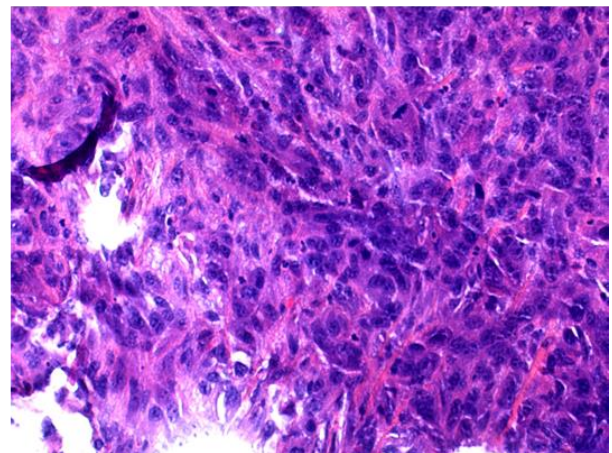


**Figure 4-1: H&E staining of tumors at the earlier time point in tumor progression**

H&E staining was performed on five tumor samples from immunocompetent mice at the earlier time point in tumor progression, five tumor samples from immunocompromised mice at the earlier time point in tumor progression, five tumor samples from immunocompetent mice at the later time point in tumor progression, and five tumor samples from immunocompromised mice at the later time point in tumor progression. Representative H&E stains from tumor samples taken at the earlier time point in tumor progression and the later time point in tumor progression



are shown in Figure 4-1 and Figure 4-2, respectively. In both of these figures, the tumors taken from the immunocompetent mice are shown on the left, and the tumors taken from the immunocompromised mice are shown on the right.

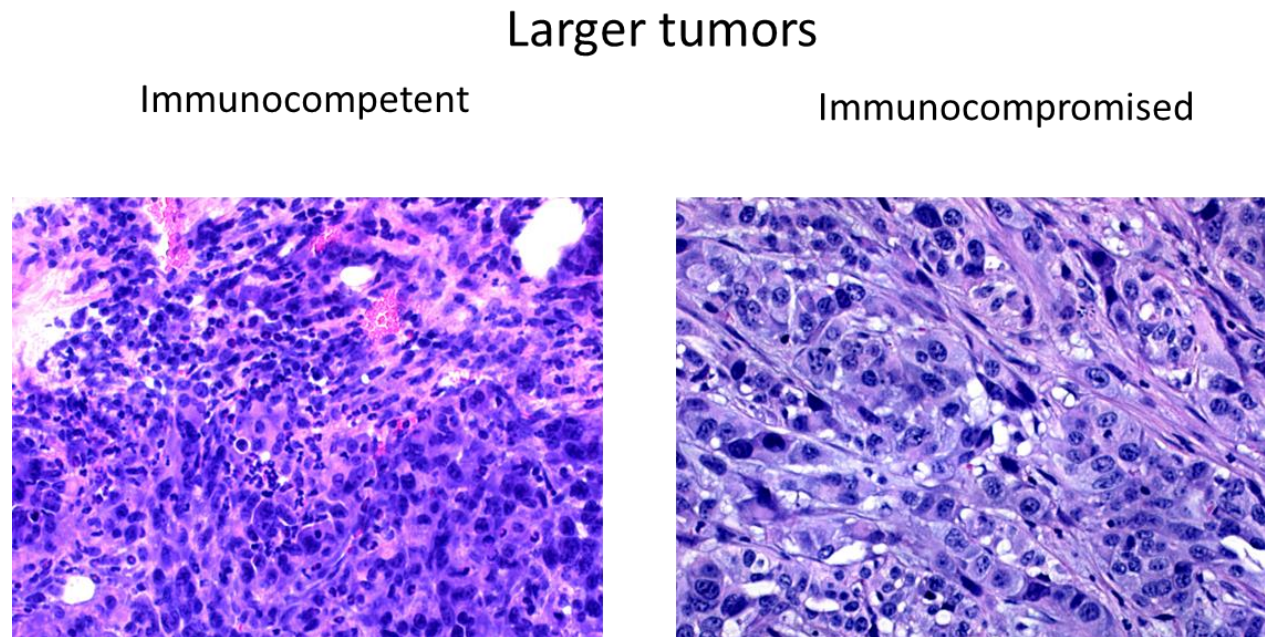


**Figure 4-2: H&E staining of tumors at the later time point in tumor progression**

One can distinguish between immune cells and cancer cells in these H&E stains by looking at their morphological features. In particular, immune cells are small and dense, while cancer cells have a large nucleus and an irregular size and shape. In the tumors taken from the C57BL/6 mice, as one would expect, we see that the immune components are very successful at infiltrating all areas of the tumor. This infiltration becomes more pronounced as the tumor becomes larger. Conversely, in the tumors taken from the nude mice, which lack the ability to produce many viable T cells, there is much less immune infiltration. This can be seen even more clearly in the color-coded H&E stains shown in Figure 4-3 and Figure 4-4. Figure 4-3 shows a stain of a tumor taken from an immunocompetent mouse at the later time point in tumor

progression, while Figure 4-4 shows a stain of a tumor taken from an immunocompromised mouse at the later time point in tumor progression. Here, immune components are shown in green, cancer cells are shown in red, and elongated stromal cells are shown in blue. In the tumor

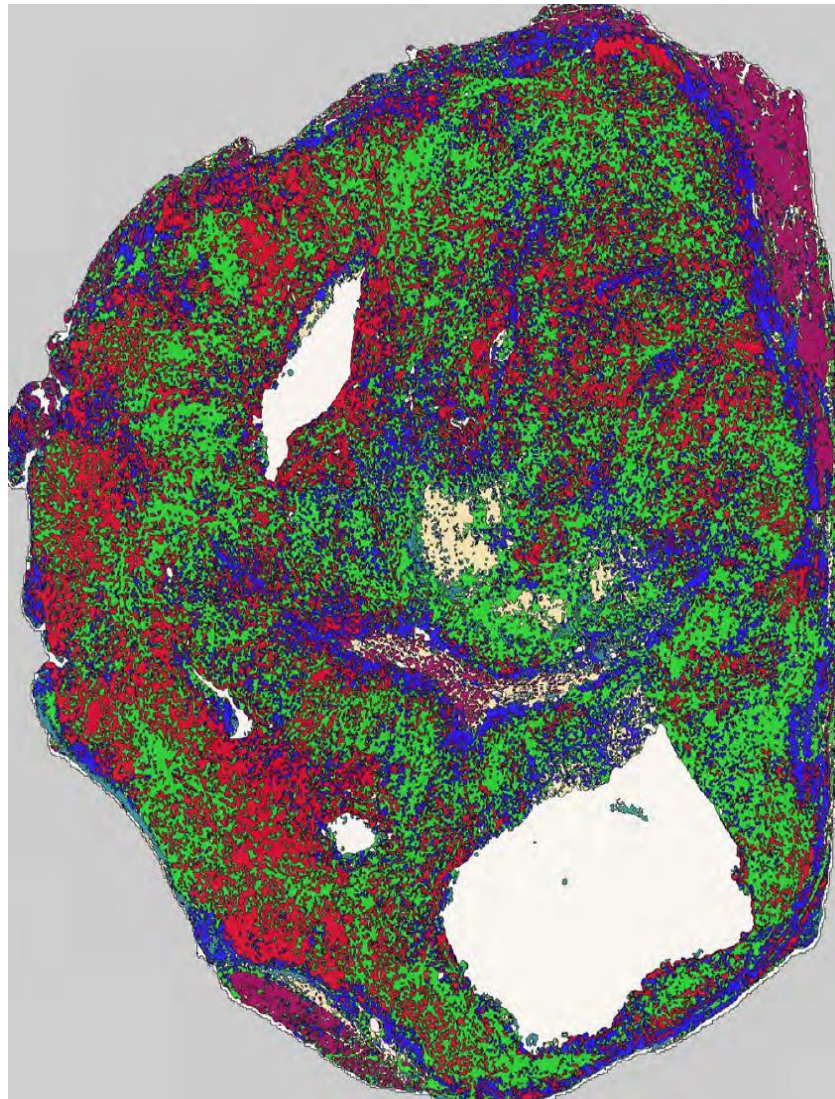


**Figure 4-3: Color coded H&E stain of a tumor taken from the immunocompetent mice**

taken from the immunocompetent mouse, the immune components clearly infiltrate all areas of the tumor, while in the tumor taken from the immunocompromised mouse, the immune



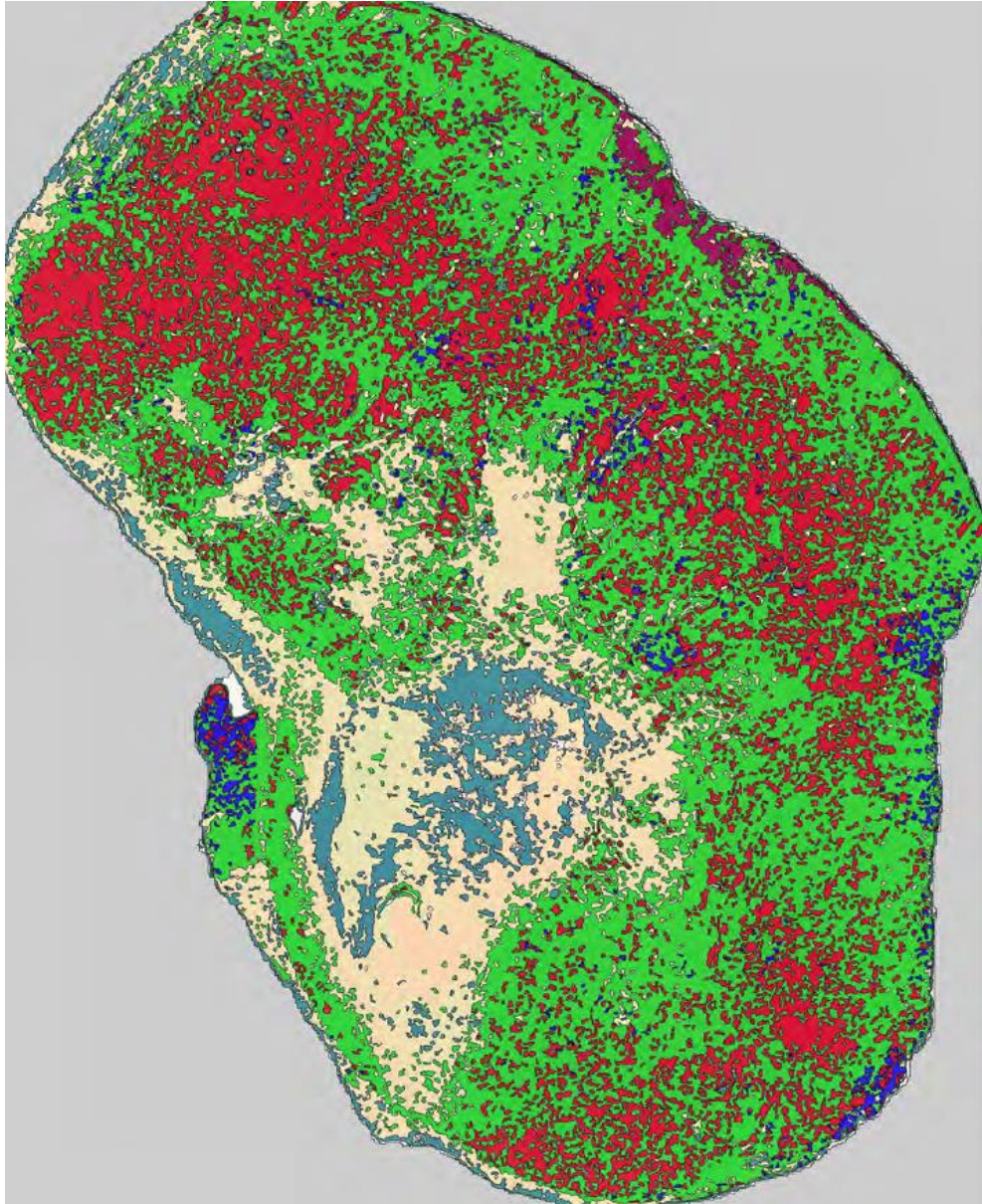


**Figure 4-4: Color coded H&E stain of a tumor taken from the immunocompromised mice**

components, which are presumably B cells, are restricted to the periphery. These observed differences in the level of immune infiltration have tremendous consequences, and these effects will be the topic of discussion in the following section.

## 4.2 The Effects of Immune Infiltration

The finding that the tumors cultivated in an immunocompetent environment exhibit higher baseline metabolic activity than in the nude mice can be explained in reference to the histological stains presented in the previous section. Tumors are typically strongly infiltrated with immune cells, and this infiltration mimics the inflammatory conditions that are seen in noncancerous tissue [271]. Thus, tumors can be thought of as wounds that never heal [272]. It is well known and, in fact, is now considered one of the hallmarks of cancer [124], that tumor cells have built-in machinery that allow them to evade this immune response. However, the problem runs deeper than this; paradoxically, the aforementioned inflammatory response induced by the immune cells actually promotes tumorigenesis and progression [273-276]. In particular, the inflammatory response adds bioactive materials to the tumor microenvironment, such as growth factors, survival factors, proangiogenic factors, and extracellular matrix modifying enzymes that promote invasion and metastasis [124,277]. In addition, inflammatory cells release mutagenic reactive oxygen species, which facilitate the tumor's genetic progression towards a greater state of malignancy [124,276].

As shown in Figure 4-1, Figure 4-2, and Figure 4-3, immune cells are successful at infiltrating the tumors cultivated in the immunocompetent mice, thus mimicking inflammatory conditions. Therefore, the tumors cultivated in the immunocompetent environment benefit from the tumorigenic properties discussed in the above paragraph. With the upregulation of growth factors, survival factors, proangiogenic factors, and mutagenic factors, it should come as no surprise that this reflected downstream as an upregulation of metabolic activity. The NMR spectroscopic data seem to suggest that the tumors cultivated in the immunocompetent background start out with a greater amount of glucose than the tumors cultivated in the

immunocompromised background since one observes an upregulation of metabolism across the board. This may be accomplished via an upregulation of glucose transporter proteins such as GLUT1, as to provide the necessary fuel required for the enhanced tumor progression induced by the inflammatory conditions. This greater initial amount of glucose present in the tumors cultivated in the immunocompetent mice would also explain why the tumors cultivated in the immunocompromised mice demonstrate a higher propensity for utilizing lactate as a glucose alternative, which is discussed in greater detail in the next section.

#### **4.3 Lactate Metabolism**

There were two major findings in this project. The first is that the tumors cultivated in the immunocompetent mice exhibit significantly higher baseline metabolic activity than the tumors cultivated in the immunocompromised mice. This was initially counterintuitive to me since I assumed that one would expect higher metabolic activity in the nude mice since tumor cells would be more successful at proliferating given that they lack an immune system. However, as discussed above, the immune components located in the tumor microenvironment, which are present in the C57BL/6 mice but missing in the nude mice, allow the tumor to mimic an inflamed state. This inflammation promotes tumorigenesis by supplying growth factors, survival factors, and proangiogenic factors to the tumor microenvironment, which is reflected downstream as upregulated metabolic activity relative to a system in which these immune components are missing.

The second major finding of this project is that the tumors cultivated in the immunocompromised mice displayed a greater level of glycolytic dependence than the tumors

cultivated in the immunocompetent mice. At first glance these two findings seem to clash with one another. How is it possible that one observes significantly higher pyruvate-to-lactate conversion in one group but a significantly higher lactate pool size in the other? This is extremely exciting, however, as it proves that additional information can be garnered via the implementation of real-time dynamic spectroscopic imaging with hyperpolarized pyruvate. Here, it can clearly be seen that the dynamic spectroscopic data are not simply redundantly corroborating the *ex vivo* data acquired using more conventional static spectroscopic techniques. Thus, the implementation of dynamic spectroscopic imaging with hyperpolarized pyruvate in patients will add undeniable value to the clinic, augmenting the radiologist's ability to study metabolic dysregulation in tumors. Whether this augmentation justifies the cost of DNP systems and outweighs the additional challenges introduced remains to be seen. It should also be clearly noted that hyperpolarization and NMR spectroscopy are measuring different things. Namely, hyperpolarization is measuring a dynamic metabolic flux in real-time, while NMR spectroscopy is simply looking at a static snapshot of tumor metabolism. Information about where a given metabolite came from cannot be discerned from NMR spectroscopy; one measures only a static pool size.

The lack of correlation between the *in vivo* data and the *ex vivo* data certainly came as a surprise. Firstly, this is due to the unpublished data acquired in our laboratory studying a different cancer system that showed a direct correlation between nLac and lactate pool size in pancreatic tumors of varying aggressiveness. Also, historically, lactate is often viewed as a dead-end waste product of glycolytic metabolism [278]. This is not the case, however, as lactate can serve as an alternative to glucose as a carbohydrate fuel source in both cancerous cells [279-281] and noncancerous cells [282] alike. It has been shown that the tumors in the

immunocompromised mice exhibit significantly lower baseline metabolic activity than the tumors in the immunocompetent mice. Thus, it is probable that the tumors in the immunocompromised mice take up less glucose than their immunocompetent counterparts, given that one observes smaller pool sizes of glucose's byproducts in the tumors in the immunocompromised mice. Having less glucose available from the beginning, it would make sense that the tumors in the immunocompromised mice would have a higher propensity for utilizing the available lactate. In 1985, Brooks introduced the lactate shuttle hypothesis, in which he contended that lactate metabolism is a critically important component in the integration and regulation of intermediary metabolism [283]. Further research has elucidated two distinct mechanisms [284] through which lactate can be metabolized: the cell-cell lactate shuttle [285,286] and the intracellular lactate shuttle [287,288].

The cell-cell lactate shuttle is a mechanism through which lactate leaves a glycolytic cell and is shuttled into another. It has long been understood in the context of exercise [289,290]. Because of its large mass and its high metabolic activity, skeletal muscle is the major utilizer of the cell-cell lactate shuttle [291]. Namely, white muscle fibers produce lactate and transport it into the blood [292]. The monocarboxylate transporters (MCTs) constitute a family of membrane transport proteins that shuttle monocarboxylates, such as pyruvate and lactate, across biological membranes [293,294]. Lactate is shuttled out of the glycolytic muscle cells via the transporter MCT4 and shuttled into erythrocytes via the transporter MCT1 [295]. In addition to the red blood cells, the heart and the brain have also been shown to consume lactate [296-298]. More recently, it has been demonstrated that this mechanism is exploited in cancer in which glycolytic tumor cells transport lactate to either oxidative tumor cells or endothelial cells lining tumor blood vessels [299]. Analogously to the mechanism described above, MCT4 mediates the movement of

lactate out of the glycolytic tumor cells, and MCT4 mediates the deposition of lactate into the oxidative tumor cells [279]. Here, the oxidative tumor cells have been shown to utilize the lactate as their main source of metabolic fuel [300].

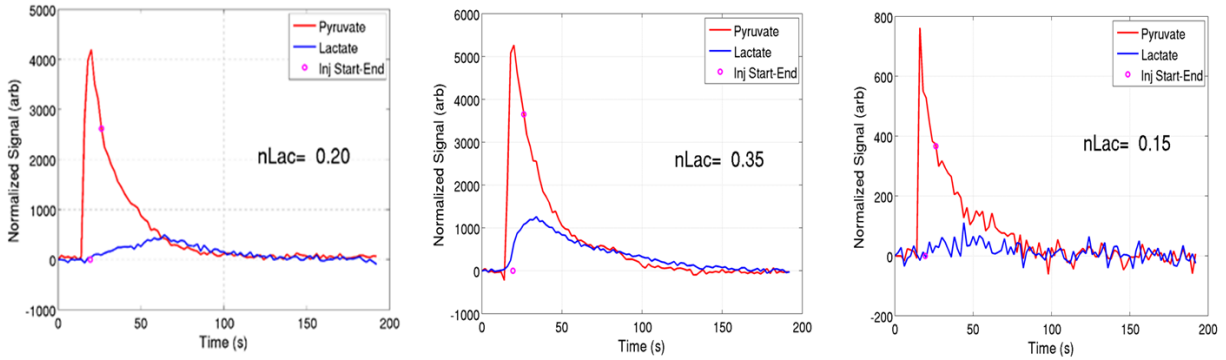
The intracellular lactate shuttle describes the process through which lactate is back converted into pyruvate [301]. Enzyme-mediated kinetics exhibit a strong concentration dependence, and the pyruvate-to-lactate forward conversion is typically more favorable than the lactate-to-pyruvate back conversion [302]. However, pyruvate is taken up by the mitochondria to be further metabolized via the tricarboxylic acid (TCA) cycle [303], while lactate is not. Thus, if one looks at the mitochondria as a pyruvate sink, then at the interface of the cytosol and the plasma membrane of the mitochondria the ratio of the concentration of lactate to the concentration of pyruvate is unusually high. Thus, the lactate-to-pyruvate back conversion, which is mediated by the enzyme lactate dehydrogenase B [304] (LDHB), becomes more kinetically favorable in this subcellular region<sup>300</sup>. Being in its immediate vicinity, this newly created pyruvate can then be taken up by the mitochondria and driven through the TCA cycle [305]. Thus, through both the cell-cell lactate shuttle and the intracellular lactate shuttle, one sees that lactate cannot be thought of as simply a dead end waste product of glycolytic metabolism and can, instead, be utilized as an alternative to glucose to fuel further downstream metabolism. Whether or not this is what is happening in these tumors will need to be verified in future studies.



## 4.4 Problems and Pitfalls

Science often progresses along a circuitous path, and this project was certainly no exception. As was mentioned previously, the biggest drawback of dynamic spectroscopic imaging with hyperpolarized pyruvate is that the hyperpolarized signal decays rapidly. Namely, the characteristic  $T_1$  decay of the hyperpolarized pyruvate is typically on the order of tens of seconds to minutes. Thus, the successful implementation of this technique relies on the assumption that the pyruvate can be delivered to the tumor in a time that is short relative to the  $T_1$  of the hyperpolarized pyruvate. This assumption can be violated when the tumor is poorly vascularized.

### Nude



### C57BL/6

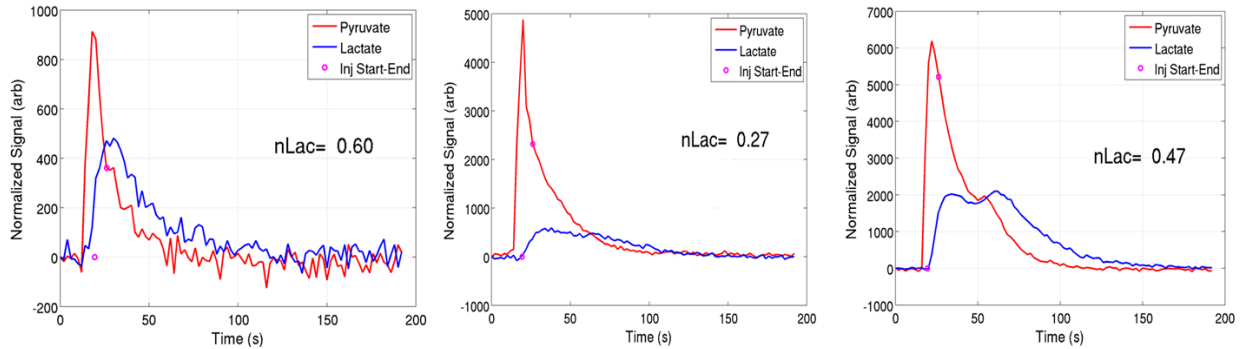


**Figure 4-5: Dynamic spectroscopy, failed experiment due to low SNR**

Poor vascularization hampered many of the experiments from this project, since some of the tumors were extremely necrotic at later stages of tumor progression. When this happens, no spectroscopic signal is observed after the injection of pyruvate. Luckily, these experiments were performed on animal subjects, so in the event of a failed injection, we were able to simply keep the mouse anesthetized and on the scanner for a repeat experiment. However, as this technology is implemented into the clinic, a more effective method to deliver the pyruvate to poorly vascularized tumors may need to be developed.

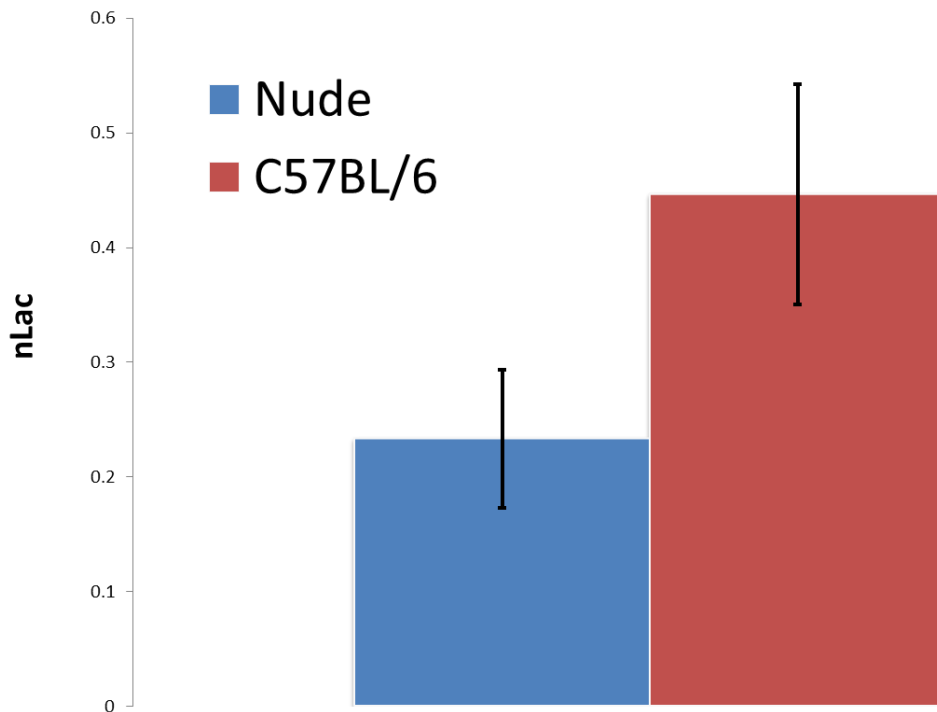


**Figure 4-6: Glycolytic dependence, failed experiment due to low SNR**

This issue not only was a nuisance; it shaped the entire course of this project. The first hyperpolarization experiment that was performed has not been shown above, since the data are not reliable. Because the large tumors were extremely necrotic, the pyruvate had difficulty perfusing to the tumor, and the signal-to-noise (SNR) ratio of the experiments was unacceptably

low. The acquired dynamic spectra are shown in Figure 4-5, where one can see extraordinarily low SNR in the third nude mouse and the first C57BL/6 mouse. As can be seen in Figure 4-6, these data suggest that the immunocompetent mice exhibit higher glycolytic dependence than the nude mice. To counteract these SNR issues, the next set of hyperpolarized experiments were performed at an earlier time point in tumor progression. At this time point, the tumors were small, and necrosis was not as much of an issue. Here, the SNR issues were circumvented, but a reversal of the previous result was observed, as the nude mice exhibited higher glycolytic dependence than the immunocompetent mice. These seemingly contradictory results led to the hypothesis that the immune-related metabolic properties of pancreatic tumors displayed temporal dependence with respect to tumor development. Later, more rigorous experiments disproved this hypothesis and showed that both NMR metabolomics experiments and hyperpolarization experiments largely did not depend on time with respect to tumor development. However, this line of reasoning explains why each experiment done in this project was repeated both at an earlier time point and a later time point in tumor development.

#### **4.5 Future Direction**

As discussed previously, the main finding of this project was that the pancreatic tumors cultivated in the immunocompetent setting exhibited significantly higher baseline *ex vivo* metabolic activity than the pancreatic tumors cultivated in the immunocompromised setting, while the pancreatic tumors cultivated in the immunocompromised setting demonstrated a significantly higher glycolytic conversion flux *in vivo* than the pancreatic tumors cultivated in the immunocompetent setting. Because this result was completely unexpected, it generated many new questions to ask and avenues to explore in order to further elucidate how the immune

environment affects pancreatic tumor metabolism. In Section 4.3, the two major mechanisms through which lactate is metabolized were discussed. To interrogate the relative importance of the cell-cell lactate shuttle, we will use antibodies to stain for both MCT4 and MCT1. Similarly, to interrogate the relative importance of the intracellular lactate shuttle, we will use an antibody to stain for LDHB. Also, the NMR metabolomics data suggests that the tumors cultivated in the immunocompetent environment may take up more glucose than the tumors cultivated in the immunocompromised environment. To test this possibility, we will also stain the tumors for glucose transporter 1 (GLUT1), a proteins that mediates the uptake of glucose into cells [306].

As shown in Section 4.1, the tumors cultivated in the immunocompetent environment are heavily infiltrated by immune cells. On one hand, as has been discussed, the heavy infiltration of immune cells seen in the immunocompetent mice initiates tumor-promoting inflammatory conditions. On the other hand, T cell activation has its own metabolic demands, as it has been shown that mitogenic-stimulated T cell activation is accompanied by an increase in glucose utilization [307-311]. Thus, when performing NMR spectroscopy on these samples, one cannot determine the relative contributions to the metabolic profile by the immune cells and the cancer cells. Thus, to determine the metabolic signature of each cell type, we will employ flow cytometry to separate the two cell types and will perform NMR spectroscopy on each.

There are multiple types of T lymphocytes located in the tumor microenvironment of the pancreatic tumors cultivated in the C57BL/6 mice. As described in Section 1.2, CD4<sup>+</sup> T cells, also known as helper T cells, aid in the activation of B and T lymphocytes and induce B and T cell proliferation [97]. CD8<sup>+</sup> T cells, also known as cytotoxic T cells [312], directly attack and kill antigens [98]. It would be advantageous to determine how each type of T cell contributes to the metabolic function of the tumor. This can be accomplished by inactivating a given type of T

lymphocyte while keeping other types active. Inactivation of specific T cell types can be accomplished in one of two ways. *In vivo* T cell depletion can be accomplished via an intraperitoneal administration of monoclonal antibodies [313]. Alternatively, one can use CD4 or CD8 knockout mice [314], in which the mouse's genome has been altered to suppress the expression of the genes that encode for the proteins utilized by helper T cells or cytotoxic T cells, respectively. Thus, the CD4 knockout blocks helper T cell development, and the CD8 knockout blocks cytotoxic T cell development. The contribution to the metabolic function of a tumor by a given T cell type will be ascertained by inactivating that specific T cell type and performing *in vivo* hyperpolarization experiments and *ex vivo* NMR spectroscopic experiments.

Lastly, we will continue to work on a project studying how the microbiome influences the efficacy of immunotherapy in pancreatic cancer. Shortly after one's birth the human intestinal tract is colonized by nearly 100 trillion commensal microorganisms [315-325]. Astonishingly, the number of bacteria living in one's gut is greater than the number of eukaryotic cells in the body [326,327]. This microbiome is known to affect the host immune system since these microbial communities in one's gut co-evolve with the immune system [328]. Specifically, it has been shown that the composition of the intestinal microbiota alters the balance between interleukin-17-producing effector T helper cells and Foxp3<sup>+</sup> regulatory T cells [329,330]. In our experiments, the microbiome is modulated by isolating the mice in a gnotobiotic facility, which implies that they are kept in a germfree environment [331]. These mice are then treated with immunotherapeutic agents, and the tumors are resected following euthanasia. These samples are then subjected to NMR spectroscopy for metabolic analysis in order to assess the efficacy of the immunotherapy.

## 5. Conclusion

Pancreatic cancer has an extremely high associated morbidity, due in part to the fact that it is resistant to both radiotherapy and many of the chemotherapeutic agents that are available in the clinic. Immunotherapy, on the other hand, has exhibited tremendous success in treating melanoma and various other forms of cancer, so it had been hoped that immunotherapy would be equally successfully implemented into pancreatic cancer. Unfortunately, this has not been the case. There is an initiative that aims to try to understand from a more mechanistic perspective why immunotherapy is not effective in treating pancreatic cancer. This, however, is an extremely complex problem that must be attacked from a variety of angles. Because metabolic dysregulation is a hallmark of malignant cells and because metabolomics is downstream from genomics and proteomics, it is advantageous to better understand how the immune system alters the metabolic function of a pancreatic tumor.

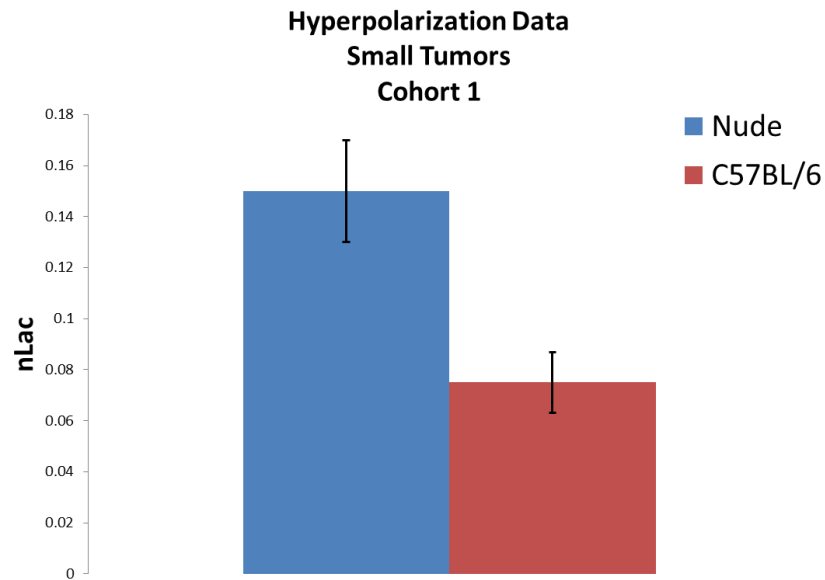
We have shown that the immune environment in which a pancreatic tumor is harvested strongly affects its metabolic expression. In particular, we have shown that pancreatic tumors cultivated in mice with a functioning immune system exhibit significantly higher baseline metabolic activity than pancreatic tumors cultivated in nude mice that lack the ability to produce viable T cells. The histological stains of these tumors indicate a high level of immune infiltration in the samples taken from the immunocompetent mice and much lower levels of immune involvement in the samples taken from the immunocompromised mice. The higher levels of immune infiltration seen in the tumors taken from the immunocompetent mice mimic the inflammatory conditions observed in wound healing. Inflammation is known to supply bioactive molecules to the tumor microenvironment. This phenomenon is reflected downstream as an

upregulation of metabolic activity, as observed here as larger static metabolite pool sizes in the NMR spectroscopic analysis of the tumor tissue samples.

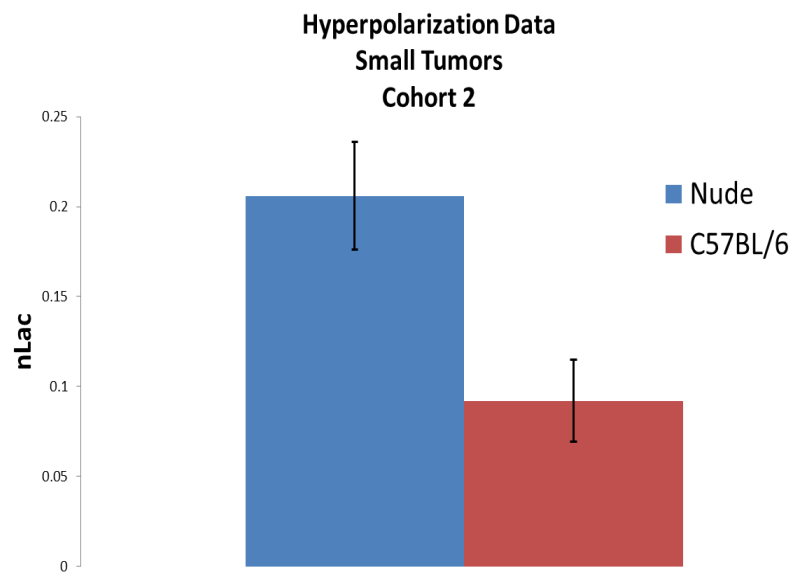
In addition, we have shown that the tumors cultivated in the immunocompromised setting demonstrate a significantly higher pyruvate-to-lactate conversion flux than the tumors cultivated in the immunocompetent setting. This measurement combined with the fact that the static lactate pool size is significantly smaller in the tumors cultivated in the immunocompromised mice relative to the tumors cultivated in the immunocompetent mice implies that the immunocompromised mice must further metabolize lactate somehow. Future histological stains will elucidate the relative importance of the cell-cell lactate shuttle and the intracellular lactate shuttle in pancreatic tumor metabolism.

Ultimately, this project has illustrated the delicate interplay between immunology and pancreatic cancer metabolic expression. In particular, the immune environment in which a pancreatic tumor is harvested strongly affects its metabolic signature, as this study has identified clear biomarkers that can facilitate the assessment of metabolic changes between immunocompromised and immunocompetent pancreatic tumors. Because cancer cells exhibit a significant increase in metabolic activity relative to normal tissue, an understanding of the metabolic function of tumors in systems with different levels of immunocompetence serves as a critical first step to develop an understanding of the immune-related metabolic properties of the tumor, which have potential application in assessing a tumor's response to immunotherapy.

## 6. Supplementary Section



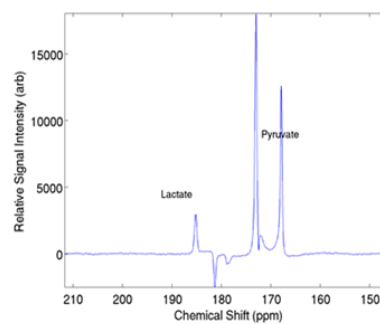
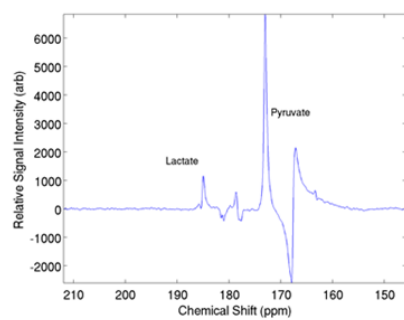
Supplementary Figure 1: Glycolytic dependence, small tumors, cohort 1



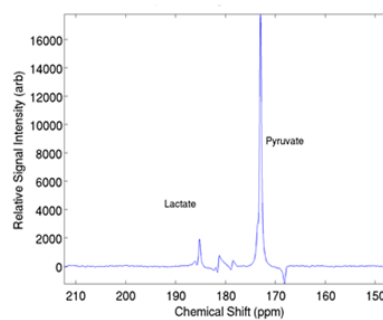
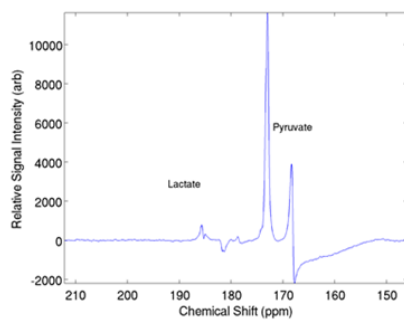
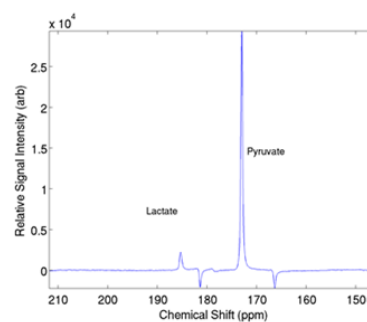
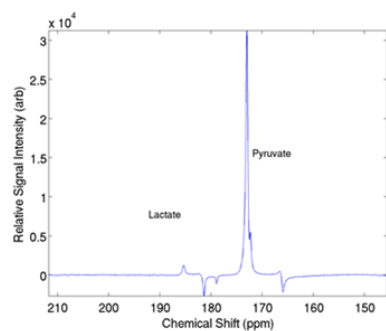
Supplementary Figure 2: Glycolytic dependence, small tumors, cohort 2



Nude

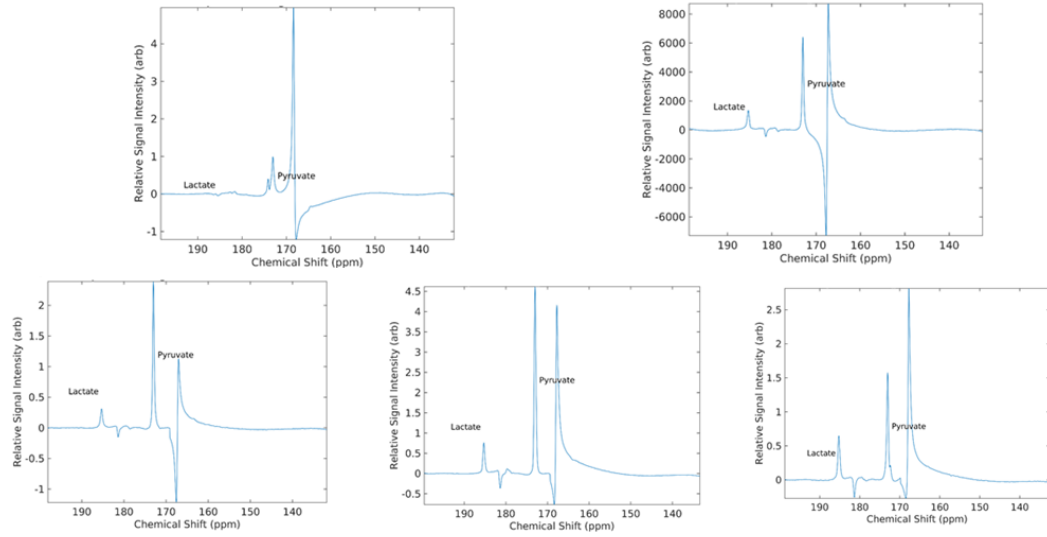


C57BL/6

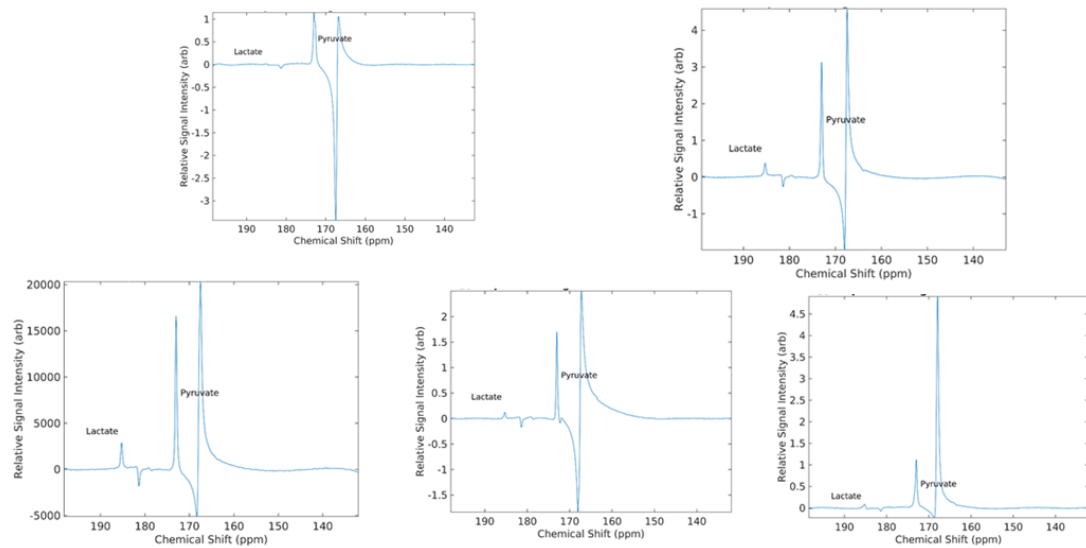


**Supplementary Figure 3: Time-integrated spectra, small tumors, cohort 1**

Nude

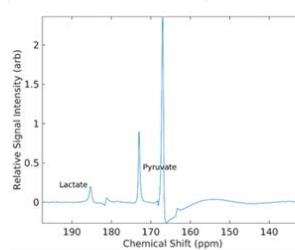
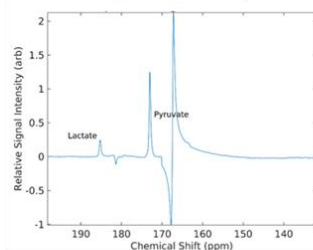
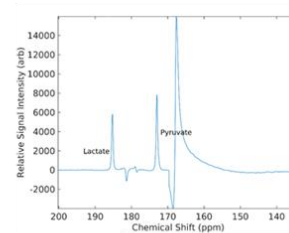
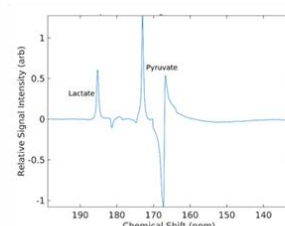
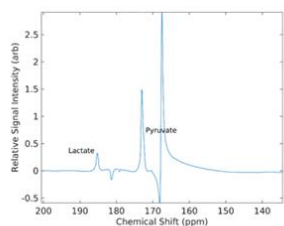


C57BL/6

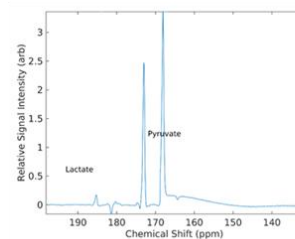
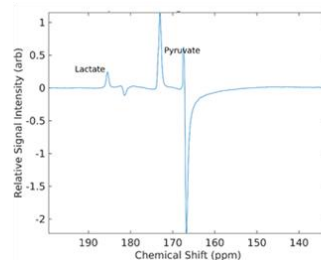
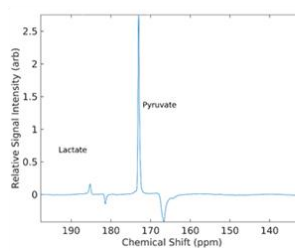
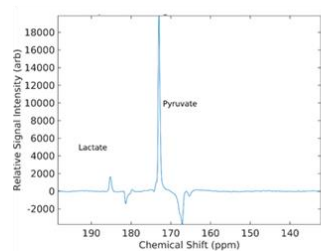


**Supplementary Figure 4: Time-integrated spectra, small tumors, cohort 2**

Nude



C57BL/6



**Supplementary Figure 5: Time-integrated spectra, large tumors**

## 7. Citations

1. American Cancer Society. Cancer Facts & Figures, 2015. Atlanta, Georgia: American Cancer Society; 2015.
2. Cameron JL, Crist DW, Sitzmann JV, Hruban RH, Boitnott JK, Seidler AJ, Coleman J. Factors influencing survival after pancreaticoduodenectomy for pancreatic cancer. *The American Journal of Surgery*. 1991; 161: 120-125.
3. Lopes RB, Gangeswaran R, McNeish IA, Wang Y, Lemoine NR. Expression of the IAP protein family is dysregulated in pancreatic cancer cells and is important for resistance to chemotherapy. *International Journal of Cancer*. 2007; 120: 2344-2352.
4. Scanlon VC, Sanders T. *Essentials of Anatomy and Physiology*. 5 ed., 2007; Philadelphia: F.A. Davis Company.
5. Fléjou JF, Potet F, Molas G, Bernades P, Amouyal P, Fékété F. Cystic dystrophy of the gastric and duodenal wall developing in heterotopic pancreas: an unrecognized entity. *Gut*. 1993; 34: 343-347.
6. Kahl S, Malfertheiner P. Exocrine and endocrine pancreatic insufficiency after pancreatic surgery. *Best Practices and Research Clinical Gastroenterology*. 2004; 18: 947-955.
7. Orci L, Unger RH. Functional subdivisions of islets of Langerhans and possible role of D cells. *The Lancet*. 1975; 306: 1243-1244.

8. Cherrington AD, Chiasson JL, Liljenquist JE, Jennings AS, Keller U, Lacy WW. The role of insulin and glucagon in the regulation of basal glucose production in the postabsorptive dog. *The Journal of Clinical Investigation*. 1976; 58: 1407-1418.
9. Hansen AP, Johansen K. Diurnal patterns of blood glucose, serum free fatty acids, insulin, glucagon and growth hormone in normal and juvenile diabetics. *Diabetologia*. 1970; 6: 27-33.
10. Pfeifer MA, Halter JB, Porte D Jr. Insulin secretion in diabetes mellitus. *The American Journal of Medicine*. 1981; 70: 579-588.
11. Maruyama H, Hisatomi A, Orci L, Grodsky GM, Unger RH. Insulin within islets is a physiologic glucagon release inhibitor. *The Journal of Clinical Investigation*. 1984; 74: 2296-2299.
12. Howard F, Yudkin J. Effect of dietary change upon the amylase and trypsin activities of the rat pancreas. *British Journal of Nutrition*. 1963; 17: 281-294.
13. Lowenfels AB, Maisonneuve P. Epidemiology and risk factors for pancreatic cancer. *Best Practices and Research Clinical Gastroenterology*. 2006; 20: 197-209.
14. Silverman DT. Risk factors for pancreatic cancer: a case-control study based on direct interviews. *Teratogenesis, Carcinogenesis, and Mutagenesis*. 2001; 21: 7-25.
15. Hassan MM, Bondy ML, Wolff RA, Abbruzzese JL, Vauthey JN, Pisters PW, Evans DB, Khan R, Chou TH, Lenzi R, Jiao L, Li D. Risk factors for pancreatic cancer: case-control study. *American Journal of Gastroenterology*. 2007; 102: 2696-2707.
16. Anderson KE, Potter JD, Mack TM. Pancreatic cancer. In: Schottenfeld D, Fraumeni JF Jr, eds. *Cancer Epidemiology and Prevention*. Oxford: Oxford University Press. 1996: 725-771.

17. Iodice S, Gandini S, Maisonneuve P, Lowenfels AB. Tobacco and the risk of pancreatic cancer: a review and meta-analysis. *Langenbeck's Archives of Surgery*. 2008; 393: 535-545.
18. Zheng W, McLaughlin JK, Gridley G, Bjelke E, Schuman LM, Silverman DT, Wacholder S, Co-Chien HT, Blot WJ, Fraumeni Jr JF. A cohort study of smoking, alcohol consumption, and dietary factors for pancreatic cancer (United States). *Cancer Causes and Control*. 1993; 4: 477-482.
19. Cuzick J, Babiker AG. Pancreatic cancer, alcohol, diabetes mellitus, and gall-bladder disease. *American Journal of Cancer*. 1989; 43: 415-421.
20. Talamini G, Bassi C, Falconi M, Sartori N, Salvia R, Rigo L, Castagnini A, di Francesco V, Fulloni L, Bovo P, Vaona B, Angelini G, Vantini I, Cavallini G, Pederzoli P. Alcohol and smoking as risk factors in chronic pancreatitis and pancreatic cancer. *Digestive Diseases and Sciences*. 1999; 44: 1303-1311.
21. Fernandez E, La Vecchia C, D'Avanzo B, Negri E, Franceschi S. Family history and the risk of liver, gallbladder, and pancreatic cancer. *Cancer Epidemiology, Biomarkers, and Prevention*. 1994; 3: 209-212.
22. Schenk M, Schwartz AG, O'Neal E, Kinnard M, Greenson JK, Fryzek JP, Ying GS, Garabrant DH. Familial risk of pancreatic cancer. *Journal of the National Cancer Institute*. 2001; 93: 640-644.
23. Kauppinen T, Partanen T, Degerth R, Ojajdrvi A. Pancreatic cancer and occupational exposures. *Epidemiology*. 1995; 6: 498-502.

24. Fryzek J, Garabrant DH, Harlow SD, Severson RK, Gillespie BW, Schenk M, Schottenfeld D. A case-control study of self-reported exposures to pesticides and pancreas cancer in Southern Michigan. *International Journal of Cancer*. 1997; 72: 62-67.
25. Hezel AF, Kimmelman AC, Stanger BZ, Bardeesy N, DePinho RA. Genetics and biology of pancreatic ductal adenocarcinoma. *Genes and Development*. 2006; 20: 1218-1249.
26. Li D, Xie K, Wolff R, Abbruzzese JL. Pancreatic Cancer. *The Lancet*. 2004; 363: 1049-1057.
27. Almoguerra C, Shibata D, Forrester K, Martin J, Arnheim N, Perucho M . Most human carcinomas of the exocrine pancreas contain mutant c-K-ras genes. *Cell*. 1988; 53: 549-554.
28. Uehara H, Nakaizumi A, Tatsuta M, Baba M, Takenaka A, Uedo N, Sakai N, Yano H, Iishi H, Ohigashi H, Ishikawa O, Okada S, Kakizoe T. Diagnosis of pancreatic cancer by detecting telomerase activity in pancreatic juice: comparison with K-ras mutations. *American Journal of Gastroenterology*. 1999; 94: 2513-2518.
29. Wenger FA, Zieren J, Peter FJ, Jacobi CA, Müller JM. K-ras mutations in tissue and stool samples from patients with pancreatic cancer and chronic pancreatitis. *Langenbeck's Archives of Surgery*. 1999; 384: 181-186.
30. Malats N, Porta M, Corominas JM, Piñol JL, Rifà J, Real FX. Ki-ras mutations in exocrine pancreatic cancer: association with clinic-pathological characteristics and with tobacco and alcohol consumption. *International Journal of Cancer*. 1997; 70: 661-667.
31. Porta M, Crous-Bou M, Wark PA, Vineis P, Real FX, Malats N, Kampman E. Cigarette smoking an K-ras mutations in pancreas, lung, and colorectal adenocarcinomas: etiopathogenic similarities, differences, and paradoxes. *Mutation Research*. 2009; 682: 83-93.

32. Berger DH, Chang H, Wood M, Huang L, Heath CW, Lehman T, Ruggeri BA. Mutational activation of K-*ras* in non-neoplastic exocrine pancreatic lesions in relation to cigarette smoking status. *Cancer*. 1999; 85: 326-329.
33. Bardeesy N, DePinho RA. Pancreatic cancer biology and genetics. *Nature Reviews*. 2002; 2: 897-909.
34. Waddell N, Pajic M, Patch AM, Chang DK, Kassahn KS, Bailey P, Johns AL, Miller D, Nones K, Quek K, Quinn MCJ, Robertson AJ, Fadlullah MZH, Bruxner TJC, Christ AN, Harliwong I, Idrisoglu S, Manning S, Nourse C, Nourbakhsh E, Wani S, Wilson PJ, Markham E, Cloonan N, Anderson MJ, Fink JL, Holmes O, Kazakoff SH, Leonard C, Newell F, Poudel B, Song S, Taylor D, Waddell N, Wood S, Xu Q, Wu J, Pinese M, Cowley MJ, Lee HC, Jones MD, Nagrial AM, Humphris J, Chantrell LA, Chin V, Steinmann AM, Mawson A, Humphrey ES, Colvin EK, Chou A, Scarlett CJ, Pinho AV, Giry-Laterriere M, Rooman I, Samra JS, Kench JG, Pettitt JA, Merrett ND, Toon C, Epari K, Nguyen, NQ, Barbour A, Zeps N, Jamieson NB, Graham JS, Niclou SP, Bjerkvig R, Grützmann R, Aust D, Hruban RH, Maitra A, Iacobuzio-Donahue CA, Wolfgang CL, Morgan RA, Lawlor RT, Corbo V, Bassi C, Falconi M, Zamboni G, Tortora G, Tempero MA, Australian Pancreatic Cancer Genome Initiative, Gill AJ, Eshleman JR, Pilarsky C, Scarpa A, Musgrove EA, Pearson JV, Biankin AV, Grimmond SM. Whole genomes redefine the mutational landscape of pancreatic cancer. *Nature*. 2015; 518: 495-501.
35. Sausen M, Phallen J, Adleff V, Jones S, Leary RL, Barrett MT, Anagnostou V, Parpart-Li S, Murphy D, Li QK, Hruban CA, Scharpf R, White JR, O'Dwyer PJ, Allen PJ, Eshleman JR, Thompson CB, Klimstra DS, Linehan DC, Maitra A, Hruban RH, Diaz Jr LA, Von Hoff DD, Johansen JS, Drebin JA, Velculescu VE. Clinical implications of genomic alterations in the tumour and circulation of pancreatic cancer patients. *Nature Communications*. 2015; 6: 1-6.



36. Schutte M, Hruban RH, Geradts J, Maynard R, Hilgers W, Rabindran SK, Moskaluk CA, Hahn SA, Schwarte-Waldhoff I, Schmiegel W, Baylin SB, Kern SE, Herman JG. Abrogation of the Rb/p16 tumor-suppressive pathway in virtually all pancreatic carcinomas. *Cancer Research*. 1997; 57: 3126-3130.
37. Moskaluk CA, Hruban RH, Kern SE. p16 and K-ras gene mutations in the intraductal precursors of human pancreatic adenocarcinoma. *Cancer Research*. 1997; 57: 2140-2143.
38. Caldas C, Hahn SA, da Costa LT, Redston MS, Schutte M, Seymour AB, Weinstein CL, Hruban RH, Yeo CJ, Kern SE. Frequent somatic mutations and homozygous deletions of the p16 (MTS1) gene in pancreatic adenocarcinoma. *Nature Genetics*. 1994; 8: 27-32.
39. Murphy KM, Brune KA, Griffin C, Sollenberger JE, Petersen GM, Bansal R, Hruban RH, Kern SE. Evaluation of candidate genes MAP2K4, MADH4, ACVR1B, and BRCA2 in familial pancreatic cancer. *Cancer Research*. 2002; 62: 3789-3793.
40. Itakuri J, Ishiwata T, Friess H, Fujii H, Matsumoto Y, Büchler MW, Korc M. Enhanced expression of vascular endothelial growth factor in human pancreatic cancer correlates with local disease progression. *Clinical Cancer Research*. 1997. 3: 1309-1316.
41. Wei D, Wang L, He Y, Xiong HQ, Abbruzzese JL, Xie K. Celecoxib Inhibits Vascular Endothelial Growth Factor Expression in and Reduces Angiogenesis and Metastasis of Human Pancreatic Cancer via Suppression of Sp1 Transcription Factor Activity. *Cancer Research*. 2004; 64: 2030-2038.
42. Waugh DJJ, Wilson C. The interleukin-8 pathway in cancer. *Clinical Cancer Research*. 2008; 14: 6735-6741.

43. Nishida N, Yano H, Nishida T, Kamura T, Kojiro M. Angiogenesis in cancer. *Vascular Health and Risk Management*. 2006; 2: 213-219.
44. Yamanaka Y, Friess H, Büchler M, Beger HG, Uchida E, Onda M, Kobrin MS, Korc M. Overexpression of acidic and basic fibroblast growth factors in human pancreatic cancer correlates with advanced tumor stage. *Cancer Research*. 1993; 53: 5289-5296.
45. Korc M. Role of growth factors in pancreatic cancer. *Surgical Oncology Clinics of North America*. 1998; 7: 25-41.
46. Schmiegel W, Roeder C, Schmielau J, Rodeck U, Kalthoff H. Tumor necrosis factor alpha induces the expression of transforming growth factor alpha and the epidermal growth factor receptor in human pancreatic cancer cells. *Proceedings of the National Academy of Sciences of the United States of America*. 1993; 90: 863-867.
47. Friess H, Yamanaka Y, Büchler M, Ebert M, Beger HG, Gold LI, Korc M. Enhanced expression of transforming growth factor  $\beta$  isoforms in pancreatic cancer correlates with decreased survival. *Gastroenterology*. 1993; 105: 1846-1856.
48. Blanchard JA II, Barve S, Joshi-Barve S, Talwalker R, Gates LK. Cytokine production by CAPAN-1 and CAPAN-2 cell lines. *Digestive Diseases and Science*. 2000; 45: 927-932.
49. Saito K, Ishikura H, Kishimoto T, Kawarada Y, Yano T, Takahashi T, Kato H, Yoshiki T. Interleukin-6 produced by pancreatic carcinoma cells enhances humoral immune responses against tumor cells: a possible event in tumor regression. *International Journal of Cancer*. 1998; 75: 284-289.

50. Warshaw AL, Gu ZY, Wittenberg J. Preoperative staging and assessment of resectability of pancreatic cancer. *Archives of Surgery*. 1990; 125: 230-233.
51. Klinkenbijl JH, Jeekel J, Sahmoud T, van Pel R, Couvreur ML, Veenhof CH, Arnaud JP, Gonzalez DG, de Wit L, Hennisman A, Wils J. Adjuvant radiotherapy and 5-fluorouracil after curative resection of cancer of the pancreas and periampullary region: phase III trial of the EORTC gastrointestinal tract cancer cooperative group. *Annals of Surgery*. 1999; 230: 776-784.
52. Yeo CJ, Cameron JL, Lillemore KD, Sitzmann JV, Hruban RH, Goodman SN, Dooley WC, Coleman J, Pitt HA. Pancreaticoduodenectomy for cancer of the head of the pancreas: 201 patients. *Annals of Surgery*. 1995; 221: 721-731.
53. Li CP, Chao Y, Chi KH, Chan WK, Teng HC, Lee RC, Chang FY, Lee SD, Yen SH. Concurrent chemoradiotherapy treatment of locally advanced pancreatic cancer: Gemcitabine versus 5-fluorouracil, a randomized controlled study. *International Journal of Radiation Oncology\*Biological\*Physics*. 2003; 57: 98-104.
54. El Kamar FG, Grossbard ML, Kozuch PS. Metastatic pancreatic cancer: emerging strategies in chemotherapy and palliative care. *The Oncologist*. 2003; 8: 18-34.
55. Conroy T, Desseigne F, Ychou M, Bouché O, Guimbaud R, Bécouarn Y, Adenis A, Raoul JL, Gougou-Bourgade S, de la Fouchardière C, Bennouna J, Bachet JB, Khemissa-Akouz F, Péré-Vergé D, Delbaldo C, Assenat E, Chauffert B, Michel P, Montoto-Grillot C, Ducreux M. FOLFIRINOX versus gemcitabine for metastatic pancreatic cancer. *The New England Journal of Medicine*. 2011; 364: 1817-1825.
56. Beck G, Habicht GS. Immunity and the invertebrates. *Scientific American*. 1996; 275: 60-71.

57. Hoebe K, Janssen E, Beutler B. The interface between innate and adaptive immunity. *Nature Immunology*. 2004; 5: 971-974.
58. Medzhitov R, Janeway Jr CA. Innate immunity: the virtues of a nonclonal system of recognition. *Cell*. 1997; 91: 295-298.
59. Pitman RS, Blumberg RS. First line of defense: the role of intestinal epithelium as an active component of the mucosal immune system. *Journal of Gastroenterology*. 2000; 35: 805-814.
60. Delves PJ, Roitt IM. The immune system. *The New England Journal of Medicine*. 2000; 343: 37-49.
61. Raulet DH, Guerra N. Oncogenic stress sensed by the immune system: role of natural killer cell receptors. *Nature Reviews Immunology*. 2009; 9: 568-580.
62. Zasloff M. Antimicrobial peptides of multicellular organisms. *Nature*. 2002; 415: 389-395.
63. Aderem A, Underhill DM. Mechanisms of phagocytosis in macrophages. *Annual Review of Immunology*. 1999; 17: 593-623.
64. Brinkmann V, Reichard U, Goosmann C, Fauler B, Uhlemann Y, Weiss DS, Weinrauch Y, Zychlinsky A. Neutrophil extracellular traps kill bacteria. *Science*. 2004; 303: 1532-1535.
65. Greenberg S, Grinstein S. Phagocytosis and innate immunity. *Current Opinion in Immunology*. 2002; 14: 136-145.
66. Henneke, P. Golenbock DT. Phagocytosis, innate immunity, and host-pathogen specificity. *The Journal of Experimental Medicine*. 2004; 199: 1-4.
67. Herberman RB, Ortaldo JR. Natural killer cells: their roles in defenses against disease. *Science*. 1981; 214: 24-30.

68. Vivier E, Tomasello E, Baratin M, Walzer T, Ugolini S. Functions of natural killer cells. *Nature Immunology*. 2008; 9: 503-510.
69. Shtrichman R, Samuel CE. The role of gamma interferon in antimicrobial immunity. *Current Opinion in Microbiology*. 2001; 4: 251-259.
70. Hoffman JA, Kafatos FC, Janeway Jr CA, Ezekowitz RAB. Phylogenetic Perspectives in Innate Immunity. *Science*. 1999; 284: 1313-1318.
71. Marieb EN, Hoehn K. *Human Anatomy and Physiology*. 8 ed., 2010; San Francisco: Pearson Education, Inc.
72. Stockert E, Jäger E, Chen YT, Scanlan MJ, Gout I, Karbach J, Arand M, Knuth A, Old LJ. A survey of the humoral immune response of cancer patients to a panel of human tumor antigens. *The Journal of Experimental Medicine*. 1998; 187: 1349-1354.
73. Bowen DG, Walker CM. Adaptive immune responses in acute and chronic hepatitis C virus infection. *Nature*. 2005; 436: 946-952.
74. Casadevall A. Antibody-mediated immunity against intracellular pathogens: two-dimensional thinking comes full circle. *Infection and Immunity*. 2003; 71: 4225-4228.
75. Pape KA, Catron DM, Itano AA, Jenkins MK. The humoral immune response is initiated in lymph nodes by B cells that acquire soluble antigen directly in the follicles. *Immunity*. 2007; 26: 491-502.
76. Dobrovolskaia MA, McNeil SE. Immunological properties of engineered nanomaterials. *Nature Nanotechnology*. 2007; 2: 469-478.

77. Ettinger R, Sims GP, Fairhurst AM, Robbins R, da Silva YS, Spolski R, Leonard WJ, Lipsky PE. IL-21 induces differentiation of human naive and memory B cells into antibody-secreting plasma cells. *The Journal of Immunology*. 2005; 175: 7867-7879.
78. Stallone DD. The influence of obesity and its treatment on the immune system. *Nutrition Reviews*. 1994; 52: 37-50.
79. Wilson IA, Stanfield RL. Antibody-antigen interactions. *Current Opinion in Structural Biology*. 1993; 3: 113-118.
80. MacCallum RM, Martin ACR, Thornton JM. Antibody-antigen interactions: contact analysis and binding site topography. *Journal of Molecular Biology*. 1996; 262: 732-745.
81. Sheriff S, Silverton EW, Padlan EA, Cohen GH, Smith-Gill SJ, Finzel BC, Davies DR. Three-dimensional structure of an antibody-antigen complex. *Proceedings of the National Academy of Sciences of the United States of America*. 1987; 84: 8075-8079.
82. Padlan EA, Silverton EW, Sheriff S, Cohen GH, Smith-Gill SJ, Davies DR. Structure of antibody-antigen complex: crystal structure of the HyHEL-10 Fab-lysozyme complex. *Proceedings of the National Academy of Sciences of the United States of America*. 1989; 86: 5938-5942.
83. Schmidt WM, Lippard VW. Human passive transfer antibody II. Neutralization of antigen. *American Journal of Diseases of Children*. 1937; 54: 777-785.
84. Huddleson IF, Abell E. Rapid macroscopic agglutination for the serum diagnosis of Bang's abortion disease. *The Journal of Infectious Diseases*. 1928; 42: 242-247.

85. Skom JH, Talmage DW. Nonprecipitating insulin antibodies. *The Journal of Clinical Investigation*. 1958; 37: 783-786.
86. Purcell RH, Holland PV, Walsh JH. A complement-fixation test for measuring Australia antigen and antibody. *The Journal of Infectious Diseases*. 1969; 120: 383-386.
87. Sakaguchi S, Yamaguchi T, Nomura T, Ono M. Regulatory T cells and immune tolerance. *Cell*. 2008; 133: 775-787.
88. Sharpe AH, Abbas AK. T-cell costimulation – biology, therapeutic potential, and challenges. *The New England Journal of Medicine*. 2006; 355: 973-975.
89. MacDonald HR. T-cell activation. *Annual Review of Cell Biology*. 1986; 2: 231-253.
90. Smith-Garvin JE, Koretzky GA, Jordan MS. T cell activation. *Annual Review of Immunology*. 2009; 27: 591-619.
91. Kubo M, Hanada T, Yoshimura A. Suppressors of cytokine signaling and immunity. *Nature Immunology*. 2003; 4: 1169-1176.
92. Baerwald KD, Popko B. Developing and mature oligodendrocytes respond differently to the immune cytokine interferon-gamma. *Journal of Neuroscience Research*. 1998; 52: 230-239.
93. Berghe WV, Vermeulen L, de Wilde G, de Bosscher K, Boone E, Haegeman G. Signal transduction by tumor necrosis factor and gene regulation of the inflammatory cytokine interleukin-6. *Biochemical Pharmacology*. 2000; 60: 1185-1195.
94. Wilson NJ, Boniface K, Chan JR, McKenzie BS, Blumenschein WM, Mattson JD, Basham B, Smith K, Chen T, Morel F, Lecron JC, Kastelein RA, Cua DJ, McClanahan TK, Bowman EP,

- de Waal Malefyt R. Development, cytokine profile and function of human interleukin 17-producing helper T cells. *Nature Immunology*. 2007; 8: 950-957.
95. Schoenberger SP, Toes REM, van der Voort EIH, Offringa R, Melief CJM. T-cell help for cytotoxic T lymphocytes is mediated by CD40–CD40L interactions. *Nature*. 1998; 393: 480-483.
96. Thompson C, Powrie F. Regulatory T cells. *Current Opinion in Pharmacology*. 2004; 4: 408-414.
97. Broder S, Edelson RL, Lutzner MA, Nelson DL, MacDermott RP, Durm ME, Goldman CK, Meade BD, Waldmann TA. The Sézary syndrome: a malignant proliferation of helper T cells. *The Journal of Clinical Investigation*. 1976; 58: 1297-1306.
98. Biron CA, Nguyen KB, Pien GC, Cousens LP, Salazar-Mather TP. Natural killer cells in antiviral defense: function and regulation by innate cytokines. *Annual Review of Immunology*. 1999; 17: 189-220.
99. Beissert S, Schwarz A, Schwarz T. Regulatory T cells. *Journal of Investigative Dermatology*. 2006; 126: 15-24.
100. Collison LW, Workman CJ, Kuo TT, Boyd K, Wang Y, Vignali KM, Cross R, Sehy D, Blumberg RS, Vignali DAA. The inhibitory cytokine IL-35 contributes to regulatory T-cell function. *Nature*. 2007; 450: 566-569.
101. Hermann PC, Huber SL, Herrler T, Aicher A, Ellwart JW, Guba M, Bruns CJ, Heeschen C. Distinct populations of cancer stem cells determine tumor growth and metastatic activity in human pancreatic cancer. *Cell Stem Cell*. 2007; 1: 313-323.



102. Ng SSW, Tsao MS, Chow S, Hedley DW. Inhibition of phosphatidylinositide 3-kinase enhances gemcitabine-induced apoptosis in human pancreatic cancer cells. *Cancer Research*. 2000; 60: 5451-5455.
103. Qian LW, Mizumoto K, Urashima T, Nagai E, Maehara N, Sato N, Nakajima M, Tanaka M. Radiation-induced increase in invasive potential of human pancreatic cancer cells and its blockade by a matrix metalloproteinase inhibitor, CGS27023. *Clinical Cancer Research*. 2002; 8: 1223-1227.
104. Rosenberg SA, Yang JC, Restifo NP. Cancer immunotherapy: moving beyond current vaccines. *Nature Medicine*. 2004; 10: 909-915.
105. Wobser M, Keikavoussi P, Kunzmann V, Weininger M, Andersen MH, Becker JC. Complete remission of liver metastasis of pancreatic cancer under vaccination with a HLA-A2 restricted peptide derived from the universal tumor antigen survivin. *Cancer Immunology, Immunotherapy*. 2006; 55: 1294-1298.
106. McKhann CF, Gunnarsson A. Approaches to immunotherapy. *Cancer*. 1974; 34: 1521-1531.
107. Blattman JN, Greenberg PD. Cancer immunotherapy: a treatment for the masses. *Science*. 2004; 305: 200-205.
108. Homey B, Müller A, Zlotnik A. Chemokines: agents for the immunotherapy of cancer? *Nature Reviews Immunology*. 2002; 2: 175-184.
109. Weiner LM, Surana R, Wang S. Monoclonal antibodies: versatile platforms for cancer immunotherapy. *Nature Reviews Immunology*. 2010; 10: 317-327.

110. Slamon DJ, Leyland-Jones B, Shak S, Fuchs H, Paton V, Bajamonde A, Fleming T, Eiermann W, Wolter J, Pegram M, Baselga J, Norton L. Use of chemotherapy plus a monoclonal antibody against HER2 for metastatic breast cancer that overexpresses HER2. *The New England Journal of Medicine*. 2001; 344: 783-792.
111. Wilbur DS, Hadley SW, Hylarides MD, Abrams PG, Beaumier PA, Morgan AC, Reno JM, Fritzberg AR. Development of a stable radioiodinating reagent to label monoclonal antibodies for radiotherapy of cancer. *Journal of Nuclear Medicine*. 1989; 30: 216-226.
112. Teeling JL, French RR, Cragg MS, van den Brakel J, Pluyter M, Huang H, Chan C, Parren PWHI, Hack CE, Dechant M, Valerius T, van de Winkel JGJ, Glennie MJ. Characterization of new human CD20 monoclonal antibodies with potent cytolytic activity against non-Hodgkin lymphomas. *Blood*. 2004; 104: 1793-1800.
113. Maloney DG, Grillo-López AJ, White CA, Bodkin D, Schilder RJ, Neidhart JA, Janakiraman N, Foon KA, Liles TM, Dallaire BK, Wey K, Royston I, Davis T, Levy R. IDEC-C2B8 (Rituximab) anti-CD20 monoclonal antibody therapy in patients with relapsed low-grade non-Hodgkin's lymphoma. *Blood*. 1997; 90: 2188-2195.
114. McLaughlin P, Grillo-López AJ, Link BK, Levy R, Czuczman MS, Williams ME, Heyman MR, Bence-Bruckler I, White CA, Cabanillas F, Jain V, Ho AD, Lister J, Wey K, Shen D, Dallaire BK. Rituximab chimeric anti-CD20 monoclonal antibody therapy for relapsed indolent lymphoma: half of patients respond to a four-dose treatment program. *Journal of Clinical Oncology*. 1998; 16: 2825-2833.
115. Bernard A, Boumsell L, Reinherz EL, Nadler LM, Ritz J, Coppin H, Richard Y, Valensi F, Dausset J, Flandrin G, Lemerle J, Schlossman SF. Cell surface characterization of malignant T

cells from lymphoblastic lymphoma using monoclonal antibodies: evidence for phenotypic differences between malignant T cells from patients with acute lymphoblastic leukemia and lymphoblastic lymphoma. *Blood*. 1981; 57: 1105-1110.

116. Miller RA, Maloney DG, Warnke R, Levy R. Treatment of B-cell lymphoma with monoclonal anti-idiotypic antibody. *The New England Journal of Medicine*. 1982; 306: 517-522.

117. Davis TA, Grillo-López AJ, White CA, McLaughlin P, Czuczman MS, Link BK, Maloney DG, Weaver RL, Rosenberg J, Levy R. Rituximab anti-CD20 monoclonal antibody therapy in non-Hodgkin's lymphoma: safety and efficacy of re-treatment. *Journal of Clinical Oncology*. 2000; 18: 3135-3143.

118. Hale G, Clark MR, Marcus R, Winter G, Dyer MJS, Phillips JM, Riechman L, Waldmann H. Remission induction in non-Hodgkin lymphoma with reshaped human monoclonal antibody CAMPATH-1H. *The Lancet*. 1988; 332: 1394-1399.

119. Ritz J, Schlossman SF. Utilization of monoclonal antibodies in the treatment of leukemia and lymphoma. *Blood*. 1982; 59: 1-11.

120. Österborg A, Fassas AS, Anagnostopoulos A, Dyer MJS, Catovsky D, Mellstedt H. Humanized CD52 monoclonal antibody campath-1H as first-line treatment in chronic lymphocytic leukaemia. *British Journal of Haematology*. 1996; 93: 151-153.

121. Adams GP, Weiner LM. Monoclonal antibody therapy of cancer. *Nature Biotechnology*. 2005; 23: 1147-1157.

122. Laheru D, Jaffee EM. Immunotherapy for pancreatic cancer- science diving clinical progress. *Nature Reviews Cancer*. 2005; 5: 459-467.

123. Hanahan D, Weinberg RA. The hallmarks of cancer. *Cell*. 2000; 100: 57-70.
124. Hanahan D, Weinberg RA. Hallmarks of cancer: the next generation. *Cell*. 2011; 144: 646-674.
125. Cavallo F, de Giovanni C, Nanni P, Forni G, Lollini PL. 2011: the immune hallmarks of cancer. *Cancer Immunology, Immunotherapy*. 2011; 60: 319-326.
126. Vinay DS, Ryan EP, Pawelec G, Talib WH, Stagg J, Elkord E, Lichtor T, Decker WK, Whelan RL, Shantha Kumara HMC, Signori E, Honoki K, Geogakilas AG, Amin A, Helferich WG, Boosani CS, Guha G, Ciriolo MR, Chen S, Mohammed SI, Azmi AS, Keith WN, Bilsland A, Bhakta D, Halicka D, Fujii H, Aquilano K, Ashraf SS, Nowsheen S, Yang X, Choi BK, Kwon BS . Immune evasion in cancer: mechanistic basis and therapeutic strategies. *Seminars in Cancer Biology*. 2015; 35: S185-S198.
127. Ganss R, Hanahan D. Tumor microenvironment can restrict the effectiveness of activated antitumor lymphocytes. *Cancer Research*. 1998; 58: 4673-4681.
128. Greenwald RJ, Boussiotis VA, Lorschach RB, Abbas AK, Sharpe AH. CTLA-4 regulates induction of anergy *in vivo*. *Immunity*. 2001; 14: 145-155.
129. Wang T, Niu G, Kortylewski M, Burdelya L, Shain K, Zhang S, Bhattacharya R, Gabrilovich DI, Heller R, Coppola D, Dalton W, Jove R, Pardoll D, Yu H. Regulation of the innate and adaptive immune responses by Stat-3 signaling in tumor cells. *Nature Medicine*. 2004; 10: 48-54.
130. Schwartz RH. T cell anergy. *Annual Review of Immunology*. 2003; 21: 305-334.

131. Oyama T, Ran S, Ishida T, Nadaf S, Kerr L, Carbone DP, Gabrilovich DI. Vascular endothelial growth factor affects dendritic cell maturation through the inhibition of nuclear factor- $\kappa$ B activation in hemopoietic progenitor cells. *The Journal of Immunology*. 1998; 160: 1224-1232.
132. Coyle AJ, Gutierrez-Ramos. The expanding B7 superfamily: increasing complexity in co-stimulatory signals regulating T cell function. *Nature Immunology*. 2001; 2: 203-209.
133. Ohm JE, Carbone DP. VEGF as a mediator of tumor-associated immunodeficiency. *Immunologic Research*. 2001; 23: 263-272.
134. Carreno BM, Collins M. BTLA: a new inhibitory receptor with a B7-like ligand. *Trends in Immunology*. 2003; 24: 524-527.
135. Ungerfrozen H, Voss M, Bernstorff WV, Schmid A, Kremer B, Kalthoff H. Immunological escape mechanisms in pancreatic carcinoma. *Annals of the New York Academy of Sciences*. 1999; 880: 243-251.
136. Elhalel MD, Huang JH, Schmidt W, Rachmilewitz J, Tykocinski ML. CTLA-4: FasL induces alloantigen-specific hyporesponsiveness. *The Journal of Immunology*. 2003; 170: 5842-5850.
137. Bellone G, Turletti A, Artusio E, Mareschi K, Carbone A, Tibaudi D, Robecchi A, Emanuelli G, Rodeck U. Tumor-associated transforming growth factor  $\beta$  and interleukin-10 contribute to a systemic Th2 immune phenotype in pancreatic carcinoma patients. *The American Journal of Pathology*. 1999; 155: 537-547.

138. Wegener AMK, Letourneur F, Hoeveler A, Brocker T, Luton F, Malissen B. The T cell receptor/CD3 complex is composed of at least two autonomous transduction modules. *Cell*. 1992; 68: 83-95.
139. Schmielau J, Nalesnik MA, Finn OJ. Suppressed T-cell receptor  $\zeta$  chain expression and cytokine production in pancreatic cancer patients. *Clinical Cancer Research*. 2001; 7: 933s-939s.
140. Kornmann M, Ishiwata T, Kleeff J, Beger HG, Korc M. Fas and Fas-ligand expression in human pancreatic cancer. *Annals of Surgery*. 2000; 231: 368-379.
141. Ito D, Fujimoto K, Doi R, Koizumi M, Toyoda E, Mori T, Kami K, Kawaguchi Y, Whitehead R, Imamura M. Chronic exposure of transforming growth factor  $\beta$ 1 confers a more aggressive tumor phenotype through down-regulation of p21 (WAF1/CIP1) in conditionally immortalized pancreatic epithelial cells. *Surgery*. 2004; 136: 364-374.
142. Klausner RD Samelson LE. T cell antigen receptor activation pathways: the tyrosine kinase connection. *Cell*. 1991; 64: 875-878.
143. Sawai H, Funahashi H, Yamamoto M, Okada Y, Hayakawa T, Tanaka M, Takeyama H, Manabe T. Interleukin-1 $\alpha$  enhances integrin  $\alpha$ 6  $\beta$ 1 expression metastatic capability of human pancreatic cancer. *Oncology*. 2003; 65: 167-173.
144. Blumberg RS, Ley S, Sancho J, Lonberg N, Lacy E, McDermott F, Schad V, Greenstein JL, Terhorst C. Structure of the T cell antigen receptor: evidence for two CD3  $\epsilon$  subunits in the T cell receptor-CD3 complex. *Proceedings of the National Academy of Sciences of the United States of America*. 1990; 87: 7220-7224.

145. Irving BA, Weiss A. The cytoplasmic domain of the T cell receptor  $\zeta$  chain is sufficient to couple to receptor associated signal transduction pathways. *Cell*. 1991; 64: 891-901.
146. Bernstorff W, Spanjaard RA, Chan AK, Lockhart DC, Sadanaga N, Wood I, Peiper M, Goedegebuure PS, Eberlein TJ. Pancreatic cancer cells can evade immune surveillance via nonfunctional Fas (APO-1/CD95) receptors and aberrant expression of Fas ligand. *Surgery*. 1999; 125: 73-84.
147. Duda DG, Sunamura M, Lefter LP, Furukawa T, Yokoyama T, Yatsuoka T, Abe T, Inoue H, Motoi F, Egawa SI, Matsuno S, Horii A. Restoration of SMAD4 by gene therapy reverses the invasive phenotype in pancreatic adenocarcinoma cells. *Oncogene*. 2003; 22: 6857-6864.
148. Clevers H, Alarcon B, Wileman T, Terhorst C. The T cell receptor/CD3 complex: a dynamic protein ensemble. *Annual Review of Immunology*. 1988; 6: 629-662.
149. Walunas TL, Bakker CY, Bluestone JA. CTLA-4 ligation blocks CD28-dependent T cell activation. *Journal of Experimental Medicine*. 1996; 183: 2541-2550.
150. Carreno BM, Collins M. The B7 family of ligands and its receptors: new pathways for co-stimulation inhibition of immune responses. *Annual Review of Immunology*. 2002; 20: 29-53.
151. Liang SC, Latchman YE, Buhlmann JE, Tomczak MF, Horwitz BH, Freeman GJ, Sharpe AH. Regulation of PD-1, PD-L1, PD-L2 expression during normal and autoimmune responses. *European Journal of Immunology*. 2003; 33: 2706-2716.
152. Jenkins MK, Schwartz RH. Antigen presentation by chemically modified splenocytes induces antigen-specific T cell unresponsiveness. *Journal of Experimental Medicine*. 1987; 165: 302-319.

153. Sugamura K, Ishii N, Weinberg AD. Therapeutic targeting of the effector T cell co-stimulatory molecule OX40. *Nature Reviews Immunology*. 2004; 4: 420-431.
154. Lane P. Role of OX40 signals in coordinating CD4 T cell selection, migration, and cytokine differentiation in T helper (Th) 1 and Th2 cells. *Journal of Experimental Medicine*. 2000; 191: 201-206.
155. Korman AJ, Peggs KS, Allison JP. Checkpoint blockade in cancer immunotherapy. *Advances in Immunology*. 2006; 90: 297-339.
156. Drake CG, Jaffee E, Pardoll DM. Mechanisms of immune evasion by tumors. *Advances in Immunology*. 2006; 90: 51-81.
157. Blank C, Brown I, Peterson AC, Spiotto M, Iwai Y, Honjo T, Gajewski TF. PD-L1/B7H-1 inhibits the effector phase of tumor rejection by T cell receptor (TCR) transgenic CD8<sup>+</sup> T cells. *Cancer Research*. 2004; 64: 1140-1145.
158. Ribas A. Tumor immunotherapy directed at PD-1. *The New England Journal of Medicine*. 2012; 366: 2517-2519.
159. Agata Y, Kawasaki A, Nishimura H, Ishida Y, Tsubat T, Yagita H, Honjo T. Expression of the PD-1 antigen on the surface of stimulated mouse T and B lymphocytes. *International Immunology*. 1996; 8: 765-772.
160. Okazaki T, Honjo T. PD-1 and PD-1 ligands: from discovery to clinical application. *International Immunology*. 2007; 19: 813-824.
161. Iwai Y, Ishida M, Tanaka Y, Okazaki T, Honjo T, Minato N. Involvement of PD-L1 on tumor cells in the escape from host immune system and tumor immunotherapy by PD-L1



blockade. *Proceedings of the National Academy of Sciences of the United States of America*. 2002; 99: 12293-12297.

162. Dong H, Chen L. B7-H1 pathway and its role in the evasion of tumor immunity. *Journal of Molecular Medicine*. 2003; 81: 281-287.

163. Khoury SJ, Sayegh MH. The roles of the new negative T cell costimulatory pathways in regulating autoimmunity. *Immunity*. 2004; 20: 529-538.

164. Francisco LM, Salinas VH, Brown KE, Vanguri VK, Freeman GJ, Kuchroo VK, Sharpe AH. PD-L1 regulates the development, maintenance, and function of induced regulatory T cells. *The Journal of Experimental Medicine*. 2009; 206: 3015-3029.

165. Keir ME, Butte MJ, Freeman GJ, Sharpe AH. PD-1 and its ligands in tolerance and immunity. *Annual Review of Immunology*. 2008; 26: 677-704.

166. Mu CY, Huang JA, Chen Y, Chen C, Zhang XG. High expression of PD-L1 in lung cancer may contribute to poor prognosis and tumor cells immune escape through suppressing tumor infiltrating dendritic cells maturation. *Medical Oncology*. 2011; 28: 682-688.

167. Azuma K, Ota K, Kawahara A, Hattori S, Iwama E, Harada T, Matsumoto K, Takayama K, Takamori S, Kage M, Nakanishi Y, Okamoto I. Association of PD-L1 overexpression with activating EGFR mutations in surgically resected nonsmall-cell lung cancer. *Annals of Oncology*. 2014; 25: 1935-1940.

168. Nakanishi J, Wada Y, Matsumoto K, Azuma M, Kikuchi K, Ueda S. Overexpression of B7-H1 (PD-L1) significantly associates with tumor grade and postoperative prognosis in human urothelial cancers. *Cancer Immunology, Immunotherapy*. 2007; 56: 1173-1182.

169. Gao Q, Wang XY, Qiu SJ, Yamato I, Sho M, Nakajima Y, Zhou J, Li BZ, Shi YH, Xiao YS, Xu Y, Fan J. Overexpression of PD-L1 significantly associates with tumor aggressiveness and postoperative recurrence in human hepatocellular carcinoma. *Clinical Cancer Research*. 2009; 15: 971-979.
170. Nomi T, Sho M, Akahori T, Hamada K, Kubo A, Kanehiro H, Nakamura S, Enomoto K, Yagita H, Azuma M, Nakajima Y. Clinical significance and therapeutic potential of the programmed death-1 ligand/programmed death-1 pathway in human pancreatic cancer. *Clinical Cancer Research*. 2007; 13: 2151-2157.
171. Topalian SL, Drake CG, Pardoll DM. Targeting the PD-1/B7-H1(PD-L1) pathway to activate anti-tumor immunity. *Current Opinion in Immunology*. 2012; 24: 207-212.
172. Herbst RS, Soria JC, Kowanetz M, Fine GD, Hamid O, Gordon MS, Sosman JA, McDermott DF, Powderly JD, Gettinger SN, Kohrt HEK, Horn L, Lawrence DP, Rost S, Leabman M, Xiao Y, Mokatrín A, Koeppen H, Hedge PS, Mellman I, Chen DS, Hodi FS. Predictive correlates of response to the anti-PD-L1 antibody MPDL3280A in cancer patients. *Nature*. 2014; 515: 563-567.
173. Leach DR, Krummel MF, Allison JP. Enhancement of antitumor immunity by CTLA-4 blockade. *Science*. 1996; 271: 1734.
174. Walunas TL, Lenschow DJ, Bakker CY, Linsley PS, Freeman GJ, Green JM, Thompson CB, Bluestone JA. CTLA-4 can function as a negative regulator of T cell activation. *Immunity*. 1994; 1: 405-413.

175. Hurwitz AA, Foster BA, Kwon ED, Truong T, Choi EM, Greenberg NM, Burg MB, Allison JP. Combination immunotherapy of primary prostate cancer in a transgenic mouse model using CTLA-4 blockade. *Cancer Research*. 2000; 60: 2444-2448.
176. Small EJ, Tchekmedyian NS, Rini BI, Fong L, Lowy I, Allison JP. A pilot trial of CTLA-4 blockade with human anti-CTLA-4 in patients with hormone-refractory prostate cancer. *Clinical Cancer Research*. 2007; 13: 1810-1815.
177. Hurwitz AA, Yu TFY, Leach DR, Allison JP. CTLA-4 blockade synergizes with tumor-derived granulocyte– macrophage colony-stimulating factor for treatment of an experimental mammary carcinoma. *Proceedings of the National Academy of Sciences of the United States of America*. 1998; 95: 10067-10071.
178. Phan GQ, Yang JC, Sherry RM, Hwu P, Topalian SL, Schwartzentruber DJ, Restifo NP, Haworth LR, Seipp CA, Freezer LJ, Morton KE, Mavroukakis SA, Duray PH, Steinberg SM, Allison JP, Davis TA, Rosenberg SA. Cancer regression and autoimmunity induced by cytotoxic T lymphocyte-associated antigen 4 blockade in patients with metastatic melanoma. *Proceedings of the National Academy of Sciences of the United States of America*. 2003; 100: 8372-8377.
179. Yuan J, Gnjjatic S, Li H, Powel S, Gallardo HF, Ritter E, Ku GY, Jungbluth AA, Segal NH, Rasalan TS, Manukian G, Xu Y, Roman RA, Terzulli SL, Heywood M, Pogoriler E, Ritter G, Old LJ, Allison JP, Wolchok JD. CTLA-4 blockade enhances polyfunctional NY-ESO-1 specific T cell responses in metastatic melanoma patients with clinical benefit. *Proceedings of the National Academy of Sciences of the United States of America*. 2008; 105: 20410-20415.

180. Peggs KS, Quezada SA, Chambers CA, Korman AJ, Allison JP. Blockade of CTLA-4 on both effector and regulatory T cell compartments contributes to the antitumor activity of anti-CTLA-4 antibodies. *The Journal of Experimental Medicine*. 2009; 206: 1717-1725.
181. Carthon BC, Wolchok JD, Yuan J, Kamat A, Tang DSN, Sun J, Ku G, Troncso P, Logothetis CJ, Allison JP, Sharma P. Preoperative CTLA-4 blockade: tolerability and immune monitoring in the setting of a presurgical clinical trial. *Clinical Cancer Research*. 2010; 16: 2861-2871.
182. Fecci PE, Ochiai H, Mitchell DA, Grossi PM, Sweeney AE, Archer GE, Cummings T, Allison JP, Bigner DD, Sampson JH. Systemic CTLA-4 blockade ameliorates glioma-induced changes to the CD4+ T cell compartment without affecting regulatory T-cell function. *Clinical Cancer Research*. 2007; 13: 2158-2167.
183. Suttmuller RPM, van Duivenvoorde LM, van Elsas A, Schumacher TNM, Wildenberg ME, Allison JP, Toes REM, Offringa R, Melief CJM. Synergism of cytotoxic T lymphocyte-associated antigen 4 blockade and depletion of Cd25+ regulatory T cells in antitumor therapy reveals alternative pathways for suppression of autoreactive cytotoxic T lymphocyte responses. *The Journal of Experimental Medicine*. 2001; 194: 823-832.
184. Hodi FS, Mihm MC, Soiffer RJ, Haluska FG, Butler M, Seiden MV, Davis T, Henry-Spires R, MacRae S, Willman A, Padera R, Jaklitsch MT, Shankar S, Chen TC, Korman A, Allison JP, Dranoff G. Biologic activity of cytotoxic T lymphocyte-associated antigen 4 antibody blockade in previously vaccinated metastatic melanoma and ovarian carcinoma patients. *Proceedings of the National Academy of Sciences of the United States of America*. 2003; 100: 4712-4717.

185. Thompson CB, Allison JP. The emerging role of CTLA-4 as an immune attenuator. *Immunity*. 1997; 7: 445-450.
186. Chambers CA, Kuhns MS, Egen JG, Allison JP. CTLA-4-mediated inhibition in regulation of T cell responses: mechanisms and manipulation in tumor immunotherapy. *Annual Reviews of Immunology*. 2001; 19: 565-594.
187. Sotomayor EM, Borrello I, Tubb E, Allison JP, Levitsky HI. *In vivo* blockade of CTLA-4 enhances the priming of responsive T cells but fails to prevent the induction of tumor antigen-specific tolerance. *Proceedings of the National Academy of Sciences of the United States of America*. 1999; 96: 11476-11481.
188. Hodi FS, Butler M, Oble DA, Seiden MV, Haluska FG, Kruse A, MacRae S, Nelson M, Canning C, Lowy I, Korman A, Lautz D, Russell S, Jaklitsch MT, Ramaiya N, Chen TC, Neuberg D, Allison JP, Mihm MC, Dranoff G. Immunologic and clinical effects of antibody blockade of cytotoxic T lymphocyte-associated antigen 4 in previously vaccinated cancer patients. *Proceedings of the National Academy of Sciences of the United States of America*. 2008; 105: 3005-3010.
189. Royal RE, Levy C, Turner K, Mathur A, Hughes M, Kammula US, Sherry RM, Topalian SL, Yang JC, Lowy I, Rosenberg SA. Phase 2 trial of single agent ipilimumab (anti-CTLA-4) for locally advanced or metastatic pancreatic adenocarcinoma. *Journal of Immunotherapy*. 2010; 33: 828-833.
190. Le DT, Lutz E, Uram JN, Sugar EA, Onners B, Solt S, Zheng L, Diaz Jr LA, Donehower RC, Jaffee EM, Laheru DA. Evaluation of ipilimumab in combination with allogeneic pancreatic

tumor cells transfected with a GM-CSF gene in previously treated pancreatic cancer. *Journal of Immunotherapy*. 2013; 36: 382-389.

191. Johansson H, Andersson R, Bauden M, Hammes S, Holdenrieder S, Ansari D. Immune checkpoint therapy for pancreatic cancer. *World Journal of Gastroenterology*. 2016; 22: 9457-9476.

192. Zhu Y, Knolhoff BL, Meyer MA, Nywening TM, West BL, Luo J, Wang-Gillam A, Goedegebuure SP, Linehan DC, DeNardo DG. CSF1/CSF1R blockade reprograms tumor-infiltrating macrophages and improves response to T-cell checkpoint immunotherapy in pancreatic cancer models. *Cancer Research*. 2014; 74: 5057-5069.

193. Yang M, Soga T, Pollard PJ. Oncometabolites: linking altered metabolism with cancer. *The Journal of Clinical Investigation*. 2013; 123: 3652-3658.

194. Brown JH, Gillooly JF, Allen AP, Savage VM, West GB. Toward a metabolic theory of ecology. *Ecology*. 2004; 85: 1771-1789.

195. Street HE, Cockburn W. *Plant Metabolism*. 2 ed., 1972; Oxford: Pergamon Press.

196. Gessaman JA, Nagy KA. Energy metabolism: errors in gas-exchange conversion factors. *Physiological Zoology*. 1988; 61: 507-513.

197. Nelson DL, Lehninger AL, Cox MM, *Lehninger Principles of Biochemistry*. 5 ed., 2008; New York: W.H. Freeman and Company.

198. Frayn KN. *Metabolic Regulation: A Human Perspective*. 2 ed., 2009; Oxford: John Wiley & Sons.

199. Hsu PP, Sabatini DM. Cancer cell metabolism: Warburg and beyond. *Cell*. 2008; 134: 703-707.
200. Wu W, Zhao S. Metabolic changes in cancer: beyond the Warburg effect. *Acta Biochimica et Biophysica Sinica*. 2013; 45: 18-26.
201. Ganapathy-Kanniappan S, Geschwind JFH. Tumor glycolysis as a target for cancer therapy: progress and prospects. *Molecular Cancer*. 2013; 12: 152.
202. Vander Heider MG, Cantley LC, Thompson CB. Understanding the Warburg effect: the metabolic requirements of cell proliferation. *Science*. 2009; 324: 1029-1033.
203. Lopez-Lazaro M. The Warburg Effect: Why and How Do Cancer Cells Activate Glycolysis in the Presence of Oxygen? *Anti-Cancer Agents in Medicinal Chemistry*. 2008; 8: 305-312.
204. Zheng J. Energy metabolism of cancer: glycolysis versus oxidative phosphorylation (Review). *Oncology Letters*. 2012; 4: 1151-1157.
205. Marín-Hernández A, Gallardo-Pérez JC, Rodríguez-Enríquez S, Encalada R, Moreno-Sánchez R, Saavedra E. Modeling cancer glycolysis. *Biochimica et Biophysica Acta (BBA) – Bioenergetics*. 2011; 1807: 755-767.
206. Xu RH, Pelicano H, Zhou Y, Carew JS, Feng L, Bhalla KN, Keating MJ, Huang P. Inhibition of glycolysis in cancer cells: a novel strategy to overcome drug resistance associated with mitochondrial respiratory defect and hypoxia. *Cancer Research*. 2005; 65: 613-621.
207. Yeung SJ, Pan J, Lee MH. Roles of p53, Myc and HIF-1 in regulating glycolysis — the seventh hallmark of cancer. *Cellular and Molecular Life Sciences*. 2008; 65: 3981-3999.

208. Lu H, Forbes RA, Verma A. Hypoxia-inducible factor 1 activation by aerobic glycolysis implicates the Warburg effect in carcinogenesis. *Journal of Biological Chemistry*. 2002; 277: 23111-23115.
209. Wang J, Weygand J, Hwang KP, Mohamed ASR, Ding Y, Fuller CD, Lai SY, Frank SJ, Zhou J. Magnetic resonance imaging of glucose uptake and metabolism in patients with head and neck cancer. *Scientific Reports*. 2016; 6: 1-7.
210. Gatenby RA, Gillies RJ. Why do cancers have high aerobic glycolysis? *Nature Reviews Cancer*. 2004; 4: 891-899.
211. Lunt SY, Vander Heiden MG. Aerobic glycolysis: meeting the metabolic requirements of cell proliferation. *Annual Reviews of Cell and Developmental Biology*. 2011; 27: 441-464.
212. Gatenby RA, Gillies RJ. Glycolysis in cancer: A potential target for therapy. *The International Journal of Biochemistry & Cell Biology*. 2007; 39: 1358-1366.
213. Garber K. Energy boost: the Warburg effect returns in a new theory of cancer. *Journal of the National Cancer Institute*. 2004; 96: 1805-1806.
214. Warburg O. The metabolism of carcinoma cells. *Cancer Research*. 1925; 9: 148-163.
215. Warburg O, Wind F, Negelein. The metabolism of tumors in the body. *The Journal of General Physiology*. 1927; 8: 519-530.
216. Warburg O. On the origin of cancer cells. *Science*. 1956; 123: 309-314.
217. Koppenol WH, Bounds PL, Dang CV. Otto Warburg's contributions to current concepts of cancer metabolism. *Nature Reviews Cancer*. 2011; 11: 325-337.



218. Schulz TJ, Thierbach R, Voigt A, Drewes G, Mietzner B, Steinberg P, Pfeiffer AFH, Ristow M. Induction of oxidative metabolism by mitochondrial frataxin inhibits cancer growth: Otto Warburg revisited. *The Journal of Biological Chemistry*. 2006; 281: 977-981.
219. Kim J, Dang CV. Cancer's molecular sweet tooth and the Warburg effect. *Cancer Research*. 2006; 66: 8927-8930.
220. Pedersen PL. Warburg, me and hexokinase 2: multiple discoveries of key molecular events underlying one of cancers' most common phenotypes, the "Warburg Effect", i.e., elevated glycolysis in the presence of oxygen. *Journal of Bioenergetics and Biomembranes*. 2007; 39: 211-222.
221. Schmidt CW. Metabolomics: what's happening downstream of DNA. *Environmental Health Perspectives*. 2004; 112: A410-A415.
222. Romero R, Espinoza J, Gotsch F, Kusanovic JP, Friel LA, Erez O, Mazaki-Tovi S, Than NG, Hassan S, Tromp G. The use of high-dimensional biology (genomics, transcriptomics, proteomics, and metabolomics) to understand the preterm parturition syndrome. *BJOG: An International Journal of Obstetrics & Gynaecology*. 2006; 113: 118-135.
223. Maxwell JC. *A Treatise on Electricity and Magnetism, Volume I*. 2 ed., 1881; London: Oxford University Press Warehouse.
224. Griffiths DJ. *Introduction to Electrodynamics*. 3 ed., 2008; San Francisco: Pearson Benjamin Cummings.
225. Jackson JD. *Classical Electrodynamics*. 1962; New York: John Wiley & Sons.

226. Weygand J, Fuller CD, Ibbott GS, Mohamed ASR, Ding Y, Yang J, Hwang KP, Wang J. “Spatial Precision in Magnetic Resonance Imaging-Guided Radiotherapy: The Role of Geometric Distortion”. *International Journal of Radiation Oncology\* Biology\* Physics*. 2016; 95: 1304-1316.
227. Rabi II, Millman S, Kusch P, Zacharias JR. The Molecular Beam Resonance Method for Measuring Nuclear Magnetic Moments. The Magnetic Moments of  $\text{Li}^{6,3}$ ,  $\text{Li}^{7,3}$  and  $\text{F}^{19,9}$ . *Physical Review*. 1939; 55: 526-535.
228. Claridge TDW. *High-Resolution NMR Techniques in Organic Chemistry*. 1999; Amsterdam: Elsevier.
229. Keeler J. *Understanding NMR Spectroscopy*. 2011; Cambridge, England: John Wiley & Sons.
230. Schempp WJ. *Magnetic Resonance Imaging: Mathematical Foundations and Applications*. 1998; New York: John Wiley & Sons.
231. Pavia DL, Lampman GM, Kriz GS, Vyvyan JA. *Introduction to Spectroscopy: A Guide for Students of Organic Chemistry*. 4 ed., 2009; Belmont, California: Cengage Learning.
232. Roberts JD. *Nuclear Magnetic Resonance: Applications to Organic Chemistry*. 1959; New York: McGraw-Hill Book Company, Inc.
233. Caravan P. Strategies for increasing the sensitivity of gadolinium based MRI contrast agents. *Chemical Society Reviews*. 2006; 35: 512-523.
234. Bushberg JT, Seibert JA, Leidholdt Jr., EM, Boone JM. *The Essential Physics of Medical Imaging*. 3 ed., 2012; Philadelphia: Lippincott Williams & Wilkins.

235. D'Esposito M, Zarahn E, Aguirre GK. Event-related functional MRI: implications for cognitive psychology. *Psychological Bulletin*. 1999; 125: 155-164.
236. Viale A, Reineri F, Santelia D, Cerutti E, Ellena S, Gobetto R, Aime S. Hyperpolarized agents for advanced MRI investigations. *The Quarterly Journal of Nuclear Medicine and Molecular Imaging*. 2009; 53: 604-617.
237. Brown RW, Cheng YCN, Haacke EM, Thompson MR, Venkatesan R. *Magnetic Resonance Imaging: Physical Principles and Sequence Design*. 2 ed., 2014; Hoboken, New Jersey: John Wiley & Sons.
238. Marx JL. Imaging technique passes muster; magnetic resonance imaging, a new but widely used technique for medical diagnosis, receives a vote of confidence from an NIH consensus panel. *Science*. 1987; 238: 888-889.
239. McClure RD, Hricak J. Magnetic resonance imaging: its application to male infertility. *Urology*. 1986; 27: 91-98.
240. Burstein D, Gray M, New MRI techniques for imaging cartilage. *The Journal of Bone & Joint Surgery*. 2003; 85: 70-77.
241. Longmaid III HE, Adams DF, Neirinckx RD, Harrison CG, Brunner P, Seltzer SE, Davis MA, Neuringer L, Geyer RP. In vivo  $^{19}\text{F}$  NMR imaging of liver, tumor, and abscess in rats: preliminary results. *Investigative Radiology*. 1985; 20: 141-145.
242. Hövener JB, Schwaderlapp N, Lickert T, Duckett SB, Mewis RE, Highton LAR, Kenny SM, Green GGR, Leibfritz D, Korvink JG, Hennig J, von Elverfeldt D. A hyperpolarized equilibrium for magnetic resonance. *Nature Communications*. 2013; 4: 1-5.

243. Zhou X, Graziani D, Pines A. Hyperpolarized xenon NMR and MRI signal amplification by gas extraction. *Proceedings of the National Academy of Sciences of the United States of America*. 2009; 106: 16903-16909.
244. Ruset IC, Ketel S, Hersman FW. Optical pumping system design for large production of hyperpolarized  $^{129}\text{Xe}$ . *Physical Review Letters*. 2006; 96: 053002-1-4.
245. Golman K, Axelsson O, Jóhannesson H, Månsson S, Olofsson C, Petersson JS. Parahydrogen-induced polarization in imaging: subsecond  $^{13}\text{C}$  angiography. *Magnetic Resonance in Medicine*. 2001; 46: 1-5.
246. Bhattacharya P, Chekmenev EY, Reynolds WF, Wagner S, Zacharias N, Chan HR, Bünger R, Ross BD. Parahydrogen-induced polarization (PHIP) hyperpolarized MR receptor imaging in vivo: a pilot study of  $^{13}\text{C}$  imaging of atheroma in mice. *NMR in Biomedicine*. 2011; 24: 1023-1028.
247. Haake M, Natterer J, Bargon J. Efficient NMR pulse sequences to transfer the parahydrogen-induced polarization to hetero nuclei. *Journal of the American Chemical Society*. 1996; 118: 8688-8691.
248. Hirsch ML, Kalechofsky N, Belzer A, Rosay M, Kempf JG. Brute-force hyperpolarization for NMR and MRI. *Journal of the American Chemical Society*. 2015; 137: 8428-8434.
249. Krjukov EV, O'Neill JD, Owers-Bradley JR. Brute force polarization of  $^{129}\text{Xe}$ . *Journal of Low Temperature Physics*. 2005; 140: 397-408.
250. Ong TC, Mak-Jurkauskas ML, Walish JJ, Michaelis VK, Corzilus B, Smith AA, Clausen AM, Cheetham JC, Swager TM, Griffin RG. Solvent-free dynamic nuclear polarization of

- amorphous and crystalline ortho-terphenyl. *The Journal of Physical Chemistry B*. 2013; 117: 3040-3046.
251. Dutta P, Martinez GV, Gillies RJ. A new horizon of DNP technology: application to in-vivo <sup>13</sup>C magnetic resonance spectroscopy and imaging. *Biophysical Reviews*. 2013; 5: 271-281.
252. Overhauser AW. Paramagnetic relaxation in metals. *Physical Review*. 1953; 89: 689-700.
253. de Boer W, Borghini M, Morimoto K, Niinikoski TO, Udo F. Dynamic polarization of protons, deuterons, and carbon-13 nuclei: Thermal contact between nuclear spins and an electron spin-spin interaction reservoir. *Journal of Low Temperature Physics*. 1974; 15: 249-267.
254. de Boer W, Niinikoski TO. Dynamic proton polarization in propanediol below 0.5 K. *Nuclear Instruments and Methods*. 1974; 114: 495-498.
255. Ardenkjaer-Larsen JH, Fridlund B, Gram A, Hansson G, Hansson L, Lerche MH, Servin R, Thaning M, Golman K. Increase in signal-to-noise ratio of >10,000 times in liquid-state NMR. *Proceedings of the National Academy of Sciences of the United States of America*. 2003; 100: 10158-10163.
256. Rodrigues TB, Serrao EM, Kennedy BWC, Hu DE, Kettunen MI, Brindle KM. Magnetic resonance imaging of tumor glycolysis using hyperpolarized <sup>13</sup>C-labeled glucose. *Nature Medicine*. 2014; 20: 93-97.
257. Golman K, in't Zandt R, Lerche M, Pehrson R, Ardenkjaer-Larsen JH. Metabolic imaging by hyperpolarized <sup>13</sup>C magnetic resonance imaging for in vivo tumor diagnosis. *Cancer Research*. 2006; 66: 10855-10860.

258. Zhang X, Lin Y, Gillies RJ. Tumor pH and its measurement. *The Journal of Nuclear Medicine*. 2010; 51: 1167-1170.
259. Harris T, Eliyahu G, Frydman L, Degani H. Kinetics of hyperpolarized  $^{13}\text{C}$ -pyruvate transport and metabolism in living human breast cancer cells. *Proceedings of the National Academy of Sciences of the United States of America*. 2009; 106: 18131-18136.
260. Chattergoon N, Martinez-Santesteban F, Handler WB, Ardenkjaer-Larsen JH, Scholl TJ. Field dependence of T1 for hyperpolarized  $[1-^{13}\text{C}]$  pyruvate. *Contrast Media and Molecular Imaging*. 2013; 8: 57-62.
261. König C, Schmid-Hempel P. Foraging activity and immunocompetence in workers of the bumble bee, *bombus terrestris* L. *Proceedings: Biological Sciences*. 1995; 260: 225-227.
262. Rygaard J. Immunobiology of the mouse mutant “nude”. *Acta Pathologica, Microbiologica et Immunologica Scandinavica*. 1969; 77: 761-762.
263. Benini J, Ehlers EM, Ehlers S. Different types of pulmonary granuloma necrosis in immunocompetent vs. TNFRp55-gene-deficient mice aerogenically infected with highly virulent mycobacterium avium. *The Journal of Pathology*. 1999; 189: 127-137.
264. Pudakalakatti SM, Uppangala S, D’Souza F, Kalthur G, Kumar P, Adiga SK, Atreya HS. NMR studies of preimplantation embryo metabolism in human assisted reproductive techniques: a new biomarker for assessment of embryo implantation potential. *NMR in Biomedicine*. 2013; 26: 20-27.

265. Dutta P, Le A, Vander Jagt DL, Tsukamoto T, Martinez GV, Dang CV, Gillies RJ. Evaluation of LDH-A and glutaminase inhibition in vivo by hyperpolarized  $^{13}\text{C}$ -pyruvate magnetic resonance spectroscopy of tumors. *Cancer Research*. 2013; 73: 4190-4195.
266. Benito J, Ramirez MS, Millward NZ, Velez J, Harutyunyan KG, Lu H, Shi YX, Matre P, Jacamo R, Ma H, Konoplev S, McQueen T, Volgin A, Protopopova M, Mu H, Lee J, Bhattacharya PK, Marszalek JR, Davis RE, Bankson JA, Cortes JE, Hart CP, Andreeff M, Konopleva M. Hypoxia-activated prodrug TH-302 targets hypoxic bone marrow niches in preclinical leukemia models. *Clinical Cancer Research*. 2016; 22: 1687-1698.
267. de Muth JE. Overview of biostatistics used in clinical research. *American Journal of Health-System Pharmacy*. 2009; 66: 70-81.
268. Hollenbeck CB. An introduction to the nutrition and metabolism of choline. *Central Nervous System Agents in Medicinal Chemistry*. 2012; 12: 100-113.
269. Lefoffe MJ. *A Photographic Atlas of Histology*. 2 ed., 2013; Englewood, CO: Morton Publishing.
270. Suvarna SK, Layton C, Bancroft JD. *Bancroft's Theory and Practice of Histological Techniques*. 7 ed., 2013; London: Churchill Livingstone.
271. Pagés F, Galon J, Dieu-Nosjean, Tartour E, Sautès-Fridman C, Fridman WH. Immune infiltration in human tumors: a prognostic factor that should not be ignored. *Oncogene*. 2010; 29: 1093-1102.
272. Dvorak HF. Tumors: wounds that do not heal. Similarities between tumor stroma generation and wound healing. *The New England Journal of Medicine*. 1986; 315: 1650-1659.

273. Colatta F, Allavena P, Sica A, Garlanda C, Mantovani A. Cancer-related inflammation, the seventh hallmark of cancer: links to genetic instability. *Carcinogenesis*. 2009; 30: 1073-1081.
274. Qian BZ, Pollard JW. Macrophage diversity enhances tumor progression and metastasis. *Cell*. 2010; 141: 39-51.
275. DeNardo DG, Andreu P, Coussens LM. Interactions between lymphocytes and myeloid cells regulate pro- versus anti-tumor immunity. *Cancer Metastasis*. 2010; 29: 309-316.
276. Grivennikov SI, Greten FR, Karin M. Immunity, inflammation, and cancer. *Cell*. 2010; 140: 883-899.
277. Karnoub AE, Weinberg RA. Chemokine networks and breast cancer metastasis. *Breast Disease*. 2007; 26: 75-85.
278. Wasserman K. The anaerobic threshold measurement to evaluate exercise performance. *American Review of Respiratory Disease*. 1984; 129: S35-S40.
279. Sonveaux P, Vegran F, Schroeder T, Wergin MC, Verrax J, Rabbani ZN, de Saedeleer CJ, Kennedy KM, Diepart C, Jordan BF, Kelley MJ, Gallez B, Wahl ML, Feron O, Dewhirst MW. Targeting lactate-fueled respiration selectively kills hypoxic tumor cells in mice. *The Journal of Clinical Investigation*. 2008; 118: 3930-3942.
280. Whitaker-Menezes D, Martinez-Outschoorn UE, Lin Z. Evidence for a stromal-epithelial “lactate shuttle” in human tumors: MCT4 is a marker of oxidative stress in cancer-associated fibroblasts. *Cell Cycle*. 2011; 10: 1772-1783.
281. Feron O. Pyruvate into lactate and back: from the Warburg effect to symbiotic energy fuel exchange in cancer cells. *Radiotherapy and Oncology*. 2009; 92: 329-333.



282. Brooks GA. Cell-cell and intracellular lactate shuttles. *The Journal of Physiology*. 2009; 587: 5591-5600.
283. Brooks GA. Lactate: glycolytic end product and oxidative substrate during sustained exercise in mammals—the “lactate shuttle”. 1985; In: *Comparative Physiology and Biochemistry: Current Topics and Trends, vol. A, Circulation, Respiration, and Metabolism*. Ed. Gilles R. Springer, Berlin.
284. Brooks GA. Intra- and extra-cellular lactate shuttles. *Medicine and Science in Sports and Exercise*. 2000; 32: 790-799.
285. Brooks GA, Hashimoto T. Investigation of the lactate shuttle in skeletal muscle mitochondria. *The Journal of Physiology*. 2007; 584: 705-706.
286. Brooks GA. Lactate shuttle – between but not within cells? *The Journal of Physiology*. 2002; 541: 333-334.
287. Gladden LB. A lactatic perspective on metabolism. *Medicine and Science in Sports and Exercise*. 2008; 40: 477-485.
288. Cruz RSO, de Aguiar RA, Turnes T, Dos Santos RP, de Oliveira MFM, Caputo F. Intracellular shuttle: the lactate aerobic metabolism. *The Scientific World Journal*. 2012; 2012: 1-8.
289. Thomas C, Perrey S, Lambert K, Hugon G, Mornet D, Mercier J. Monocarboxylate transporters, blood lactate removal after supramaximal exercise, and fatigue indexes in humans. *Journal of Applied Physiology*. 2005; 98: 804-809.

290. Overgaard M, Rasmussen P, Bohm AM, Seifert T, Brassard P, Zaar M, Homann P, Evans KA, Nielsen HB, Secher NH. Hypoxia and exercise provoke both lactate release and lactate oxidation by the human brain. *The FASEB Journal*. 2012; 26: 3012-3020.
291. Gladden LB. Lactate metabolism: a new paradigm for the third millennium. *The Journal of Physiology*. 2004; 558: 5-30.
292. Skelton MS, Kremer DE, Smith EW, Gladden LB. Lactate influx into red blood cells of athletic and nonathletic species. *American Journal of Physiology*. 1995; 268: R1121-R1128.
293. Halestrap AP, Price NT. The proton-linked monocarboxylate transporter (MCT) family: structure, function and regulation. *Biochemical Journal*. 1999; 343: 281-299.
294. Halestrap AP, Meredith D. The SLC16 gene family - from monocarboxylate transporters MCTs to aromatic amino acid transporters and beyond. *Pflügers Archiv – European Journal of Physiology*. 2004; 447: 619-628.
295. Garcia CK, Goldstein JL, Pathak RK, Anderson RGW, Brown MS. Molecular characterization of a membrane transporter for lactate, pyruvate, and other monocarboxylates: implications for the Cori cycle. *Cell*. 1994; 76: 865-873.
296. Gertz EW, Wisneski JA, Stanley WC, Neese RA. Myocardial substrate utilization during exercise in humans. Dual carbon-labeled carbohydrate isotope experiments. *The Journal of Clinical Investigation*. 1988; 82: 2017-2025.
297. Stanley WC. Myocardial lactate metabolism during exercise. *Medicine and Science in Sports and Exercise*. 1991; 23: 920-924.

298. Ide K, Secher NH. Cerebral blood flow and metabolism during exercise. *Progress in Neurobiology*. 2000; 61: 397-385.
299. Végran F, Boidot R, Michiels C, Sonveaux P, Feron O. Lactate influx through the endothelial cell monocarboxylate transporter MCT1 supports an NF- $\kappa$ B/IL-8 pathway that drives tumor angiogenesis. *Cancer Research*. 2011; 71: 2550-2560.
300. Draoui N, Feron O. Lactate shuttles at a glance: from physiological paradigms to anti-cancer treatments. *Disease Models and Mechanisms*. 2011; 4: 727-732.
301. Gladden LB. Is there an intracellular lactate shuttle in skeletal muscle? *The Journal of Physiology*. 2007; 582: 899.
302. Brooks GA. Mammalian fuel utilization during sustained exercise. *Comparative Biochemistry and Physiology Part B: Biochemistry and Molecular Biology*. 1998; 120B: 89-107.
303. Kim JW, Tchernyshyov I, Semenza GL, Dang CV. HIF-1-mediated expression of pyruvate dehydrogenase kinase: A metabolic switch required for cellular adaptation to hypoxia. *Cell Metabolism*. 2006; 3: 177-185.
304. Doherty JR, Cleveland J. Targeting lactate metabolism for cancer therapeutics. *The Journal of Clinical Investigation*. 2013; 123: 3685-3692.
305. Stainsby WN, Brooks GA. Control of lactic acid metabolism in contracting muscles and during exercise. *Medicine and Science in Sports and Exercise*. 1990; 18: 29-63.
306. Bell GI, Kayano T, Buse JB, Burant CF, Takeda J, Lin D, Fukumoto H, Seino S. Molecular biology of mammalian glucose transporters. *Diabetes Care*. 1990; 13: 198-208.

307. Roos D, Loos JA. Changes in the carbohydrate metabolism of mitogenically stimulated human peripheral lymphocytes. II. Relative importance of glycolysis and oxidative phosphorylation on phytohaemagglutinin stimulation. *Experimental Cell Research*. 1973; 77: 127-135.
308. Sagone DA Jr, LoBuglio AF, Balcerzak SP. Alterations in hexose monophosphate shunt during lymphoblastic transformation. *Cellular Immunology*. 1974; 14: 443-452.
309. Culvenor JG, Weidemann MJ. Phytohaemagglutinin stimulation of rat thymus lymphocytes glycolysis. *Biochimica et Biophysica Acta (BBA) – General Subjects*. 1976; 437: 354-363.
310. Hume DA, Radik JL, Ferber E, Weidemann MJ. Aerobic glycolysis and lymphocyte transformation. *Biochemical Journal*. 1978; 174: 703-709.
311. Frauwirth KA, Thompson CB. Regulation of T lymphocyte metabolism. *The Journal of Immunology*. 2004; 172: 4661-4665.
312. Fung-Leung WP, Schilham MW, Rahemtulla A, Kündig TM, Vollenweider M, Potter J, van Ewijk W, Mak TW. CD8 is needed for development of cytotoxic T but not helper T cells. *Cell*. 1991; 65: 443-449.
313. Handisurya A, Day PM, Thompson CD, Bonelli M, Lowy DR, Schiller JT. Strain-specific properties and T cells regulate the susceptibility to papilloma induction by *Mus musculus* papillomavirus 1. *PLOS Pathogens*. 2014; 10: 1-15.
314. Krieger NR, Yin DP, Fathman CG. CD4+ but not CD8+ cells are essential for allojection. *The Journal of Experimental Medicine*. 1996; 184: 2013-2018.

315. Gill SR, Pop M, DeBoy RT, Eckburg PB, Turnbaugh PJ, Samuel BS. Metagenomic analysis of the human distal gut microbiome. *Science*. 2006; 312: 1355-1359.
316. Turnbaugh PJ, Ley RE, Hamady M, Fraser-Liggett C, Knight R, Gordon JI. The human microbiome project: exploring the microbial part of ourselves in a changing world. *Nature*. 2007; 449: 1-17.
317. Damman CJ, Miller SI, Surawicz CM, Zisman TL. The microbiome and inflammatory bowel disease: is there a therapeutic role for fecal microbiota transplantation? *American Journal of Gastroenterology*. 2012; 107: 1452-1459.
318. Proctor LM. The human microbiome project in 2011 and beyond. *Cell Host & Microbe*. 10: 287-291.
319. Wu GD, Lewis JD. Analysis of the human gut microbiome and association with disease. *Clinical Gastroenterology and Hepatology: The Official Clinical Practice Journal of the American Gastroenterological Association*. 2013; 11: 1-7.
320. Donohoe DR, Garge N, Zhang X, Sun W, O'Connell TM, Bunger MK, Bultman SJ. The microbiome and butyrate regulate energy metabolism and autophagy in the mammalian colon. *Cell Metabolism*. 2011; 13: 517-526.
321. Turnbaugh PJ, Gordon JI. The core gut microbiome, energy balance and obesity. *The Journal of Physiology*. 2009; 587: 4153-4158.
322. Trivedi B. Microbiome: the surface brigade. *Nature*. 2012; 492: S60-S61.
323. Bäckhed F, Ley RE, Sonnenburg JL, Peterson DA, Gordon JI. Host-bacterial mutualism in the human intestine. *Science*. 2005; 307: 1915-1920.

324. McKenna P, Hoffman C, Minkah N, Aye PP, Lackner A, Liu Z, Lozupone CA, Hamady M, Knight R, Bushman FD. The macaque gut microbiome in health, lentiviral infection, and chronic enterocolitis. *PLOS Pathogens*. 2008; 4: 1-12.
325. Flint HJ. The impact of nutrition on the human microbiome. *Nutrition Reviews*. 2-12; 70: S10-S13.
326. Ley RE, Knight R, Gordon JI. The human microbiome: eliminating the biomedical / environmental dichotomy in microbial ecology. *Environmental Microbiology*. 2007; 9: 3-4.
327. Foster JA, Neufeld KAM. Gut–brain axis: how the microbiome influences anxiety and depression. *Trends in Neuroscience*. 2013; 36: 305-312.
328. Kau AL, Ahern PP, Griffin NW, Goodman AL, Gordon JI. Human nutrition, the gut microbiome and the immune system. *Nature*. 2011; 474: 327-336.
329. Ivanov II, de Llanos Frutos R, Manel N, Yoshinaga K, Rifkin DB, Sartor B, Finlay BB, Littman DR. Specific microbiota direct the differentiation of IL-17-producing T-helper cells in the mucosa of the small intestine. *Cell Host & Microbe*. 2008; 4: 337-349.
330. Ivanov II, Littman DR. Segmented filamentous bacteria take the stage. *Mucosal Immunology*. 2010; 3: 209-212.
331. Thompson GR, Trexler PC. Gastrointestinal structure and function in germ-free or gnotobiotic animals. *Gut*. 1971; 12: 230-235.

## 8. Vita

Joseph Weygand was born in Abington, Pennsylvania, son of Donna M. Weygand and Joseph L. Weygand. In high school, he was a multiple time national champion in Greco-Roman wrestling and spent countless hours of his life perfecting this craft. After retiring from the sport of wrestling, he completed an A.S. degree in mathematics in 2010 from the Community College of Philadelphia and a B.A. degree in physics in 2014 from Columbia University. He pursued graduate studies in medical physics at the University of Texas Health Science Center at Houston and completed his master's degree in 2017. He will be continuing his graduate education in medical physics at the German Cancer Research Center (DKFZ) in Heidelberg, Germany.